TURBULENT DIFFUSION
IN A STRATIFIED FLUID

by

HAROLD RUSSEL GRIGG

M.Sc., University of Saskatchewan, 1957

A THESIS SUBMITTED IN PARTIAL FULFILMENT OF
THE REQUIREMENTS FOR THE DEGREE OF
DOCTOR OF PHILOSOPHY

in the Department
of
Physics

We accept this thesis as conforming to the
required standard

THE UNIVERSITY OF BRITISH COLUMBIA
July, 1960

In presenting this thesis in partial fulfilment of the requirements for an advanced degree at the University of British Columbia, I agree that the Library shall make it freely available for reference and study. I further agree that permission for extensive copying of this thesis for scholarly purposes may be granted by the Head of my Department or by his representatives. It is understood that copying or publication of this thesis for financial gain shall not be allowed without my written permission.

Department of Physics

The University of British Columbia,
Vancouver 8, Canada.

Date Aug. 8 1960

GRADUATE STUDIES

Field of Study: Physical Oceanography

Synoptic Oceanography	G. L. Pickard
Fluid Dynamics	R. W. Stewart
Dynamic Oceanography	G. L. Pickard R. W. Stewart
Turbulence	R. W. Stewart

Related Studies:

Waves and Tides	J. C. Savage
Numerical Analysis	C. Froese
Biological Oceanography	R. F. Scagel

The University of British Columbia

FACULTY OF GRADUATE STUDIES

PROGRAMME OF THE

FINAL ORAL EXAMINATION

FOR THE DEGREE OF

DOCTOR OF PHILOSOPHY

of

HAROLD R. GRIGG

B.Sc. Saskatchewan, 1949
M.Sc. Saskatchewan, 1957

IN ROOM 301, PHYSICS BUILDING

FRIDAY, AUGUST 5, 1960 AT 10:30 A.M.

COMMITTEE IN CHARGE

DEAN G. M. SHRUM, Chairman

R. W. STEWART	F. A. FORWARD
F. A. KAEMPFFER	R. F. SCAGEL
R. W. BURLING	R. F. HOOLEY
G. V. PARKINSON	R. BARRIE

External Examiner: DR. A. PATTERSON
Pacific Naval Laboratory, Esquimalt

TURBULENT DIFFUSION IN A STRATIFIED FLUID

ABSTRACT

In natural fluids, stratification of density is common. Observations of natural turbulence in the presence of a density stratification are difficult since the stratification usually occurs in regions not readily accessible. In the laboratory, maintenance of a stratification in a shear flow presents equal difficulties.

Observations were made of isolated puffs of fluid injected vertically downwards into a uniform fluid of the same density, and into a stably stratified fluid of greater density. The observations demonstrate that such isolated puffs in uniform fluid are subject to the same decay laws as is the turbulent energy in an extended turbulent fluid. This implies that a turbulent field, made up of randomly oriented puffs of fluid of varying volumes and velocities, would display many of the characteristics of a fluid in which the turbulence is a result of shear flow, and that observations made on such puffs can be applied with some confidence to natural turbulence.

The apparatus was so constructed that the detailed mixing between the injected fluid and the surrounding fluid resulted in the formation of a finely divided precipitate which rendered the puffs visible, and permitted measurements of their path by means of moving picture photographs.

The results demonstrate that mixing with the surroundings occurs throughout the puff, which retains its identity and a relatively uniform density.

Measurements of the rate of formation of precipitate permit an estimate of the rate at which the injected fluid became mixed with the entrained fluid. The density stratification had very little influence upon this rate until after the puff had reached its maximum penetration.

The rate of horizontal spreading of the puff during its motion also showed little effect of the stratification.

Measurement of the penetration and ultimate position of the center of a puff in a density stratification together with measurements of the position of the center of a puff in uniform fluid permit the calculation of a number of dimensionless ratios. These are displayed graphically as a function of a dimensionless number made up from the initial conditions of velocity, volume, density gradient, density, and the acceleration of gravity. This number resembles the reciprocal of a Richardson's number and is referred to as $1/R_i$.

The maximum conversion of initial kinetic energy to potential energy observed was 20 percent, being greatest for small values of $1/R_i$.

The portion of the initial energy which contributes to the breakdown of the stratification was found to be approximately 3 percent and nearly independent of $1/R_i$. Some writers have thought the loss to density stratification would be much greater than this.

A figure representative of the transport of properties during the history of a puff varied by a factor 35 over the possible range of initial conditions, being greater for high values of $1/R_i$.

ABSTRACT

In natural fluids, stratification of density is common. Observations of natural turbulence in the presence of a density stratification are difficult since the stratification usually occurs in regions not readily accessible. In the laboratory, maintenance of a stratification in a shear flow presents equal difficulties.

Observations were made of isolated puffs of fluid injected vertically downwards into a uniform fluid of the same density, and into a stably stratified fluid of greater density. The observations demonstrate that such isolated puffs in uniform fluid are subject to the same decay laws as is the turbulent energy in an extended turbulent fluid. This implies that a turbulent field, made up of randomly oriented puffs of fluid of varying volumes and velocities, would display many of the characteristics of a fluid in which the turbulence is a result of shear flow, and that observations made on such puffs can be applied with some confidence to natural turbulence.

The apparatus was so constructed that the detailed mixing between the injected fluid and the surrounding fluid resulted in the formation of a finely divided precipitate which rendered the puffs visible, and permitted measurements of their path by means of moving picture photographs.

The results demonstrate that mixing with the surroundings occurs throughout the puff, which retains its identity and a relatively uniform density.

Measurements of the rate of formation of precipitate permit an estimate of the rate at which the injected fluid became mixed with the entrained fluid. The density stratification had very little influence upon this rate until after the puff had reached its maximum penetration.

The rate of horizontal spreading of the puff during its motion also showed little effect of the stratification.

Measurement of the penetration and ultimate position of the center of a puff in a density stratification together with measurements of the position of the center of a puff in uniform fluid permit the calculation of a number of dimensionless ratios. These are displayed graphically as a function of a dimensionless number made up from the initial conditions of velocity, volume, density gradient, density, and the acceleration of gravity. This number resembles the reciprocal of a Richardson's number and is referred to as $1/R_i$.

The maximum conversion of initial kinetic energy to potential energy observed was 20 percent, being greatest for small values of $1/R_i$.

The portion of the initial energy which contributes to the breakdown of the stratification was found to be approximately 3 percent and nearly independent of $1/R_i$. Some writers have thought the loss to density stratification would be much

greater than this.

A figure representative of the transport of properties during the history of a puff varied by a factor 35 over the possible range of initial conditions, being greater for high values of $1/R_i$.

An estimate of the possible effect of density stratification upon the production of turbulent energy shows that production is reduced by as much as a factor 10 for small $1/R_i$. This arises from the reversal and rebound of the puff of fluid in the stratification.

TABLE OF CONTENTS

LIST OF TABLES

LIST OF PLATES

LIST OF FIGURES

ACKNOWLEDGEMENTS

I wish to express my appreciation for the advice and suggestions given to me during the course of this research by my supervisor, Dr. R. W. Stewart.

I also wish to thank the Institute of Oceanography, University of British Columbia, for providing laboratory and office space in which to carry out the work.

1 INTRODUCTION

1.1 Background

At the present time, several volumes are available in which the literature on turbulent flow is summarized in a systematic manner, or which are particularly concerned with their author's special field of interest. In these, references to most of the original publications can be found (Hinze, J. O. 1959, Townsend, A. A. 1956, and Batchelor, G. K. 1953).

Regarding the influence of density stratification upon turbulent motions and diffusion, no such compilations have yet been made in a separate volume. Sverdrup et al (1942) contains a discussion of the subject, and gives references to some of the original papers up to that time. More recent literature is found in a large number of journals, which indicates that the subject is important to people in fields ranging from the geophysical sciences to the industrial handling of fluids. This is understandable since almost all fluids are stratified to some extent unless special precautions are taken to produce uniformity.

In one of the first series of papers on the subject, Richardson, (1920), (1925), develops a criterion for the degree of density stratification necessary to damp out turbulent motions resulting from a velocity shear. Richardson uses the usual approximation of representing the transport of momentum, and the transport of density-producing properties, due to turbulent motions, by austausch or transfer coefficients K_M and K_H

respectively, defined by Flux = K (Gradient), in analogy with a kinematic viscosity and diffusion coefficient. He introduces the dimensionless ratio $\frac{g \rho \frac{d(1/\rho)}{dZ}}{(dU/dZ)^2} = R_i$, where

g is the acceleration due to gravity,

ρ is the fluid density,

Z is the vertical displacement,

U is the non-fluctuating part of the horizontal velocity, and

R_i is now known as the ordinary Richardson's number.

Richardson proposed that for $R_i > 1$, turbulent motions could not persist but would be damped out by the energy loss to the density stratification. This was based upon the mistaken idea that $K_M = K_H$, an assumption that is approximately true in a uniform fluid (Ellison, 1957). In a stably stratified fluid, the ratio K_H/K_M can assume very small values as will be seen below.

The uncertainty about the magnitude of K_H/K_M has led to defining a new number, called the Flux Richardson's number, defined by $R_f = K_H/K_M(R_i)$. This represents the ratio $\frac{\text{Loss of mean flow energy to buoyancy}}{\text{Total loss of mean flow energy}}$ (Stewart, 1959) (a).

Taylor (1931) enlarged upon Richardson's work. Using some observations taken by Jacobsen in the Kattegat, he was able to determine R_i, K_M and K_H. He found the ratio K_H/K_M to be at all times less than 1, and to range from .13 where the stability $\rho \frac{d\,1/\rho}{dz}$ was $11.2 \times 10^{-7} cm.^{-1}$ to .021 where the

stability was 105. x 10^{-7} $cm.^{-1}$. In addition, the observations indicated that as R_i increased, it approached the ratio K_M/K_H. Taylor proposed that turbulent motions could be maintained provided $R_f < 1$.

A recent argument by Ellison (1957) indicates a critical value of R_f in the range of .14. A discussion of this subject with comments from others interested in the field is given by Stewart, (1959) (a).

The observation is often made (Sverdrup et al, 1947) that the fact that K_H/K_M is less than 1 in a stratified fluid, although the transfer of momentum and of density-producing properties is caused by the same turbulent motions, can be qualitatively understood as follows: If a fluid blob is displaced vertically by turbulent motions, momentum can be exchanged with the surroundings by pressure forces, while heat or salt can be enchanged, to any appreciable extent, only if mixing occurs between the displaced fluid and its surroundings. In my opinion, this statement requires qualification. It is true that a drop of oil moving in water can share its momentum with the water without breaking up, although, if the motion is sufficiently violent, breaking up will occur. In this case, surface tension defines a boundary which permits the dissipation of the energy, lost by momentum sharing, to occur in each fluid separately. For the case of mutually miscible fluids, no such boundary exists. The forces which are exerted on a body moving in a fluid can be broken down into viscous forces

at the interface (skin friction), and pressure forces due to the formation of a wake (form drag). Both of these imply the development of turbulent motions which must result in some degree of intermixing in the absence of any surface tension.

That there need not be any strict proportionality between these two phenomena, however, is shown by the experimental fact that K_H/K_M assumes different values. It is also reasonable that K_H/K_M should depend to some extent upon the factor controlling density, that is heat, salinity, water vapor, etc. (When it is necessary, the notation in the literature distinguishes between these by using K_H, K_S, K_W, etc., as the respective coefficients). In the limit, as turbulent motions become negligible, each coefficient must approach the corresponding molecular coefficient. They may be expected to differ somewhat until turbulent transport becomes large; with the exception of K_M, they should then approach equality, provided the hypothetical displaced blob of fluid is representative of the region from which it originated.

If the penetrating fluid is moving under its own buoyancy, as in bubbles of hot gas rising from a heated plate, it will not, in general, be representative of its point of origin, (Ellison, 1956). In this case, the relationship between the coefficients becomes more complicated, and the above remarks do not apply. In stable conditions, however, it seems reasonable to expect a displaced blob to be a representative one, since the motions are initiated by non-buoyant forces.

In natural conditions, observations of the effect of density stratification upon the turbulent motions are few. The experimental technique is difficult. Velocity-measuring instruments such as pressure-tube or pressure-plate anemometers can respond to larger scales of turbulence only. To record small details, the hot wire anemometer is the only successful instrument at this time, (Ellison, 1956) and is quite dependable in clean air or water. The hot wire, or wedge, velocity-sensing elements must be small and delicate. They are liable to become contaminated or destroyed by abrasion with foreign material in the fluid. The amplification, required to build the signal to recordable values, introduces noise which is difficult to separate from the noise-like signal. The sensing elements must be supported at considerable distances from the amplifier and supported in such a way that their velocity relative to the surroundings can be determined.

The difficulties are being overcome, (Grant et al, 1959), (Patterson, A. M. 1958, 1960). Good data on the turbulent components together with gradients of mean velocity and density, will cast light on the whole problem.

Stewart, (1959) (b), discusses the question of natural turbulence. He points out that stability is at least as important as Reynold's number in determining whether or not a natural flow will be turbulent. He gives a bibliography of recent literature on natural diffusion and related subjects.

Townsend, (1958) develops a relationship which

indicates that, in a stably-stratified atmosphere, arbitrarily small values of turbulent energy are not possible. He suggests that turbulent energy must have a certain finite amplitude or die out completely. Stewart (1959) (a), points out that Townsend's analysis requires a constant correlation between temperature fluctuations and the vertical turbulent velocity. Its conclusion, therefore, is open to question.

A density discontinuity between two miscible fluids represents an extreme example of the effect of stability on turbulent motions and turbulent mixing. Such a region will support internal waves, which in themselves, result in little increase in mixing above the molecular diffusion rate. The following two experiments show that, when a critical wave amplitude is exceeded, turbulent motions are produced which can break down the stratification.

Keulegan, (1949) conducted experiments on the effect of internal waves upon a density stratification. He found that there was little mixing across the gradient until the internal waves started to break. The principal effect of the breaking appeared to be the transport of dense material into the upper layer. The waves were caused by a shear flow in the upper fluid which was turbulent in consequence. The lower fluid was held stationary. A complementary experiment with a moving lower fluid and a stationary upper fluid has not been done to my knowledge. There is therefore some doubt as to the interpretation of the results.

In an early experiment by Taylor, (1927) a velocity shear was established by running a light fluid over a stationary dense fluid held in a shallow depression in the bottom of a channel. Little mixing occurred until a certain critical velocity of the upper fluid was reached. Once mixing commenced, the dense fluid was swept out completely.

Most of the preceding papers and experiments imply the concept of a displaced mass of fluid transferring properties of density and momentum across a density stratification. Broadly stated, they explain the alterations of the turbulent motions and the density structure by means of a ratio between the coefficients K_H and K_M.

If the concept of a penetrating fluid mass is taken literally, some further insight into the nature of the mixing process may be gained by direct observation of a single fluid mass penetrating into quiet surrounding fluid.

Scorer, (1957), (1958), made observations on discrete volumes of fluid moving under their own buoyancy into quiet surroundings. Such movements occur as thermals in a still atmosphere. Observations of displaced turbulent fluid moving against buoyant forces, or in surroundings of the same density have not been made to my knowledge.

1.2 Purpose

The object of this research is to study a volume of fluid penetrating into a quiet surrounding fluid. Buoyant forces are either zero or oppose the initial motion. The

initial motion is caused by injecting a cylinder of fluid into the still fluid.

The penetrating fluid will be called a puff. This will mean the original fluid plus any increase in volume or change in properties resulting from the entrainment of surrounding fluid. The puff will be regarded as possessing a uniform density as far as buoyant forces are concerned. The turbulent motions inside the puff were not measured.* They will not be considered in detail although the average effect of these motions in mixing the original and entrained fluids will be considered, and referred to as the detailed mixing.

The density of the injected fluid is adjusted to have nearly the same density as the surroundings at the point of injection. When the surroundings are uniform, therefore, no buoyancy forces exist. When the surroundings are stratified in density, buoyant forces are zero at the onset of motion. They increase in a manner dependent upon the details of the entrainment process, and upon the density stratification existing.

The information desired from this experiment is first, the effect of the density stratification on the penetration and the entrainment rate, and second, the rate at which the entrained fluid becomes mixed with the original fluid.

As these factors can be expected to depend upon initial conditions of velocity and volume, various values of initial conditions have been used. The details of experimental

* The hot wire anemometer will not operate in the absence of a mean flow (Hinze, 1959).

methods and measurements will be given in the next section.

Estimates of the coefficient K_M for a simple penetrative flow as described would require the presence of a vertical velocity shear. The experimental complications appear formidable. However, it can be hoped that the technique outlined above is sufficiently realistic that insight into the nature and magnitude of K_H can be obtained.

1.3 Method

The initial motion is caused by injecting a cylinder of fluid vertically downwards into a tank of still fluid through a nozzle which projects below the surface. If a simple tube is used as a nozzle, the result is almost always the formation of a vortex ring. This is particularly the case when the length of the cylinder injected is nearly the same as the diameter. The motion of vortex rings in a real fluid has been extensively studied by Northrup, (1912) and more recently by Turner (1957). It is quite possible that such rings are formed in the ocean from breaking waves and may play a part in mixing the upper layer. On a small scale it is difficult to introduce a drop of fluid into a quiet fluid without some vortex-ring formation. However, we are concerned here with turbulent mixing and the motion required is of another type. Sufficient turbulence must be present in the injected fluid to distribute the concentrated vorticity, and destroy the ring. This was accomplished by placing a coarse screen on the end of the nozzle. Even with this device, rings formed

occasionally. When this happened, the data were discarded.

In order to study the detailed mixing, some physically observable quantity must be introduced which alters when molecular mixing occurs between the injected and entrained fluid. The chemical reaction between aqueous solutions of sodium carbonate in the injected fluid, and calcium hydroxide in the tank fluid, appears to fulfil the requirements quite well. The reaction between ions in solution occurs very rapidly when the fluids are thoroughly mixed (Moelwyn-Hughes, 1957). The rate of formation of calcium carbonate will therefore be controlled by the rate at which physical mixing brings the reactants into intimate contact.

The method of measuring the amount of calcium carbonate formed, which was by measuring the light scattered from the calcium carbonate precipitate, requires justification. The tank fluid is saturated with calcium carbonate and is well supplied with condensation nucleii after being used a few times. This is evidenced by the increase of background light scatter. Supersaturation is not liable to occur. Evidence supporting the assumption of a linear relationship between volume of precipitate and light scattered is available in the data obtained. It is given in section 2.1 on page 24.

When a density gradient was required, sodium chloride was added to the fluid in the lower part of the tank, as described in the section 1.4. An experiment was conducted to show that the presence of the sodium chloride does not affect

the formation of calcium carbonate significantly. The results of this experiment are given in section 2.1 on page 25.

The cloud of fine calcium carbonate particles settles sufficiently slowly that its settling velocity can be neglected compared with the fluid velocities. The cloud apparently comes to rest. It settles out or disperses in a matter of two or three hours so the tank can be used again without renewing the fluid.

The position of the puff in the tank, as shown by the presence of the precipitate, was recorded photographically, together with the face of the oscilloscope (Plate II). The method used to measure the displacement of the center of the puff from the nozzle is given in the following section.

1.4 Apparatus

A sketch of the apparatus is shown in Fig. 1 and a photograph in Plate I. The titles on the figure correspond to the description in the text below or to the bracketed expressions. When it is necessary, specific reference will be made to the photograph.

Initiation of the fluid puff was accomplished by injecting a small volume of fluid into a tank at a depth of 3 cm. below the surface. The pressure required for the injection was provided by gravity. A fluid container (400 ml. beaker) was mounted at a height of 65 cm. above the surface of the fluid in the tank. A siphon tube dipped into this container and led vertically downwards through a fall tube to the nozzle. The

small container, fall tube, and nozzle system were movable vertically, so the nozzle could be removed from the tank between experiments, (Plate I, a). This was necessary to prevent a slow reaction between the injected and tank fluids with a consequent fouling of the nozzle. While removed from the tank, the nozzle was protected by raising a test tube, containing some of the upper fluid, to cover the nozzle. This prevented evaporation at the nozzle and loss of fluid from dripping. The screen on the end of the nozzle provided sufficient support that surface tension would prevent any dripping in the short time interval between removal from the tank and protection by the means mentioned above.

The on-off valve to start and stop the flow was a rubber hemisphere held by a spring against the end of the siphon tube which dipped into the upper container. This simple method avoided the use of packing glands. A vertical tappet rod, which supported and controlled the rubber valve, led up to a cam. The cam was operated by a small motor (Plate I a) which was so arranged that when switched on, it would open the valve once only, then shut off. A number of cams were provided to give a range of valve-opening times from .1 sec. to .8 sec.

The contact between the cam and tappet rod was used to provide the timing for an electrical pulse from a battery source, (Timing Contact). This pulse gave a vertical deflection on one beam of the dual beam oscilloscope and thus an accurate value of the valve-opening time.

An adjustable valve in the fall tube provided a means of volume regulation independent of the on-off valve. In combination with the various cams this arrangement made a limited range of velocity-volume combinations possible.

The injected volume was measured by means of a loosely-fitting polythene bead (volume measuring bead) in a graduated glass section of the fall tube. Polythene being slightly less dense than water, the bead would float slowly upwards to a constriction in the tube when the on-off valve was closed. When the valve opened, the bead fell with the fluid and the graduations permitted a volume determination accurate to .02 ml. A piece of burette tube was used for the calibrated section.

The nozzle was a section of glass tubing .540 cm. in diameter with a coarse screen on the end. The screen consisted of .033 cm. diameter plastic wire spaced approximately 0.1 cm. apart. The cross sectional area of the nozzle without the screen was .229 cm^2. The screen reduced this area to .19 cm^2.

The average initial velocity of the puff w_o was calculated from the valve-opening time, the volume measurement, and the nozzle area not decreased by the area of the screen. This initial velocity was taken to be equal to the maximum velocity attained assuming constant acceleration, that is to twice the volume divided by the product of the nozzle area and the valve-opening time. To check that this gives a reasonable figure for the average imput velocity, estimates of the volume

and velocity of the moving puff of fluid were made from moving-picture photographs. It was not possible to make these volume measurements with much precision, but the values of momentum determined by this means, agreed, on the average, with the initial momentum calculated from the initial volume and the velocity determined as stated. It appears that the fluid which first leaves the nozzle is accelerated by the fluid which follows so that the entire puff of fluid attains the velocity of the latter part.

In order to facilitate filling the siphon tube, which operation was complicated by the volume-measuring bead, a hole was drilled in the top of the inverted U of the siphon. A tube fitted with a stop cock was soldered on to the copper U tube, (Filling vent and valve). Removal of air at this point with the nozzle immersed in a beaker of the upper fluid made the operation quite simple, although it took time to get all the air bubbles out.

The large tank was of plate glass with a metal frame and an open top, (Plate I, d). The outside dimensions were 43 cm. on each side. The outside was painted with dull black paint except for windows on two adjacent sides. This blackening reduced the background light scatter to a small amount when the solution was freshly filtered and the inside of the tank walls were clean. The two windows were to permit light to enter on one side and for observation at right angles. They were made as small as was consistent with their purpose.

The calcium hydroxide solution in the tank, which will be described later, was covered with 1 cm. of kerosene to prevent evaporation and to protect it from the carbon dioxide in the air. It was necessary to remove the solution from the tank after a period of a few weeks, depending upon how often it had been used, and to clean the walls free of encrusted calcium carbonate. This was done by a dilute solution of sulphuric acid. A new solution of calcium hydroxide was then prepared and filtered into the tank.

The tank fluid, of which about 70 litres was required, was made up by mixing distilled water with 1.28 gm./l. or .017 mole/l. of $Ca(OH)_2$ in a large carboy. This mixture was stirred for several hours by a motor stirrer and allowed to settle for several days. There was always sufficient $CaCO_3$ formed during the handling of this fluid to cause cloudiness. The solution was filtered through glass wool while being transferred to the tank, and covered immediately with kerosene.

When a density gradient was required in the tank, the $Ca(OH)_2$ solution was divided into two carboys, one containing about 45 litres and the other the remainder. The fluid in the 45 litre carboy was mixed with 10% by weight of NaCl and thoroughly stirred for four or five hours. The presence of NaCl in solution has a large effect upon the solubility of $CaCO_3$ in water (Revelle & Fleming 1934). To ensure that the mixture was saturated with $CaCO_3$, some Na_2CO_3 $10H_2O$ in solution was added until a permanent cloudiness appeared with continued stirring.

When required for use the solution was filtered into the tank as before, and the unsalted $Ca(OH)_2$ solution added slowly, so as to form a two layer system. A nearly linear density gradient of about .003 gm. $cm.^{-4}$ was produced by stirring in the region of the interface. The measurement of the density gradient will be described later. The linear portion could be made sufficiently extensive to cover a depth from about 2 cm. below the surface to 12 cm. below the surface. This included all of the range covered by the experimental puffs.

When the interface was being stirred, a cloudiness appeared in the tank. This has been attributed to the details of solubility of $CaCO_3$ in water containing varying amounts of NaCl. This cloud would settle out in two days leaving the fluid clear.

Measurement of the density gradient without disturbing the fluid in the tank was accomplished by means of small glass floats approximately .5 cm. in diameter. Twelve of these were made with density covering the range in the tank. They were put into a tall cage with a glass front and back, and with coarse plastic screen sides. The cage was set on the bottom of the tank near one of the windows so the floats could be observed from outside. Depth markings on one of the glass faces permitted visual determination of the density-depth relationship. The glass floats were blown from soft glass tubing. They were calibrated by placing them in distilled water, titrating in a 20% NaCl solution with constant stirring until each

float separately became neutrally buoyant. The temperature was held at 20°C. which was approximately the temperature of the room and tank. The density of the mixture was determined from tables (Handbook of Chemistry and Physics) and checked with a sensitive hydrometer. The physical variations of size and shape in the different floats made it possible to distinguish them from one another so each could be recognized and assigned its proper density. After being in use for some time, $CaCO_3$ deposited on several of the floats as ascertained by sudden unrealistic variations of the apparent density gradient. The cage was then lifted out of the tank, the floats cleaned with dilute H_2SO_4 and re-calibrated.

The fluid in the upper container, which was the fluid injected into the tank, contained 10. g./l or .035 mole/l. of $Na_2CO_3 10H_2O$. in distilled water. In terms of the reaction to form $CaCO_3$, this fluid was twice as concentrated as the tank fluid. It was made up in 2 litre lots. For use in the density stratified tank, a number of batches were made with an increased density by adding NaCl and measuring the density with a sensitive hydrometer. As far as practical the density of the injected fluid was kept close to the density of the tank at the end of the nozzle. It was always slightly lighter, to prevent interchange of the fluids before the injection valve opened.

The heat developed by the reaction in the minimum possible volume of tank fluid could cause a density change of 1×10^{-4} gm/cm^3. In practice it would be considerably less

than this since the volume ratio was always larger than 2:1 before completion of the reaction. Density changes of this size were smaller, by an order of magnitude, than could be measured by the system of floats, and have been neglected.

The center of the tank was illuminated through one of the windows previously mentioned. A 300 watt incandescent lamp was mounted 100 cm. from the center of the tank, (Plate Ic) sufficiently far to produce reasonably uniform illumination over the portion of the tank in which the reaction occurred. Tests showed that the illumination was within 10% of its value at the center, throughout a cylinder 5 cm. in radius extending from the top to the bottom of the tank. As only about half of this volume was used in the experiment, the variation in light intensity was probably less than 5% from that at the center.

To exclude other light from the system, a dull black plywood shield covered everything except the upper fluid container and the fall tube. The tank cover had a small hole above the tank center so the nozzle could be let into the fluid when required.

A General Electric PV3 photovoltaic cell was used to measure the scattered light. With a load resistance of 100 ohms, the frequency response shows a drop of about 3% at 1000 cycles/sec, (Zworykin, 1949). This linearity is more than adequate for the purpose since the minimum rise time is about .8 seconds. The linearity of response to illumination was checked by determining the increment above the background due

to a single spherical translucent bead (.5 cm. diameter) at a number of values of incident illumination covering the range used in the experiment. The ratio, incremental output/background output, varied by 10% in a random manner.

The output of the photocell was amplified by a Kin Tel model 111BF D.C. amplifier giving amplification in 5 steps to 1000 times. The output of the amplifier was fed to one of the vertical inputs of the oscilloscope.

A DuMont type 333 double-beam oscilloscope was used to display the valve-timing pulse and the photocell-amplifier output, (Plate I d). The sweep speed was calibrated periodically against the line frequency which is closely controlled in this geographical area as it is served by a large interconnected grid. The sweep speed of the oscilloscope was found to require no adjustment and has been taken as correct. It was chosen to display the valve timing pulse on from 1/4 to 3/4 of the face and varied from .25 sec/in. to .10 sec./in.

To ensure that the valve-timing pulse was displayed on a single scan, the scope was used on external sweep control until the valve closed. A pulse, provided by an additional contact on the valve-operating cam, triggered the sweep about .1 sec. before the valve started to open. When the valve closed, the scope was switched manually to automatic sweep to show the photocell output and provide a calibration for the camera film speed.

The camera was a Bolex H. 16 standard model with an

f:1.8 lens of focal length 2.5 cm. (Plate I b). It was mounted at 75 cm. from the center of the tank inside a light-tight removable shield. The film speed was set at 16 frames per second. The exact speed was determined from the displacement of the spot on the oscilloscope and the known sweep speed. Actual camera film speeds varied from 18 to 22 frames per second. The variation during any one experiment was small. Eastman Plus X Panchromatic negative film was used at f:1.8.

Two plane mirrors were used to reflect the face of the oscilloscope into the field of the camera. These are shown in the diagram (Fig. 1). The tips of the mirrors are visible in Plate I a. Two mirrors were used to permit the puff to occupy the center of the field. The image of the oscilloscope face was split and occupied two adjacent corners of the field, this being the most convenient physical arrangement.

Plate II shows a representative series of photographs. The upper strip (a) shows the progress of a puff in a uniform tank fluid. The lower strip (b) shows a similar puff when a density gradient of .003 gm. $cm.^{-4}$ existed in the tank. The initial conditions of volume and velocity were nearly the same in each case, being .78 $cm.^3$ and 31. cm./sec. for the upper series and .83 $cm.^3$ and 32. cm./sec. for the lower series.

Experiments were carried out with volumes ranging from .8 $cm.^3$ to .065 $cm.^3$ For the larger volumes, average initial velocities of from 9.4 cm./sec. to 55 cm./sec. were possible. For the smallest volume, an average initial velocity of

9.4 cm./sec. was the greatest that could be obtained from the apparatus. The acceleration provided by gravity would not permit higher average velocities at this volume unless the apparatus were considerably modified by putting in larger diameter tubes throughout, while keeping the nozzle diameter the same as before.

Up to ten repeat runs were made with the same initial conditions, to permit an estimate of the standard deviation.

To obtain the position of the center of the puffs from the film record, an enlarged image of the puff and the tip of the nozzle was projected onto a screen. To convert from distances on the enlarged image to distances in the tank, a photograph was taken of a graduated vertical scale immersed in the tank fluid at the center of the tank. From the enlarged image of this scale, a grid was made up reading directly in cm. of actual distance in the tank. When a density gradient was used in the tank, frequent photographs were taken of the scale to compensate for the distortion due to the unequal refraction of the fluid.

The centers of the puffs were estimated visually and their displacement from the tip of the nozzle recorded. The accuracy of estimation of the center was checked on four dissimilar puffs by scanning the image of the puff and the background with a photocell. The photocell was screened off except for a square opening 2 mm. on each side. A graduated step exposure was placed on individual films using the camera shutter

stops to control the exposure. For this operation, a white card was placed temporarily in the field of the camera, and illuminated by the incandescent bulb shown in the foreground of Plate I a. Using the graduated exposure a table was drawn up for the relative response of the photocell as a function of film exposure. The centers of the puffs were calculated as a horizontal line about which the first moment of the exposure was zero. In the four cases tested, this agreed with the visual estimate to within 3 mm. of depth in the tank, (Table 1, page 22). The tendency appeared to be to estimate the displacement slightly too large. This may have been due to systematic differences in the appearance of the top and bottom of the puff. Errors in velocities calculated from the estimated displacements may thus be even less than errors in the displacements themselves.

Table 1. Comparison of visual estimates of displacement with calculated values.

Calculated	Estimated
4.6 cm.	4.7 cm.
5.1 cm.	5.3 cm.
3.8 cm.	4.1 cm.
4.8 cm.	5.0 cm.

2 DATA OBTAINED

2.1 Detailed Mixing

The use of the output of the photocell as a means of calculating the detailed physical mixing, requires justification. The quantity of light, scattered from the precipitate, will depend upon the incident illumination, and upon the details of the scattering process. It will be proportional to the volume of precipitate formed if the following conditions are met:

a. The incident illumination is constant.
b. The particles are large with respect to the maximum wavelength of incident light.
c. The distribution of particle size is uniform so that the ratio of surface area to volume is constant.
d. The particle concentration is low so that single scattering only, need be considered.

To show that these conditions are met approximately, consider two series of results, (Table 2, page 24). In one, the initial volume was .40 cm^3 and the initial velocity 9.4 cm./sec. In the other the initial volume was .80 cm^3 and the initial velocity 34. cm./sec. The time for the photocell output to reach a maximum was 7 sec. in the first case, and 1 sec. in the second case. The two sets of data were taken consecutively over a period of six days. Relative to the first set, an amplifier gain lower by a factor 3/5 was used for the second set to compensate for the increase in volume injected.

Q'_M signifies the maximum increment of photocell-amplifier output above the background value.

Table 2. Proportionality between input volume and photocell response.

Q'_M	Vol.	Q'_M/Vol.	Q'_M	Vol.	Q'_M/Vol.	Q'_M/Vol. x 5/3
3.8	.42	9.0	3.8	.88	4.3	7.2
3.9	.43	9.1	4.0*	.74	5.4	9.0
3.9	.42	9.3	3.5	.77	4.5	7.5
4.05*	.50	8.1	3.9*	.79	4.9	8.2
3.0*	.33	9.1	3.8	.80	4.8	8.0
3.2*	.37	8.7	3.6	.78	4.6	7.7
	av. 8.89 ± .39 std. dev.				av. 7.93 ± .57 std. dev.	

The two sets of data represent quite different initial conditions and different mixing processes as is shown by the fact that the time to reach Q'_M differs by a factor of seven between the two sets. The constancy achieved in Q'_M/Vol. x gain is not as high as could be desired but is not unreasonable considering the nature of the experiment. The reduction in the second set with reference to the first, may be partially attributed to the increase of deposits on the windows with a consequent reduction of light intensity.

The relative progress of the reaction is computed as the ratio $Q = Q'/Q'_M = \frac{\text{Increment of output over background}}{\text{Maximum increment}}$, which compensates for variations in illumination and changes in amplifier gain.

Q is plotted as a function of time in Fig. 2. For

* These data were not used in plotting Fig.2. Their volume and velocity do not match corresponding runs made in a stratified fluid.

similar initial conditions of volume and velocity, the data for a uniform surrounding fluid, and for one with a density gradient, are plotted together.

In Fig. 3, Q is plotted as a function of t for two experiments which had the same initial conditions and no density gradient. In one however the solutions contained no salt, while in the other both upper and lower solutions contained about 6% sodium chloride mixed thoroughly to a uniform density of 1.038 gm/cm^3. From the figure, it is apparent that the salt does not affect the formation of calcium carbonate to any appreciable extent.

2.2 Center Displacement

The displacement z of the center of the puff as a function of time is shown in Fig. 4. It requires no explanation except to say that distances were measured from the point of injection in all cases, and the positions of the centers were determined as described in section 1.4. Again for similar initial conditions of volume and velocity, the data for a uniform surrounding fluid, and for one with a density gradient, are plotted together.

2.3 Horizontal Spreading

The horizontal spread of the puff is most meaningful when plotted as a function of vertical displacement. For a uniform surrounding fluid, the envelope of successive outlines of the puff defines a cone. The outline of the cone was obtained by superimposing successive exposures and observing the

extremeties. The half angle of the cone varied from 15° to 21° and showed no systematic dependence upon the initial volume or velocity of the puff. An example is shown in Fig. 5. The successive outlines of the puff are not taken for equal increments of time.

For the cases where a density gradient was present, this method could not be used since the vertical displacement increases to a maximum and then decreases. The total horizontal width of the puff, as defined by the extremities of the precipitate, was measured on an enlarged image. This distance, converted to actual distance in the tank, is called 2 r, since a fair degree of cylindrical symmetry exists. The corresponding vertical displacement of the center z, measured as previously described (Sec. 1.4), was then plotted against r. For given values of initial volume, velocity, and density gradient, all points were plotted on one sheet. The results are shown in Fig. 6 where the outline only, of the extremeties of the experimental points is shown.

3. ANALYSIS IN NEUTRALLY BUOYANT FLUID

3.1 Detailed Mixing in Uniform Surroundings

To obtain a quantity representative of the average detailed mixing, free from the effects of chemical concentrations and gross physical entrainment, the following concepts are required:

(a) The total momentum of the puff is constant and equal to

$\rho_o V_o w_o$, the initial density, volume, and velocity of the puff.

(b) The total final volume of precipitate formed is proportional to the initial volume of fluid injected, ($Q'_m \propto V_o$).

(c) The instantaneous volume of precipitate is given by Q' and the remaining unreacted chemical in the injected fluid by $Q'_m - Q'$.

(d) From (a) the volume of fluid entrained will be $V_o(\frac{w_o}{w} - 1)$ since the density is constant.

The original amount of chemical in the entrained fluid (in terms of Q'_m) will be proportional to $Q'_m/2\ (w_o/w - 1)$ since, in terms of the reaction, the entrained fluid is only half as concentrated as the tank fluid. The remaining active material in the entrained fluid will then be proportional to $Q'_m/2(w_o/w - 1) - Q'$.

If we let A represent the injected fluid and B the entrained fluid, we can write for the reaction rate:

$dQ'/dt = k'$(Total volume) (Concentration of A) (Concentration of B)

where k' is a function which represents the average state of mixing between two fluids. This can be written:

$$dQ'/dt = k'(\text{active material in A})\ \frac{(\text{Active material in B})}{\text{Total Volume}}. \qquad (1,a)$$

Putting in the values,

$$dQ'/dt = k'(Q'_M - Q') \quad \left\{ \frac{Q'_M/2\ (w_o/w - 1) - Q'}{V_o\ w_o/w} \right\} \qquad (1,b)$$

Divide by Q'_M, let $Q'/Q'_M = Q$, substitute V_o for Q'_M absorbing all constants of proportionality in k, to obtain,

$$dQ/dt = k(1-Q)\ \left[1-w/w_o(1-2Q)\right] \qquad (2)$$

With the exception of k, the quantities in expression (2) can be obtained from the experimental curves and from the slopes of the curves. The slopes are subject to considerable error. At the point Q = .5, the dependence on w drops out and dQ/dt is observed to vary slowly. A fairly accurate value of k can be obtained in this range. For a single set of initial conditions, k is found to be nearly the same at other values of Q. An example is given in Table 3.

Table 3. Mixing function k calculated using the slopes of the mixing curves.

Initial conditions: V_o = .42 cm^3 w_o = 32. cm./sec.

Time (sec.)	.3	.4	.5	.6	.7	.8
Q	.52	.76	.88	.94	.98	1.0
dQ/dt	3.1	1.7	.90	.45	.25	0.0
w/w_o	.16	.11	.083	.068	.053	0.0
k	6.6	6.8	7.0	7.7	12.	

The last two values of k, 7.7 and 12., are determined for Q = .94 and .98 respectively. In expression (2), the

factor (1 - Q) is sensitive to small errors in Q when Q is near to 1. The calculated value of k in this range, must be regarded with suspicion.

If we assume k to be nearly constant, expression (2) can be integrated numerically in the form

$$Q = k \int_o^t (1-Q) \left[1 - w/w_o \, (1-2Q)\right] \quad dt. \qquad (3)$$

Equation (3) is not so sensitive to small errors in Q and does not make use of the slopes of the Q-t curves. These slopes are inaccurate, being obtained by numerical differentiation.

Since w is not known in the early part of the range, before two observations have been taken, the value of the integral is known only above a constant. This constant could be found by assuming the value of k determined above at Q = .5 to be correct, or alternatively to determine, for two different times, what constant would make k have identical values. Since this is, to some extent, a distinct calculation from the previous one, it has been used. Calculations are shown in Table 4, page 30 for the same data as used previously. (Table 3, page 28) The integrand in expression (3) is called B. C signifies $\int_o^{.3} B\,dt$, since t = .3 is the earliest time for which w, and therefore B, is known.

Table 4. Calculation of mixing function k using an integral expression for Q.

Time (sec.)	.3	.4	.5	.6	.7
B	.48	.25	.128	.058	.021
$\int_o^t Bdt$	c =.081	c+.036 =.117	c+.055 =.136	c+.064 =.145	c+.068 =.149
Q	.52	.76	.88	.94	.98
$k = Q/\int_o^t Bdt$	6.5	6.5	6.45	6.5	6.55

c was calculated by letting $\frac{c + \int_o^t Bdt}{Q_t}$ = const.

Choosing two points at t = .3 and t = .6, this yields $\frac{c}{.52} = \frac{c + .064}{.94}$ from which c $\simeq$ .081. Over the range where Q and w are available, the computed value of k in Table 4 varies by less than 1% from its value at Q = .5. For the other sets of initial conditions, k varied by less than 10% from its value at Q = .5 in each case.

The average values of k computed by this method are listed in Table 5 with the corresponding initial conditions.

Table 5. Mixing function k for various initial conditions.

V_o	w_o	k
.42	32.	6.5
.065	9.5	3.3
.82	55.	12.3
.80	9.4	.86
.42	9.6	.95
.81	32.	4.5
.63	32.	5.8

From equation (1) it is apparent that k has dimensions t^{-1} since Q is dimensionless. Since k is some function of the initial conditions and possibly the kinematic viscosity ν, it may be possible to determine what function.

A least squares approximation done on the logarithms of k, V_o and w_o yields the expression,

$$k = m\, w_o^{1.53}\, V_o^{-.55} \tag{4}$$

where m is a constant. This gives the approximate dependence upon w_o and V_o.

A dimensionally correct expression between k, ν, V_o, and w_o consistent with the observations, can be obtained if V_o is interpreted as a length instead of a volume. Since only one nozzle diameter was used, volume and length are proportional. In this interpretation, the relationship $k = m\, \nu^{-\frac{1}{2}} w_o^{3/2}\, V_o^{-\frac{1}{2}}$ has the correct dimensions and fits the observations reasonably well, as will be shown later. In Fig. 7, k is plotted against $w_o^{3/2} V_o^{-\frac{1}{2}}$ and the constant $m\nu^{\frac{1}{2}}$ is found to be .023. Putting in the relationship between volume and length, we obtain

$$k = .0050\, \nu^{-\frac{1}{2}} w_o^{3/2} L_o^{-\frac{1}{2}} \tag{5}$$

where L_o is the initial length of the injected cylinder.

A simple graphical method of finding an approximate power law relationship between 3 variables, is given in Appendix 1. This method was used initially to determine equation (4). By use of this method, Fig. 8 shows the agreement of the data with equation (4). Fig. 8 also shows the agreement of the data with an equation similar to (4) but with indices 3/2

and $-\frac{1}{2}$ instead of 1.53 and -.55.

The function k is a measure of the average state of mixing which exists inside the puff. It does not involve gross entrainment or concentration effects. It must be regarded as an imperical relationship which serves to express the experimental mixing data in a compact form.

The action of turbulent motions in mixing two miscible fluids can be thought of as a stretching of the initial interface to produce a greater interfacial area through which molecular diffusion can proceed. Molecular diffusion tends to reduce concentration gradients at the interface while turbulent stretching tends to sharpen these gradients and to increase the interfacial area.

The experimental evidence that k is relatively constant over the range in which observations have been taken, indicates that, in this type of flow, the initial conditions determine a relationship between the interfacial area per unit volume, and the gradient of transition from one fluid to the other. This relationship thereafter is relatively constant. The variations in chemical reaction rate are determined by the total volume occupied by the two fluids, and the undepleted active materials in this volume.

3.2 Velocity of a Puff in Uniform Fluid of the Same Density.

The superposition of successive outlines of a puff, penetrating into a uniform fluid of the same density, indicates that the puff is contained in a cone of half angle approximately

20 degrees, (Fig. 5). The values found varied from 15 degrees to 21 degrees with an average value of 19 degrees. The vertex of the cone is located at an indefinite distance from the tip of the nozzle. No systematic dependence of this distance, or of the cone angle, upon the initial conditions was determined.

If the shape of the puff remains similar, which is roughly true, the fact that its outline is contained in a cone implies that the turbulent velocities inside the puff must be proportional to the velocity of the center of the puff with respect to the surroundings. This is so since the turbulent velocities are responsible for, and proportional to, the rate of spreading.

If all velocities are proportional to one another, and remain so, the flow is of the type called self-preserving, and is independent of the Reynold's number providing this is sufficiently large. For a self-preserving flow, the form of the self-preserving functions are universal for any one type of flow, (Townsend, 1956). It follows that a non-dimensional plot of any two variables should show the same form for all flows of a given type.

In Fig. 10 a plot of $z/V_o^{1/3}$ against $tw_o/V_o^{1/3}$ is shown for all the data obtained. The considerable scatter is attributed to two factors:

a. The flows are not self-preserving at the origin and become so only after an interval of time and distance which are not related in the same manner as they are after self-

preservation becomes established.

b. The initial values V_o and w_o separately relate to the initial conditions and not necessarily to the flow after it has become self-preserving.

If we assume self-preservation, a dimensional argument yields an expression for the displacement and velocity of a puff as a function of time measured from a virtual origin where $z = 0$, and $w = \infty$ at $t = 0$.

Since the density of the surrounding fluid is the same as that of the puff, no buoyant forces are developed, and the vertical momentum of the puff, which includes the injected and entrained fluid, is a constant. Then

$$Vw = \text{const}$$

$$\text{Dimensionally} \quad L^4 = ct, \text{ or } L = c_1 t^{\frac{1}{4}},$$

where L can be any length typical of the puff depending on the choice of c_1. Interpreting L as the displacement from the virtual origin,

$$z = c_2 t^{\frac{1}{4}} \quad \text{and} \quad w = c_3 t^{-\frac{3}{4}}.$$

The line drawn on Fig. 10 as $(Z')^4 = 100(t' - 2.5)$ where Z' and t' are dimensionless displacement and time corresponding to the ordinate and abscissa of Fig. 10, indicates the trend of the data.

It may be instructive to consider the problem from the point of view of the turbulent energy density E. We require, in addition to the concept of self-preservation, the rate of turbulent energy dissipation dE/dt. In a self-preserving flow,

this is proportional to $\frac{E^{3/2}}{L}$, where L is a scale length typical of the turbulence, therefore proportional to $V^{1/3}$, (Townsend, 1956).

The rate of production of turbulent energy per unit mass will be equal to the average rate at which a unit mass of the puff loses energy, that is, to $-\frac{d}{dt}(\frac{1}{2}w^2)$.

The turbulent energy equation becomes,

$$\frac{dE}{dt} = -\frac{d}{dt}(\tfrac{1}{2}w^2) - B' \frac{E^{3/2}}{V^{1/3}} \qquad (6)$$

where B' is a proportionality constant. Since turbulent velocities are proportional to the mean center velocity, $E \propto w^2$. From momentum conservation, $V^{-1/3} = \frac{w^{1/3}}{(V_o w_o)^{1/3}}$.

Putting in these values,

$$\frac{dw^2}{dt} = -A\frac{dw^2}{dt} - B\, w^{10/3} \qquad (7)$$

where A and B are constants.

Subject to $w = w_o$ at $t = t_o$, the solution is,

$$w^{-4/3} = ct + (w_o^{-4/3} - ct_o) \qquad (8)$$

where c is a constant.

The values of w obtained numerically from the displacement curves, Fig. 4, if plotted in the form $w^{-4/3}$ vs t, show this straight line tendency except for a region where t is small. An example is given in Fig. 11.

The distance from the nozzle at which the experimental

points start to follow the relation given, is largely controlled by the initial length of the injected fluid cylinder, if this length is large with respect to the radius. If z_c is this critical distance and L_o is the original length of the injected cylinder, $z_c = f(R)L_o$, where f(R) varies from 1 to 2, increasing with increasing initial velocity. For one case, where L_o was nearly equal to the radius, the value of f(R) was 8.1. It appears that in this case, the process of adjustment to similarity conditions is altered. The values of c in equation (8) are listed in Table 6, page 39, for the various initial conditions.

3.3 Displacement of a Puff in Uniform Fluid of the Same Density

From the last section, (Sec. 3.2), the displacement of a puff follows the relationship $z \propto t^{\frac{1}{4}}$ if z and t are measured from the correct origin. This origin is not always well defined by the cone obtained by superimposing successive positions of the puff. It can be determined more precisely by using two nearby displacement values occurring after similarity conditions are established, that is after the velocity begins to follow the relation $w^{-4/3} \propto t$.

Consider two displacements, z_a at t_a and z_b at t_b, where $z_b - z_a = \delta$, and is small with respect to z_a and also with respect to the displacement from the virtual origin. If we represent displacement and time measured from the virtual origin by z^* and t^*, then $z_b^* - z_a^* = \delta$, and $t_b^* - t_a^* = t_b - t_a = \epsilon$.

From the virtual origin, $w^{*-4/3} = ct^*$, and, $z^4 = \frac{4^4}{c^3} t$. Now,

$$z_b^{*4} - z_a^{*4} = \frac{4^4}{c^3} (t_b^* - t_a^*) \tag{9}$$

Expand the left hand side, discard a term in δ^2, let $z_b^* = z_a^* + \delta$, and simplify to obtain,

$$\left(z_a^* + \frac{\delta}{2}\right) \left(z_a^*\right) \left(z_a^* + \delta\right) = \left(\frac{4}{c}\right)^3 \frac{\epsilon}{\delta} ,$$

or approximately $$\left(z_a^* + \frac{\delta}{2}\right)^3 = \left(\frac{4}{c}\right)^3 \frac{\epsilon}{\delta} . \tag{10}$$

The constant c can be obtained from the slope of the corresponding velocity curve, $w^{-4/3} = ct + \text{const.}$ and ϵ and δ are known. Hence z_a^* can be approximated. This approximate value can be checked in (9) and small corrections made if necessary.

The displacement of the virtual origin from the tip of the nozzle is given by $z_a - z_a^*$. These displacements were calculated from the data in Fig. 4, and found to vary from -.58 cm. to 5.6 cm. No systematic dependence on the initial conditions could be observed.

This lack of system with respect to the position of a virtual origin, is a feature which often occurs in turbulent flows (Hinze, 1959, page 216). This phenomenon may be due, in the present case, to the fact that in initiating the flow, the apparatus presents several lengths and velocities, and consequently many Reynold's numbers which become critical at

different mean velocities. This may influence the behaviour of the puff for a short distance. After the small scale effects have had time to decay, the behaviour of the puff will be controlled by the gross features of initiation.

A sample plot of z^4 against t is shown in Fig. 12. No correction for a virtual origin of time has been made since time is involved linearly. The points follow a straight line reasonably well except for small values of t. In one set (not shown) the equation is not obeyed. The initial conditions in this case were $V_o = .065$ cm^3, and $w_o = 9.5$ cm./sec. It is possible that similarity conditions are not reached in this case, at least not during the time of observation.*

No systematic dependence of the slope of the straight line portion of the z^4 vs t curve upon the initial conditions has been observed. The same holds for the velocity curves since the two slopes are related.

The values of the constant c in equations (8) and (10) are listed in Table 6, page 39, together with the corresponding initial conditions.

* This is the same set which showed anomalous behaviour with respect to the velocity law (Equation 8, page 35). This set had a Reynold's number ($w_o V_o^{1/3}/\nu$) equal to 380, the lowest used. For other runs, Reynold's numbers ranged from 870 to 5100.

Table 6. Values of slope constant in velocity and displacement curves.

V_o cm.^{3}	w_o cm./sec.	c cm.$^{-4/3}$ sec.$^{1/3}$
.42	32.	.82
.82	55.	2.5
.80	9.4	.68
.42	9.6	1.3
.81	32.	1.8
.63	32.	.90

4 ANALYSIS IN STABLY STRATIFIED SURROUNDINGS

4.1 Motion Across a Density Discontinuity

A volume V_o of fluid of density ρ_o, if injected downwards into a uniform fluid of greater density ρ_z will experience a constant buoyant force equal to $V_o(\rho_z - \rho_o)g$, as can be seen by the following:

Increase in mass = mass entrained.

or $d(\rho V) = \rho_z\, dV$; $\rho dV + V\, d\rho = \rho_z dV$; $dV/V = d\rho/(\rho_z - \rho)$

Subject to $V = V_o$ when $\rho = \rho_o$, the solution of this is $V(\rho_z - \rho) = V_o(\rho_z - \rho_o)$.

The buoyant force $V(\rho_z - \rho)g$ is therefore given by $V_o(\rho_z - \rho_o)g$ and is constant. This is understandable since any entrained fluid contributes no buoyant force whatever.

The time for such an injected puff to become stationary is readily calculable by setting the momentum loss

equal to the initial momentum to obtain

$$t = (\rho_o w_o)/(\rho_z - \rho_o)g \ .$$

To obtain the depth of penetration would require a knowledge of the entrainment rate.

4.2 Motion in a Uniform Stratification

Where the surrounding fluid has a density which increases with depth, the buoyant force is also a function of the entrainment rate. The additional notation used in this section is given below:

ρ instantaneous mean density of the puff

Z instantaneous depth of the puff.

ρ_o mean density of the puff at the point of injection Z_o.

ρ_{zo} density of surroundings at the point of injection Z_o.

ρ_m mean density of the puff at the point of maximum penetration Z_m.

ρ_{zm} density of surroundings at Z_m.

ρ_z density of the soundings at depth Z.

$\rho_{eq} = \rho_{zeq}$ density of puff and surroundings at the point where the puff eventually comes to rest Z_{eq}.

Although in recording the data (Fig. 4), Z_o was taken as zero, and displacements measured from this point, it is convenient in this section to refer to displacement from the point of injection as $Z - Z_o$.

The changes which a fluid puff undergoes when injected vertically downwards into a similar fluid with density stratification are as follows: Assuming $\rho_o = \rho_{zo}$, the volume

increases by entrainment of surrounding, more dense, fluid with resulting increase of average density. The kinetic energy decreases from losses due to entrainment, and from work done against the buoyant forces. The potential energy of the puff, zero at the start, increases, since it is necessarily positive at the point of maximum penetration due to the density difference between the puff and its surroundings. After coming to rest, the puff rises under buoyant forces, usually overshoots the equilibrium position, and eventually comes to rest at some point below the point of injection.

The experimental displacements, measured from the point of injection, are plotted against time in Fig. 4 for the various initial conditions.

From the measured displacements, an estimate of the instantaneous velocity can be made. The density of the surrounding fluid increases nearly linearly with depth at rates varying from .0025 to .0031 gm./cm^4. Initial values of volume and velocity are known.

From the data it is possible, in principle, to determine the volume and density at all times by numerical methods as follows:

Decrease of momentum = mean buoyant force x time, $\Delta (\rho_n V_n w_n) = -(\rho_{z+\frac{1}{2}} - \rho_n) V_n g \Delta t$, where $\rho_{z+\frac{1}{2}}$ is the mean density of the surroundings during the time interval Δt. From this we can obtain the momentum at the next observed point $(\rho V w)_{n+1}$. From this obtain the mass at n+1 by dividing

by the observed velocity w_{n+1}. The volume of fluid entrained ΔV is equal to (mass change/mean surrounding density). Then $\rho_{n+1} = \frac{\rho_n V_n + \rho_{z+\frac{1}{2}} \Delta V}{V_{n+1}}$.

This process can be iterated using mean values of volume and density in the interval, to calculate the momentum loss.

In practice, the method does not work well because the momentum is not known precisely at any one time. The time of injection is an appreciable portion of the time for the whole process. Some entrainment of fluid occurs before the puff has attained its maximum velocity, hence the initial conditions are not known exactly. Similar objections apply to working backwards from the point of zero momentum at Z_m. The precise time at which w is zero cannot be determined. Several trial calculations were made but proved so sensitive to small changes in initial conditions that no reliance could be placed upon them.

In the lack of detailed information on instantaneous volume and density, the following section gives a method of calculating the minimum value of the potential energy at Z_m.

4.3 Potential Energy of a Puff at Maximum Penetration

To obtain a minimum estimate of the potential energy of a puff at Z_m the following assumptions are made:

(a). Assume the density of the puff at Z_m is equal to the density of the fluid at the level where the puff eventually

comes to rest ($\rho_m = \rho_{zeq}$). This must give a maximum value for the density of the puff at Z_m since the greater part of the ensuing path is through fluid of greater density than ρ_{zeq}, and the puff must end up with a density of ρ_{zeq}.
(b) Assume the volume of the puff at Z_m is determined from mixing of the initial volume V_o at density ρ_o with fluid of the maximum density encountered, that is ρ_{zm}. This yields the smallest volume of the puff and therefore the smallest potential energy consistent with assumption (a).

To examine whether assumption (a) gives a minimum value for potential energy, consider the potential energy if the density of the puff at Z_m is less than ρ_{zeq} (it cannot be greater). In this case the equilibrium point will not be at Z_{eq} but at some higher point Z_a.

The potential energy is given by,

$$PE = \int_{za}^{zm} Vg\ (\rho_z - \rho_m)\ dZ \qquad (11)$$

$\rho_m = \rho_{za}$, and $\rho_z = \rho_{za} + (Z - Z_a)\ d\rho/dZ$, since $d\rho/dZ$ is constant. Making these substitutions, and evaluating the integral, we obtain,

$$PE = \tfrac{1}{2}\ Vg\ (Z_m - Z_a)^2\ d\rho/dZ. \qquad (12)$$

To obtain an equation for PE in terms of ρ_m and known quantities, we require the relation between depth and density,

$$Z_m - Z_a = \frac{(\rho_{zm} - \rho_m)}{d\rho/dZ}\ , \qquad (13)$$

and also an expression for V determined from assumption (b),

$$V\rho_m = V_o\rho_o + \rho_{zm}\,(V - V_o), \text{ from which}$$

$$V = V_o\,\frac{(\rho_{zm} - \rho_o)}{(\rho_{zm} - \rho_m)}\,. \tag{14}$$

Substituting (13) and (14) into (12) we obtain after simplification,

$$PE = V_o\,\frac{(\rho_{zm} - \rho_o)\,(\rho_{zm} - \rho_m)}{2\,d\rho/dZ}\,g\,. \tag{15}$$

It is apparent that the minimum value of PE will be obtained when ρ_m has the greatest value consistent with the observations, that is when $\rho_m = \rho_{eq}$.

The computations were made using the observations on a single puff, and not the averaged values of several observations as shown in Fig. 4. This applies to all the computations in this section where the critical points were used, and accounts for the fact that the number of plotted points in Figs. 13, 15, 17, and 18, is greater than the number of curves in Fig. 4.

The scatter in the individual observations as indicated in Fig. 4, is only partly due to variations in input conditions and errors in observations. Even in cases where the input conditions were nearly identical as far as could be determined, considerable variations in displacement were noted. The progress of the fluid puff appears to be influenced to some considerable extent by conditions in the fluid which are

beyond immediate control, and the observations are valid only in a statistical sense. Since, in any real case, these small perturbations will be present, the resulting scatter must be regarded as an essential part of the observations.

Calculations have been made from the data using equation (15) with ρ_{eq} substituted for ρ_m. This minimum value of potential energy at maximum penetration had been compared with the initial energy at the point of injection (the sum of initial kinetic and potential energy when the latter was not zero), to form the ratio

$$\frac{\text{potential energy at maximum penetration}}{\text{initial total energy}} .$$

In order to show the results in the most general manner possible, a dimensionless ratio is made up from the initial conditions which might be expected to influence the flow. These are ρ_o, w_o, g, $d\rho/dz$, and V_o. The kinematic viscosity has been omitted since the Reynold's number is sufficiently high that it is not expected to affect the flow. A suitable dimensionless combination is $\frac{\rho_o w_o^2}{g \, d\rho/dz \, V_o^{2/3}}$ which involves a comparison between kinetic forces and buoyant forces. This dimensionless form has a resemblance to the reciprocal of the Richardson's number, differing from it by the replacement of $(du/dz)^2$ by $w_o^2/V_o^{2/3}$, and will be referred to as $1/R_i$.

All dimensionless ratios obtained are plotted as a function of the reciprocal of this Richardson's number, and

will vary with it in the same general manner as if it were the usual Richardson's number. The actual numerical values of $1/R_i$ given in Figs. 13 and following figures, bear no relation to the values of reciprocal Richardson's number which might be found in practice.

In Fig. 13, the ratio of the potential energy at maximum penetration to the initial total energy is plotted against $1/R_i$. The points are distinguished as to the initial volume, and, when plotted in this manner, show no variation of the ratio with initial volume.

The results indicate that as much as 20 percent of the initial energy appears as potential energy for small values of $1/R_i$. For higher values of $1/R_i$, the ratio decreases rapidly, and approaches zero for $1/R_i$ approximately equal to 1000.

For an initial velocity of 54 cm./sec. the puff showed no perceptible rise after reaching the point of maximum penetration. At this velocity, the puff dissipates rapidly, and cannot be observed for long. Since the equilibrium position is not known, no value can be assigned to the energy ratio in this case. It cannot be zero, however, but must possess some small value. The density gradients used were all very nearly the same at about .003 gm./cm^4 so the principal part of the change in R_i is due to the variations in initial velocity and volume.

4.4 Effect of a Puff Upon the Surrounding Fluid

Regarding the alteration of the density structure of the ambient fluid by a penetrating puff, the information we should like to obtain is, (a) what part of the initial energy is dissipated in altering the density structure, and (b) where, with respect to the point of origin, does this alteration occur.

Exact calculation of the effect of a puff on the surroundings is not possible since the details of entrainment along the path cannot be made with any precision. An approximate value for the energy lost to the density stratification, and for the location of this density alteration, can be obtained using the same assumptions as were used before, that is, that the equilibrium density is achieved by mixing of fluid from the path extremeties at Z_o and Z_m.

In this approximation, the effect upon the surroundings is as follows. A quantity of fluid V_o is removed from depth Z_o, mixed with sufficient fluid from depth Z_m to produce a density ρ_{eq}, and the total volume deposited at Z_{eq}. The fluid above Z_{eq} will rise slightly to replace that removed from Z_o. The fluid below Z_{eq} will fall to replace that removed from Z_m. A sharp gradient will be produced at Z_o and at Z_m. A short region of uniform density will be produced at Z_{eq}. Fig. 14 is an exaggerated illustration of the alterations in density stratification produced by such a puff. The solid line represents the original linear density gradient.

The cross hatched areas represent, in exaggerated form, the alterations produced by the puff, under the assumption of mixing at the maximum depth only. The dashed line represents the probable alterations in density structure which would be produced assuming entrainment along the entire path. In actuality, since the tank is large with respect to the puff, the discontinuities at Z_o and Z_m are very small, as is the uniform portion at Z_{eq}.

Referring to Fig. 14, the areas A and B are equal since the area under the curve must remain unchanged. This can be expressed as follows:

$$\Delta\rho_a\,(Z_{eq} - Z_o) = \Delta\rho_b(Z_m - Z_{eq}) \quad \text{or,}$$

$$\frac{\Delta\rho_a}{\Delta\rho_b} = \frac{Z_m - Z_{eq}}{Z_{eq} - Z_o} \tag{16}$$

The ratio (16) is also equal to $V_o/\Delta V$, where ΔV is the volume of fluid removed from Z_m. This can be seen by use of equation (14), page 44, and some algebra, setting ρ_m equal to ρ_{eq}.

The ratio in (16), which represents the initial volume divided by the volume entrained at Z_m from assumption (b) Sec. 4.3, has been calculated for the various initial conditions and is shown graphically as a function of $1/R_i$ in Fig. 15. The ratio (16) has an approximate value of 2 for $1/R_i$ equal to 30, and drops to less than 1 for $1/R_i$ equal to 500. For $1/R_i$ equal to 1000. which corresponds to an initial

velocity of 55. cm./sec. and initial volume of .80 cm^3, the puff was not observed to rise. (Fig. 4 c) The calculated ratio is therefore zero. Actually there must be some small rise and a small finite value for the ratio (16).

Fig. 16 is a plot of the experimental values of maximum penetration Z_m and equilibrium depth, Z_{eq}, obtained from the same data as were used to produce Fig. 4. The depths are plotted against initial velocity. No systematic dependence of these depths upon the initial volume was observable. Figs. 15 and 16 are related through equation 16, page 48.

The work done upon the surrounding fluid can be calculated in this simplified picture as follows: Referring to Fig. 14, the work done will be equal to the work required to restore the density gradient to its original linear form. This will be the work required to carry the product of density defect and volume represented by region B to the position of region A. This product is independent of the size of the tank, provided the tank is sufficiently large. In the actual case, $\Delta\rho_a$ and $\Delta\rho_b$ will be small, and the volume large. The uniform density region at Z_{eq} will be negligibly small with respect to the other distances involved. Let E_ρ represent the work required, then

$$E_\rho = (\text{tank cross section})\,\Delta\rho_a\,(Z_{eq} - Z_o)\,x \left(\frac{Z_{eq} - Z_o}{2} + \frac{Z_m - Z_{eq}}{2}\right) g \cdot \qquad (17)$$

Consider a unit cross sectional tank area and unit

volume injected. The fluid above Z_{eq} must rise unit distance to replace the displaced volume. Then $\Delta \rho_a = d\rho/dZ$ and (17) becomes,

$$E_\rho = d\rho/dZ\ (Z_{eq} - Z_o)\ (Z_m - Z_o)\ \frac{g}{2}\ , \text{ per unit } V_o. \qquad (18)$$

From equation (18) the values of E have been calculated from the original data. The ratios E_ρ/E_o, where E_o is the initial total energy of the puff per unit volume, were computed and the results are plotted in Fig. 17 as a function of the reciprocal Richardson's number.

The variation in this ratio with $1/R_i$ is small. At low values of $1/R_i$, where the penetrations are small and relative errors in measurement are proportionately large, the points are badly scattered. At higher values of $1/R_i$ the points are well grouped near to a value of .03. As a representative figure, we could say that approximately 3 percent of the initial energy is used to alter the density stratification, for the range of Richardson's number covered in the experiment.

4.5 Transfer Coefficient

Strictly speaking, a transfer coefficient has little meaning for the single displaced puff or fluid. Nevertheless, computations can be made of the transfer of density difference during the lifetime of the puff, and the results of these computations can be compared for the various initial conditions of volume and velocity.

As has been shown in the preceding sections, and

making the same assumptions as before of mixing at the path extremity Z_m only, the result of the puff is the following. A volume of fluid V_o is removed from position Z_o, mixed with fluid at Z_m to make a total volume V, and the whole is deposited at Z_{eq}. This amounts to moving a volume V_o from Z_o to Z_{eq}, and a volume ΔV from Z_m to Z_{eq}. The product of mass difference and distance transported will be given by

$$\Delta M\, L = V_o\, (\rho_o - \rho_{eq})\, (Z_{eq} - Z_o) + \Delta V\, (\rho_{eq} - \rho_m)\, (Z_m - Z_{eq}). \tag{19}$$

By use of equation 16, page 48, and the fact that the density gradient is linear, (19) can be written

$$\frac{\Delta M\, L}{V_o} = - \left[(Z_{eq} - Z_o)^2 + \frac{Z_{eq} - Z_o}{Z_m - Z_{eq}}\, (Z_m - Z_{eq})^2 \right] \frac{d\rho}{dZ}. \tag{20}$$

If we let K_H' be a net density transfer coefficient for this process, such that

$$\frac{\Delta M\, L}{V_o} = -K_H' \frac{d\rho}{dZ} \quad \text{then,} \tag{21}$$

$$K_H' = (Z_{eq} - Z_o)\, (Z_m - Z_o) \tag{22}$$

where K_H' has dimensions L^2. These net density transfer coefficients have been calculated from the original data for single experiments. K_H' is made dimensionless by division by $V_o^{2/3}$ and is plotted against the dimensionless reciprocal Richardson's number in Fig. 18. The values range from 1 where $1/R_i$ is approximately 30, to 35 when $1/R_i$ is approximately 1100. In the range covered, $K_H'/V_o^{2/3}$ varies nearly linearly with $1/R_i$.

Another dimensionless ratio which can be made up from the density gradient data is the ratio of the equilibrium distance $Z_{eq} - Z_o$ to the distance of maximum penetration $Z_m - Z_o$. This ratio is plotted in Fig. 19 as a function of the reciprocal Richardson's number. The ratio approaches 1 when $1/R_i$ is approximately 1100. It falls in a roughly linear manner to a value of .4 when $1/R_i$ is approximately 30.

5 COMPARISON OF NEUTRALLY BUOYANT AND STABLE SURROUNDINGS

5.1 Horizontal Spreading

Figs. 5 and 6 show the horizontal spread of a puff in both uniform and stably stratified surroundings as a function of vertical displacement.

If the horizontal extension is plotted as a function of time, (not shown) the curves obtained for uniform and stably stratified surroundings fall very closely together for the same initial conditions of volume and velocity. This fact can be observed in Plate II where two puffs with nearly the same initial conditions penetrate a uniform fluid (upper strip) and a stratified fluid (lower strip). During the active motion of the puff, the radii in the two cases are nearly identical. After the motion ceases, the puff in stratified fluid spreads at its own density level under the influence of gravity, indicating that its density is relatively uniform throughout. This can not be seen in Plate II since the photographs do not continue to that time.

5.2 Vertical Spreading

No readings were made for vertical spreading due to the difficulty in delineating the upper boundary of the puff. The last few frames on Plate II indicate that the vertical extent of the puff is reduced relative to the puff in neutral surroundings. This reduction does not appear to commence until after the puff has reached its maximum penetration. Once the puff commences to rise however, the vertical extent decreases relative to the neutral case. The net result is that the volume of the puff in stable surroundings is reduced over that in neutral surroundings roughly by a factor of 2 by the time the equilibrium position is reached.

5.3 Energy Loss

A comparison can be made between the energy of a puff at the point of maximum penetration, and the energy of a similar puff in neutral surroundings at the same elapsed time. The time of maximum penetration t_m is read from the data for a stratified fluid in Fig. 4. The velocity of the puff in uniform fluid at the same time is computed numerically from the same figure. The ratio $\frac{\text{Kinetic Energy at } t_m}{\text{Initial Kinetic Energy}} = \frac{KE_{tm}}{KE_o}$ is simply the ratio of $\frac{\text{Velocity at } t_m}{\text{Velocity at } t_o}$, since momentum is conserved. Dividing the ratio plotted in Fig. 13 by the ratio above, for the same initial conditions, we obtain

$$\frac{PE_m}{KE_{tm}} = \frac{\text{Potential energy at maximum penetration}}{\text{Kinetic energy at same time in neutral surroundings}}.$$

These energy ratios are plotted in Fig. 20 as a function of reciprocal Richardson's number. Except near $1/R_i$ equal to 1100, where the ratio PE_m/KE_{tm} has a value approaching zero, the points are scattered with a mean value near to .8. As has been mentioned previously, in the experiment with high reciprocal Richardson's number, the puff dissipated rapidly, and was not observable for long. It may, therefore, have had a higher value of PE_m/KE_{tm} at $1/R_i$ equal to 1100 than is shown in Fig. 20. Since the values of potential energy were derived from a minimum expression (equation 15, page 44), it seems probable that the actual value of the ratio in Fig. 20 does not differ greatly from 1 over a large range of Richardson's number.

This approximate equality of energy content between a puff in neutral surroundings and one in a density stratification, at the time when the latter has become stationary, implies that they have lost nearly the same amount of energy to turbulent motions. This is rather surprising, in view of the fact that the velocities in the two cases have been considerably different as can be seen by the relative displacements in Fig. 4. This subject will be considered further in the next section.

5.4 Detailed Mixing

In Fig. 2, the detailed mixing curves for a puff penetrating neutrally buoyant and stable surroundings are plotted together to permit direct comparison. From the accuracy of

observation, as indicated by the standard deviation marked on the curves, and the number of observations taken, it is apparent that little distinction can be made between the two sets of results.

In equation 2, page 28, if w/w_o is replaced by its equivalent V_o/V, the equation is valid for stable as well as neutrally buoyant fluid, since we are no longer implying the conservation of momentum. The equation becomes,

$$\frac{dQ}{dt} = k(1-Q)\left[1 - \frac{V_o}{V}(1-2Q)\right] \qquad (23)$$

From the similarity between the mixing curves, (Fig. 2) we know that dQ/dt, (1-Q), (1-2Q) are not greatly different in the two cases. Also, since k is a function of the initial conditions which are the same, and of the turbulent energy available to mix the two fluids, which does not differ greatly at the point of maximum penetration, (Fig. 20) k must also be substantially unchanged. This implies that the ratio V_o/V is not greatly altered by the presence of the stratification.

We can infer from these facts, that the entrainment in the two cases has been substantially the same up to this time, and that the details of the mixing process have not been greatly altered by the presence of the density stratification.

6 DISCUSSION

6.1 Mixing Length

Mixing-length theories of turbulent transport processes

assume that a lump of fluid, when displaced, will retain its identity for a certain distance before mixing with its surroundings. They try to account for the transport process in terms of this mixing-length.

In assuming that observations of the behaviour of an isolated volume of fluid moving relative to quiet surroundings can lead to useful information on the behaviour of a turbulent fluid, we are implying that the mixing-length idea has more than a formal significance.

Mixing-length theories are among the first theories which attempt to account for diffusion in a turbulent fluid, and are discussed by Hinze (1959), who states (page 275): "A complete solution of the transport problem can be expected only if there is complete knowledge of the statistical functions describing the turbulent motion. As long as such a complete knowledge is lacking, any solution of the transport problem must be incomplete and, at best, approximate."

While no one believes that a mixing-length theory can be correct in detail, it has proven successful in yielding useful semiempirical relationships. More modern theories have not yet advanced to a stage where they can replace the mixing-length where practical answers are required.

6.2 Momentum Conservation and Ratio of Transfer Coefficients

In considering the motion of a moving puff in neutrally buoyant surroundings we have made use of the fact that the total momentum is constant in the absence of buoyant forces.

The total momentum involves the momentum of the injected and entrained fluid. If some of the entrained fluid does not mix with the injected fluid, it will not be visible in the experiment, and the momentum of the visible portion will be reduced.

A series of measurements of volume and velocity of the moving fluid were made. Volume measurements are difficult to make from a series of photographs, so the results serve only as a rough guide. From these measurements, the momentum in the visible moving puff was constant within 25 percent during the time the puff was visible. The measurements are not inconsistent with a constant momentum.

In determining an expression for the displacement of a puff in neutral surroundings, the assumption of a constant momentum was used. The agreement between this expression and the experimental points is shown in Fig. 12.

While the preceding two paragraphs indicate that the sharing of momentum is accompanied by mixing, a strict application of this principle would lead to difficulties. Equation 22, page 51, gives an expression for a density transfer coefficient for a displaced puff of fluid in stratified surroundings. If, in addition to being stratified, a uniform velocity gradient were present, the application of momentum sharing only by detailed mixing, would result in an identical expression for a momentum transfer coefficient. It appears therefore, either that a moving volume of fluid can lose some

momentum to its surroundings without mixing with them in any way, or that the difference between the transfer coefficients for density and momentum depend upon something more subtle than can be shown by the decay of a single puff.

Recent work (Ellison and Turner, 1960) indicates that, in uniform fluid, the ratio of the transfer coefficients K_H/K_M has a value near to 1.3. In a fluid with density stratification, K_H/K_M falls to small values. If we consider the possibility that a displaced volume of fluid can exchange momentum with its surroundings without mixing, the variations in K_H/K_M can be understood qualitatively.

Let C be the instantaneous average concentration of some property in a displaced fluid volume, and C_z the concentration of the same property in the surroundings at depth Z. Then C_z-C is the difference in concentration between the displaced fluid and its surroundings. If V is the volume of the displaced fluid, the total transport of the property by the puff will be given by $T = \int_0^L V(C_z-C)\, dZ.$ (24)
In (24) the integral is taken over the path of the puff to the point L where the puff comes to the average velocity of the surroundings.

If the concentration C is determined completely by mixing with the surroundings, then C will be a function of V and C_z, and will be the same for any property if we neglect molecular diffusion. If, as we are supposing to be the case with momentum, some means exists of reducing the difference

C_z-C without mixing, then with V having the same values as before, C_z-C will be smaller and T will be reduced. This would give a ratio for K_H/K_M greater than one.

In a density-stratified fluid where the displaced fluid will penetrate a certain distance and then reverse direction, dZ will change sign but C_z-C will not do so immediately. The sign of the integral will be reversed for a distance which will be greater as C_z-C is greater. It is easy to visualize a case in which the total value of the integral will be larger if C_z-C is relatively small. We can suppose that this is the case with momentum, giving small values to the ratio K_H/K_M as the stratification becomes great and mixing lengths reduced.

Examination of equation (20) and considering vertical momentum as the property being transported in a uniform fluid of the same density, we obtain $T = \int_0^L V(w_z-w)\,dz$, where w is the velocity of the puff and w_z is the velocity of the surroundings which is equal to zero in still surroundings. If momentum is conserved, the integrand in (20) becomes -Vw, a constant. The path of integration will have no limit and T becomes infinite.

We must conclude, therefore, that vertical momentum is not exactly conserved in the puff throughout its history. The expressions for velocity and displacement of a puff in uniform fluid of the same density obtained in sections 3.2 and 3.3 are then only approximately correct. The agreement of the data

with equations (8) and (9) as shown in Figs. 11 and 12, indicate that the assumption of momentum conservation in the puff is justified over the range of observation, where the momentum is apparantely large with respect to the losses. If it were possible to continue observations to longer times, the experimental points in Figs. 11 and 12 must fall below the straight lines indicated.

If vertical momentum is not conserved, it seems reasonable to assume that the horizontal momentum of a puff of fluid penetrating a region of variable mean horizontal velocity should not be determined entirely by the horizontal momentum in the fluid entrained. The difference in horizontal velocity between the puff and its surroundings will be less than calculated strictly by mixing, and the value of C_z-C in equation 20 therefore smaller when C refers to horizontal velocity than when it refers to a property such as temperature or salinity.

6.3 Turbulent Energy Dissipation

Some arguments on the effect of density stratification upon a turbulent fluid (Bolgiano, 1959) imply that the energy transfer from turbulent motions to density stratification occurs over all length scales of turbulence, and might form a considerable portion of the total loss of turbulent energy. In this case the total viscous dissipation would be considerably reduced. The results of the experimental work reported here, in particular Fig. 17, do not support this view.

Fig. 17 indicates that only about 3 percent of the total energy goes to potential energy of the stratification.

The observations of mixing rate indicate that the molecular mixing, which is closely associated with viscous dissipation, is much the same when the surrounding fluid is stratified and when it is not stratified. Observations of the puff show that it behaves as a unit which suggests that it is mixed to a fairly uniform density and that the smaller turbulent scales are not influenced to any great extent by the stratification.

In section 3.2 it was shown that the assumption of momentum conservation and similarity lead to an equation of the form

$$w^{-4/3} = ct, \tag{25}$$

where w is the velocity of the puff, t is the time, and c is an experimental constant.

In a turbulent fluid, if the Reynold's number is sufficiently large, the flow is independent of Reynold's number. The only factors which enter into the rate of turbulent energy decay will be the turbulent velocities and the scale of turbulence. Dimensional homogeneity then requires that the rate of decay of turbulent density will be given by

$$\frac{dw^2}{dt} \propto \frac{w^3}{L} \tag{26}$$

where w now represents turbulent velocities and L is a scale length.

To demonstrate that an isolated puff satisfies equation

(26), consider that the turbulent velocity is given by w in (25). A suitable scale length will be the radius R of the puff equal to $z \tan \alpha$ where z is penetration and α is the half angle of the cone of expansion of the puff. Integrating w in (25) to obtain z, and comparing $\frac{dw^2}{dt}$ with $\frac{w^3}{z \tan \alpha}$ we obtain,

$$\frac{dw^2}{dt} = 6 \tan \alpha \frac{w^3}{R}. \qquad (27)$$

The experimental value of α was near to 19° which makes $6 \tan \alpha$ equal to 2 approximately. The value of this constant depends upon what is chosen as a suitable scale length. The figure 2 is of the same order of magnitude but somewhat larger than is associated with a decaying turbulent field.

The foregoing remarks imply that if a turbulent field were built up of randomly oriented moving puffs of fluid such as have been studied in this experiment, it would have many of the properties actually found in a field of turbulence resulting from a shear flow. The results of a study of isolated puffs can perhaps be applied with some confidence to an actual turbulent flow.

6.4 Turbulent Energy Production

The production of turbulent energy per unit mass can be shown (Hinze 1960, page 65) to depend upon the term $- \overline{u_i u_j} \partial U_i / \partial x_j$. In a two dimensional case with mean flow U in the horizontal direction and a velocity gradient $\partial U / \partial z$ in the vertical direction, this becomes $- \overline{uw} \, \partial U / \partial z$ (28)

where the lower case letters refer to turbulent velocity components and the upper case to mean values.

Consider a steady state of turbulence established in a uniform fluid where the production is counter-balanced by diffusion, by loss to pressure fluctuations and by loss to viscosity. Now consider that a density gradient is set up. One effect of the density gradient, as has been shown by the experimental work (Sec. 4) is that the vertical motion w is partially reversed by buoyant forces. The partial reversal of w will result in partial reversal of the sign of (28), which will be greatly reduced. In addition, there will be a small but significant loss of turbulent energy to the density stratification (Sec. 4.4). Although the diffusion and viscous dissipation of turbulent energy will also be reduced, the net effect of the density stratification will be that the turbulent energy will establish a new equilibrium at a much reduced level.

It is possible to make a rough estimate of the effect of the density gradient upon the turbulent energy production if we assume that the stratification influences only the vertical motions. A figure representative of the total turbulent energy produced by a puff will be $-uz_n \partial U/\partial z$, where z_n is the net displacement of the puff, equal to the largest observed displacement in the case of a uniform surrounding fluid, and equal to z_{eq} (Sec. 4.2) in the case of a stratified fluid.

The ratio z_{eq}/z_n, which represents roughly turbulent

energy production in (stratified fluid/uniform fluid) varies from .1 when $1/R_i$ (Sec. 4.3) is equal to 30, to .8 when $1/R_i$ is equal to 1100.

6.5 Turbulent Scales

The scale of the turbulent motions are commonly described (Hinze 1960) by either a Lagrangian scale or an Eulerian scale. If $u_{(x')}$ is the velocity component of a particular particle of fluid at position x', and $u_{(x'+x)}$ is the velocity component of the same particle at some later time when the particle is at x'+x, then the Lagrangian scale is given by

$$\int_0^\infty \frac{\overline{u(x')\ u(x'+x)}}{\left(\overline{u^2_{(x')}}\right)^{\frac{1}{2}}\left(\overline{u^2_{(x'+x)}}\right)^{\frac{1}{2}}}\ dx \qquad (29)$$

where the integral is taken over a large number of realizations of the product average.

The Eulerian scale is given by an expression similar to (29) but the averages are taken over different particles at the same instant of time.

We are concerned here with particle movements along the axis of the puff, that is, in the vertical direction. In order to obtain an estimate of the ratio of Lagrangian scale/Eulerian scale, we will take the denominator of (29) in each case to be equal to $\overline{u^2_{x'}}$.

From equation (25), page 61, we can obtain an expression for w in terms of z,

$$w = az^{-3} \qquad (30)$$

where a is a constant.

Substitution of this value of w for u in (29) yields Lagrangian scale $= z_1^3 \int_{z_1}^{\infty} z^{-3}\, dz$, which, when evaluated is equal to $z_1/2$.

The Eulerian scale can be approximated by considering that as we measure instantaneous velocities in a puff the correlations will be high as long as measurements are made inside the puff. When the boundary is reached, the correlation will drop to zero. The Eulerian scale will therefore be approximately equal to R or to $z_1 \tan \alpha$ where α is the half angle of the cone of successive outlines of the puff and approximately equal to 19°.

The ratio Lagrangian scale/Eulerian scale is therefore approximately equal to 1.4.

The relationship between the Lagrangian and Eulerian scales is discussed by Corrsin (1959). Hinze (1960) (page 49) states that the two scales are roughly of the same magnitude.

No estimate of the expected accuracy of the results in terms of the errors in the measurement of the determining parameters has been given. As was stated in Sec. 4.3, page 44, the error in the results is dominated by statistical scatter. A significant improvement in accuracy can be achieved only by greatly increasing the number of observations.

7 SUMMARY AND CONCLUSIONS

Turbulent transport mechanisms in a density-stratified fluid have been studied by comparison of observations of a puff of fluid projected vertically downwards into a tank containing a stratified fluid, with similar observations of a puff penetrating a uniform fluid of its own density. The injected and tank fluids contained chemicals which produced a finely divided precipitate when mixing occurred on a molecular scale. Observation of this precipitate, both as to amount and position, permitted estimates of the detailed mixing process occurring between the injected and ambient fluid, and of the progress of the puff as a whole.

The results of the observations taken with a uniform surrounding fluid show that the velocity of the center of the puff obeys the relationship $w^{-4/3} = ct + \text{const.}$ after an initial period of orientation. This relationship can be obtained by assuming self-preservation of the puff, which means that a moving equilibrium is set up in which all velocities remain proportional.

From the variation of velocity and scale with time, the energy decay rate per unit mass is shown to be $\frac{dw^2}{dt} \propto \frac{w^3}{L}$ where L is a length typical of the puff. The same energy decay rate per unit mass holds in a turbulent fluid (Townsend, 1956). This implies that a fluid with a large number of randomly oriented puffs would have many features in common with a naturally turbulent fluid resulting from a shear flow, and

that calculations made on the basis of isolated puffs can be applied with some confidence to a turbulent fluid.

Since the puffs can be observed closely throughout their history, it is possible to determine the rate at which they mix with the surroundings, how this mixing proceeds inside the puff, and the details of motion of the puff as a whole. In a turbulent fluid, the effects of all scales of turbulence are superimposed, and turbulent velocities have all directions. Thus only the integrated effects of all scales and orientations can be observed.

For these reasons, it is possible to obtain estimates of detailed mixing and energy changes as a function of the determining parameters which can not be obtained from studies of a turbulent fluid directly. Numerical values for quantities useful in turbulence theory have thus been obtained which were previously unknown to an order of magnitude.

In order to display these values in the most general manner, they are expressed in terms of dimensionless ratios, and plotted against a dimensionless combination of the initial conditions which resembles the reciprocal of a Richardson's number. This number is given by $1/R_i = \frac{\rho_o w_o^2}{g \frac{\partial \rho}{\partial z} V_o^{2/3}}$. It can be thought of as the ratio of inertial forces to buoyant forces. In the experiment $1/R_i$ varies from 37 to 1140, changes in the initial velocity and volume being the principal cause of variation.

One quantity determined was the ratio of potential

energy of a puff at maximum penetration to the initial energy, which was found to vary from .2 at small values of $1/R_i$ to zero at $1/R_i$ equal to 1100 as is shown in Fig. 13. The order of magnitude of this ratio was not known previously.

Since, in a turbulent field, it is often possible to determine the turbulent energy, the knowledge of the energy ratio in the preceding paragraph permits an estimate of the distance a displaced volume of fluid may be from its equilibrium position.

Another quantity is the fraction of the initial energy which goes to altering the density gradient, shown in Fig. 17 as a function of $1/R_i$. Over a large range of $1/R_i$, this quantity shows no systematic dependence on $1/R_i$ and has a mean value of .03. No estimate of its magnitude has been obtained from studies of turbulent fluid. It has been suggested that a large portion of the energy in larger turbulent scales would be lost to the density structure since energy would be lost by all stages of the decay cascade. The evidence presented here demonstrates that this is not the case.

Values have also been obtained for the variation of density transport and turbulent energy production with the determining parameters. This variation agrees in kind with what is known from studies of turbulent fields. The agreement in these cases gives added confidence to the application of isolated puff observations to a turbulent field.

A number K_H' representative of the density transport

due to a single displaced blob of fluid was computed. K_H' was made dimensionless by division by $V_o^{2/3}$, and is plotted as a function of $1/R_i$ in Fig. 18. $K_H'/V_o^{2/3}$ varies from 1 for $1/R_i$ equal to 30, to 35 for $1/R_i$ equal to 1100. To the accuracy obtained, the variation is linear over this range. Density transport estimations for a turbulent fluid are known to vary in a similar manner.

An estimate was obtained of the effect upon the production of turbulent energy of the sudden application of a stratification of density upon a turbulent field. A comparison of the equilibrium depth of a puff in a stratified fluid with the maximum penetration of a similar puff in uniform fluid gives a measure of the relative production. The ratio varies linearly with $1/R_i$ from .1 at $1/R_i$ equal to 35 to .8 at $1/R_i$ equal to 1200. It is known that the presence of a density stratification will cause a great reduction of turbulent energy density in a given shear flow.

An estimate of the detailed mixing between the injected and surrounding uniform fluid was obtained by removing volume and concentration effects from the observed rate of formation of precipitate. For each set of initial conditions, the detailed mixing per unit volume of the puff can be represented by a single number k, (eq. 2, p. 28) which varies by less than 10% of its mean value from the time of initiation until the time the chemical reagents are exhausted (1 to 7 sec.). The values of k were found to depend upon the initial

conditions of velocity, length and viscosity according to the relationship $k = .0050\nu^{-1/2}w_o^{3/2}L_o^{-1/2}$.

The detailed mixing in a stratified fluid was found to be unchanged from that in a uniform fluid within the experimental error.

Comparison of the horizontal width of a puff in a stratified fluid with the width of a similar puff in uniform fluid shows that there is no significant difference in the spreading rate in the two cases. The vertical kinetic energy which the puff loses to potential energy is returned to vertical energy or to the alteration of the density structure and does not enhance the horizontal spreading rate. It has been suggested, (Parr, 1936) that horizontal turbulence is increased by the presence of a stratification. The observations do not support this view.

A comparison has been made between the potential energy of a puff at maximum penetration in a stratified fluid and the kinetic energy of a similar puff at the same time after initiation, but in a neutrally buoyant fluid. The results in Fig. 20 show that over the range of $1/R_i$ from 30 to 500 this ratio has a mean value of 0.8, not greatly different from 1. The value of zero shown at $1/R_i$ equal to 1100 must be regarded with suspicion. In this case the puffs were not observed to rise from the point of maximum penetration. A slight unobserved rise would yield a value for the energy ratio. Since, for large $1/R_i$ due to a very small density gradient, the

surroundings would be nearly identical in the two cases, the energies should also approach equality.

The expression used to deduce the potential energy yielded a minimum value. It therefore seems probable that the ratio does not differ significantly from 1 over the whole range. This indicates that the loss of energy to turbulence has not been greatly altered by the stratification up to this time in the history of the puff.

The fact that a puff in stratified fluid retains a definite shape, does not break up into separate portions, and particularly, the reduction in vertical extent when it finally stops, indicate that it has a nearly uniform density structure compared with the surroundings.

This uniformity of density structure inside the puff together with the observed similarity in the detailed mixing of a puff with uniform and stratified surroundings, indicates that all conditions inside the puff are little influenced by the stratification. The equality in the horizontal spreading rate and the equality of the energy of the puff as a whole in uniform and in stratified fluid are consistent with this concept.

We can conclude therefore that the effect of the density stratification is principally upon the initial (large) turbulent scales in which turbulent energy is produced, and only slightly upon the small scales in which turbulent energy decays.

8 APPENDIX

A graphical method of finding an approximate power law relationship between 3 variables was used initially on the data for V_o, w_o, and k. It may be of interest, and will be described below.

If three variables A, B, and C are related by

$A = mB^{\alpha} C^{\beta}$, where m is a constant, then

$\text{Log } A = \log m + \alpha \log B + \beta \log C$, or

$A = m' + \alpha B' + \beta C'$, where the prime indicates a logarithm. The linear relationship between A', B', and C', defines a plane, and the power law relationship between A, B, and C, also defines a plane in space where the distances are proportional to logarithms of the variables. It is desired to find the traces of this plane on two orthogonal planes, one where B is constant and other where C is constant. The slopes of these traces will give the values of β and α respectively. Use is made of the principles or orthographic projection. Any two sets of experimental points determine one point on each trace. If the experimental data obey a power law, all the trace points will lie on a line, or nearly so.

For two sets of experimental points, the method of finding the two trace points is illustrated in Fig. 9.

Let the experimental points be A_1, B_1, C_1 and A_2, B_2, C_2, represented by open circles in Fig. 9. The line x--x indicates the intersection of the B = constant plane and the C = constant plane. It can be chosen in any convenient position.

The directions of increasing A, B, and C, as shown are convenient so that ordinary log-log paper can be used. Any origin for A, B, C, = 1 may be chosen. B and C = 1 may be coincident if desired. The marked points, (open circles) are the projections of the data points on these two orthogonal planes. It is necessary to know which plane, therefore the projections must be labelled as A_1B_1 if on the B = constant plane, or as A_1C_1 if on the C = constant plane. To fine the trace of the line defined by $A_1B_1C_1$ and $A_2B_2C_2$ on the C = constant plane, join A_1B_1 and A_2B_2 and produce to intersect the x--x line at O. Erect a perpendicular to x--x at O to intersect A_1C_1, A_2C_2 produced at P. P, represented by a solid circle, is the required trace point. The trace point Q, on C = constant, is found similarly, as shown on the diagram. It is represented by an open triangle.

For the experimental data in Table 6, page 39, a plot of the points made in this manner, and the traces of the planes determined by all possible pairs of points is shown in Fig. 8. (Some of the trace points lie off the paper, as do some of the experimental points).

The relation $k = m\, w_o^{1.53}\, V_o^{-.55}$ is shown by the dashed line. The relation $k = m\, w_o^{1.5}\, V_o^{-.5}$, is shown by the solid line. In each case the intersection of the two traces must lie on the x--x line. This point was chosen by eye to give the best fit.

REFERENCES

Batchelor, G. K., (1953). The theory of homogeneous turbulence. Cambridge University Press.

Bolgiano, R. Jr., (1959). Turbulent spectra in a stably stratified atmosphere. Jour. Geophys. Res., 64, 12.

Corrsin, S., (1959). Lagrangian correlation and some difficulties in diffusion experiments. Advances in Geophysics, 6.

Ellison, T. H., (1956). Atmospheric Turbulence. Surveys in mechanics. Camb. Univ. Press.

Ellison, T. H., (1957). Turbulent transport of heat and momentum from an infinite rough plane. Jour. of Fluid Mech., 2, 5, pp. 456.

Ellison, T. H. and Turner J. S., (1960). In press Jour. Fluid Mech.

Grant, H. L., Moilliet, A., Stewart, R. W., (1959). A spectrum of turbulence at very high Reynold's number. Nature 811, pp. 808.

Handbook of Chemistry and Physics, (1948). Chemical Rubber Publishing Co., Cleveland, Ohio.

Hinze, J. O., (1959). Turbulence. McGraw-Hill.

Keulegan, G. H., (1949). Interfacial instability and mixing in stratified flows. Jour. of Research, 43; 487-500.

Moelwyn-Hughes, (1957). Physical Chemistry. Pergamon Press, p 1128 and 1260.

Northrup, E. F., (1911). Experimental study of vortex motions in liquids. Franklin Inst. Jour., 172, pp 211-216.

Parr, A. E., (1936). On the possible relationship between vertical stability and lateral mixing processes. Conseil Perm. Internat. p. l'Explor. de la Mer, Journal du Conseil, v.11, p. 308-313.

Patterson, A. M., (1958). Turbulence spectrum studies in the sea with hot wires. Limnology and Oceanography III, 2, p. 171-180.

Patterson, A. M., (1960). Hot wire turbulence measurements in a tidal channel. (P.C.C. D12-95-20-08). Pacific Naval Laboratory, Esquimalt, B. C.

Revelle, R. and Fleming, R. H., (1934) as discussed in The Oceans, Prentice Hall. 1942.

Richardson, L. F., (1920). The supply of energy from and to atmospheric eddies. Proc. Roy. Soc. London, A, 97: 354-373.

Richardson, L. F., (1925). Turbulence and vertical temperature difference near trees. Phil. Mag., 49: 81-90.

Scorer, R. S., (1957). Experiments on convection of isolated masses of buoyant fluid. Jour. Fluid Mech. 2, 583.

Scorer, R. S., (1958). Natural Aerodynamics, Pergamon Press.

Stewart, R. W., (1959) (a). The problem of diffusion in a stratified fluid. Atmospheric Diffusion and pollution, Advances in Geophysics, 6, 303-311.

Stewart, R. W., (1959) (b). The natural occurrence of turbulence. Jour. Geophys. Res., 64, 12, 2112-2115.

Sverdrup, H. U., Johnson, M. W. and Fleming, R. H., (1942). The Oceans, Prentice Hall.

Taylor, G. I., (1927). An experiment on the stability of superposed streams of fluid. Proc. Camb. Phil. Soc., 23, 1927, pp. 730-731.

Taylor, G. I., (1931). Internal waves and turbulence in a fluid of variable density. Conseil. Perm. Intern. pour l'Expl. mer, Rapp et Proc. Verb., 76: 35-43.

Townsend, A. A., (1956). The structure of turbulent shear flow. Cambridge Univ. Press.

Townsend, A. A., (1958). Turbulent flow in a stably stratified atmosphere. Jour. Fluid Mech., 3, 4, pp. 361-372.

Turner, J. S., (1957). Buoyant vortex rings. Proc. Roy. Soc. A., 239, pp. 61-75.

Zworykin, V. K. and Ramberg, E. G., (1949). Photoelectricity. John Wiley & Sons, New York.

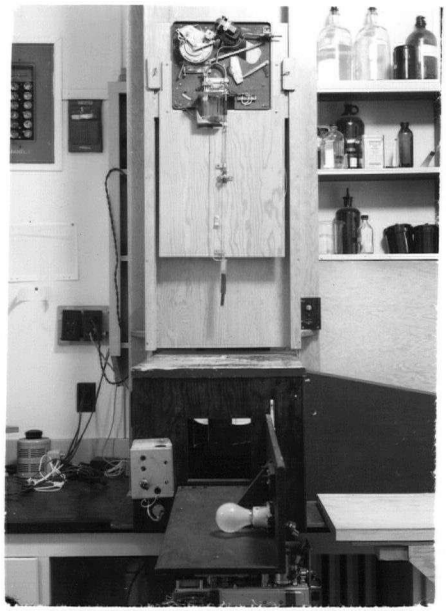

a.

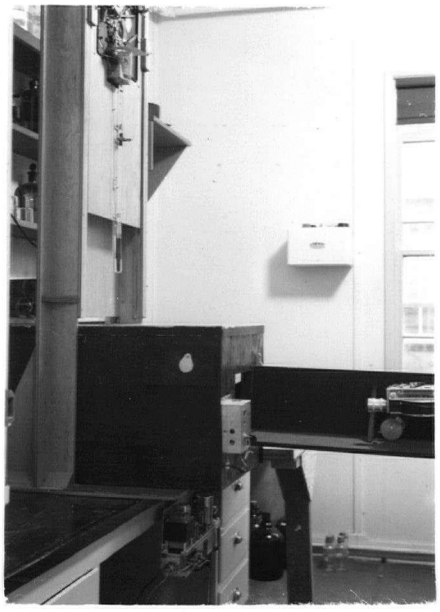

b.

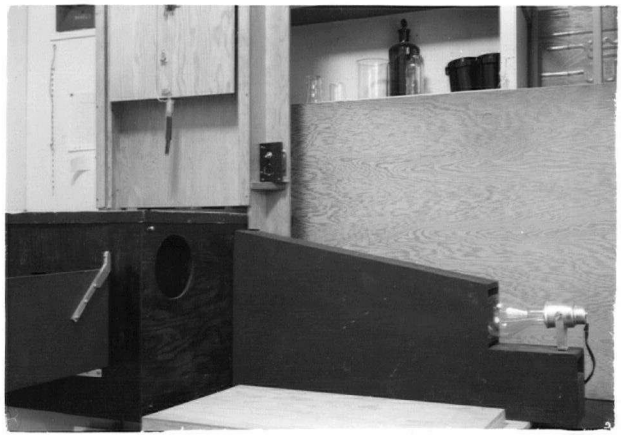

c.

d.

PLATE I

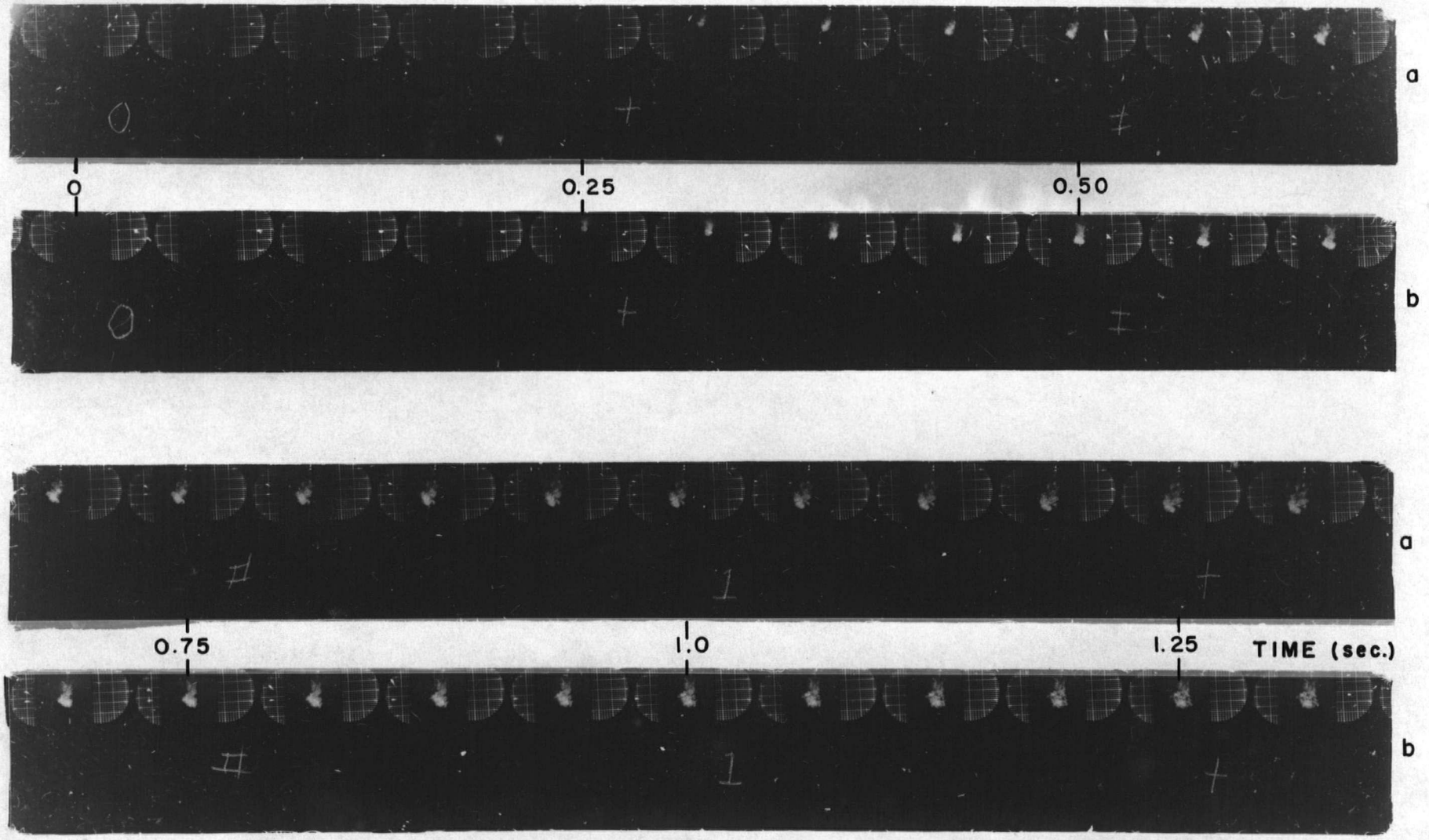

Plate II

REPRESENTATIVE SERIES OF PHOTOGRAPHS OF A PUFF

a. In Uniform Fluid

b. In Stratified Fluid

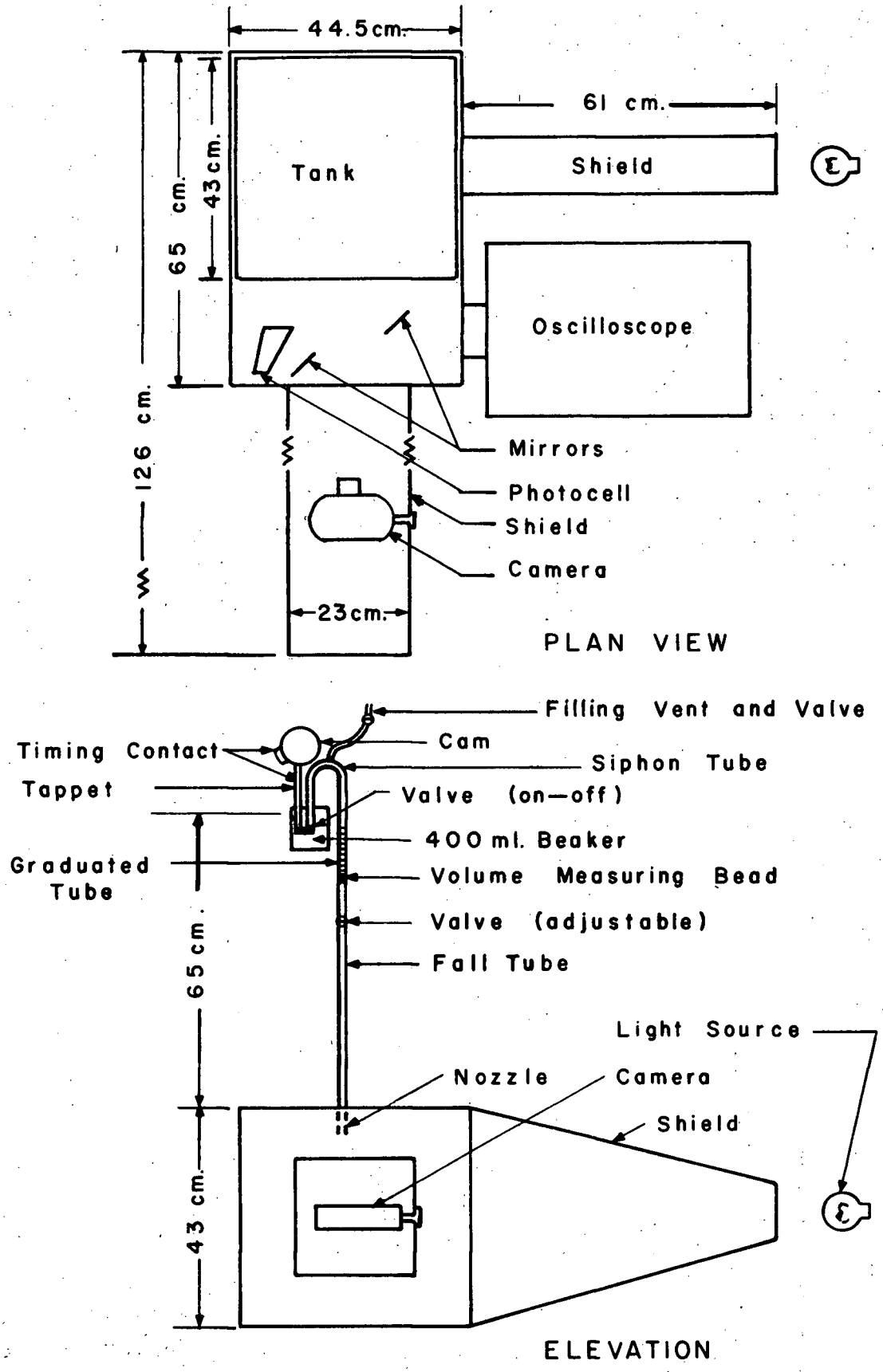

Fig. 1 APPARATUS

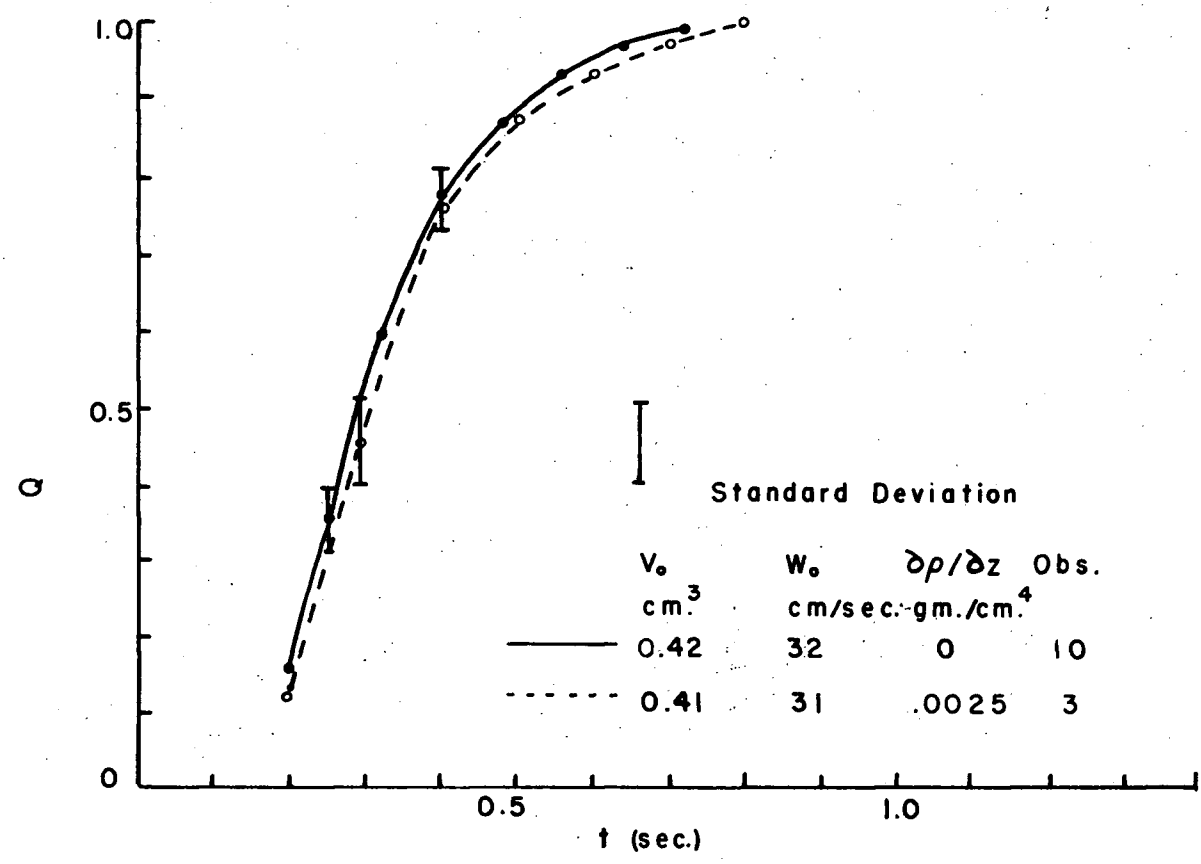

Fig. 2a

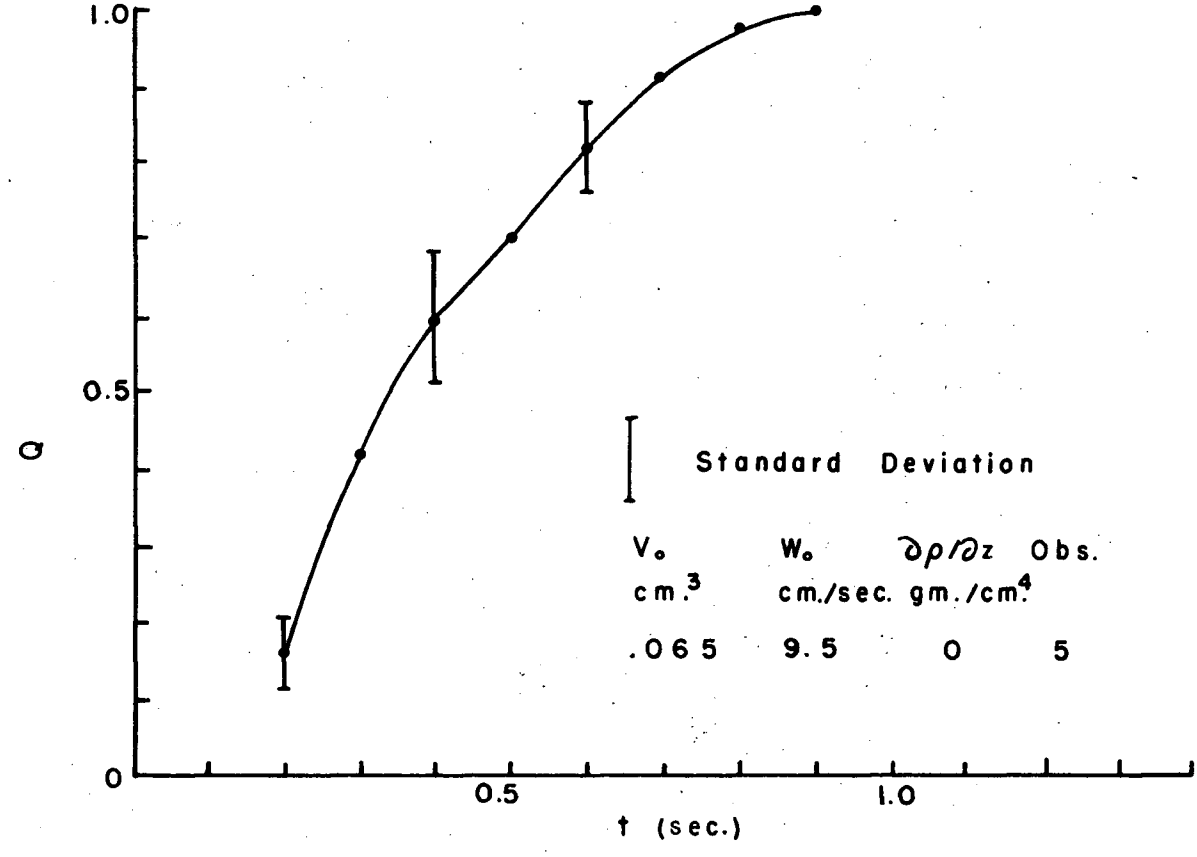

Fig. 2b DETAILED MIXING

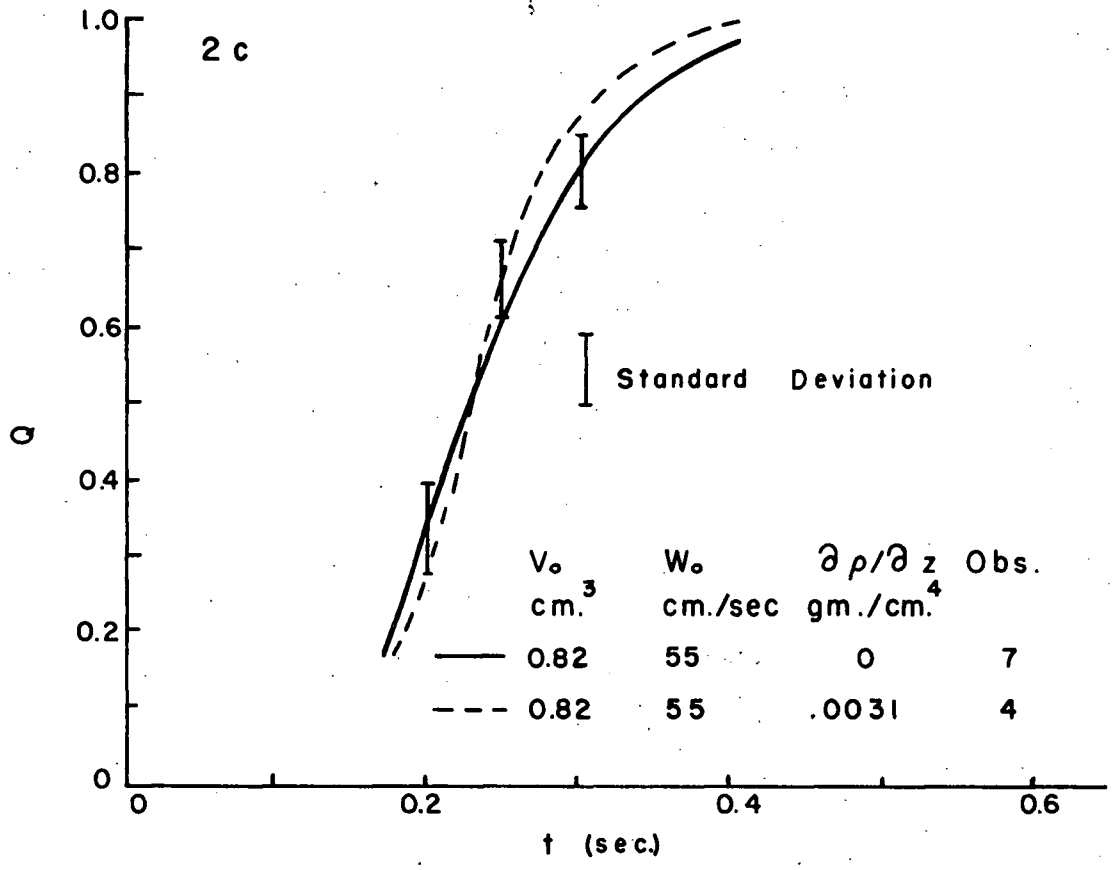

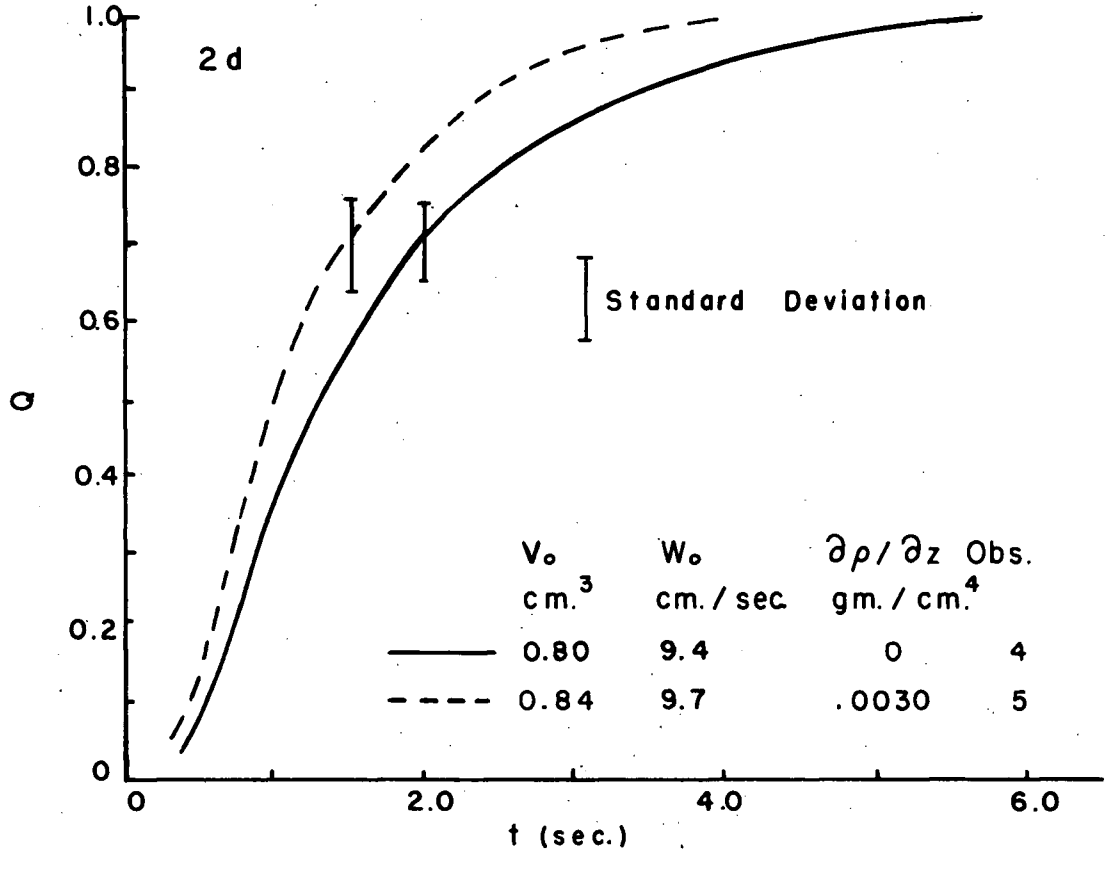

Fig. 2 DETAILED MIXING

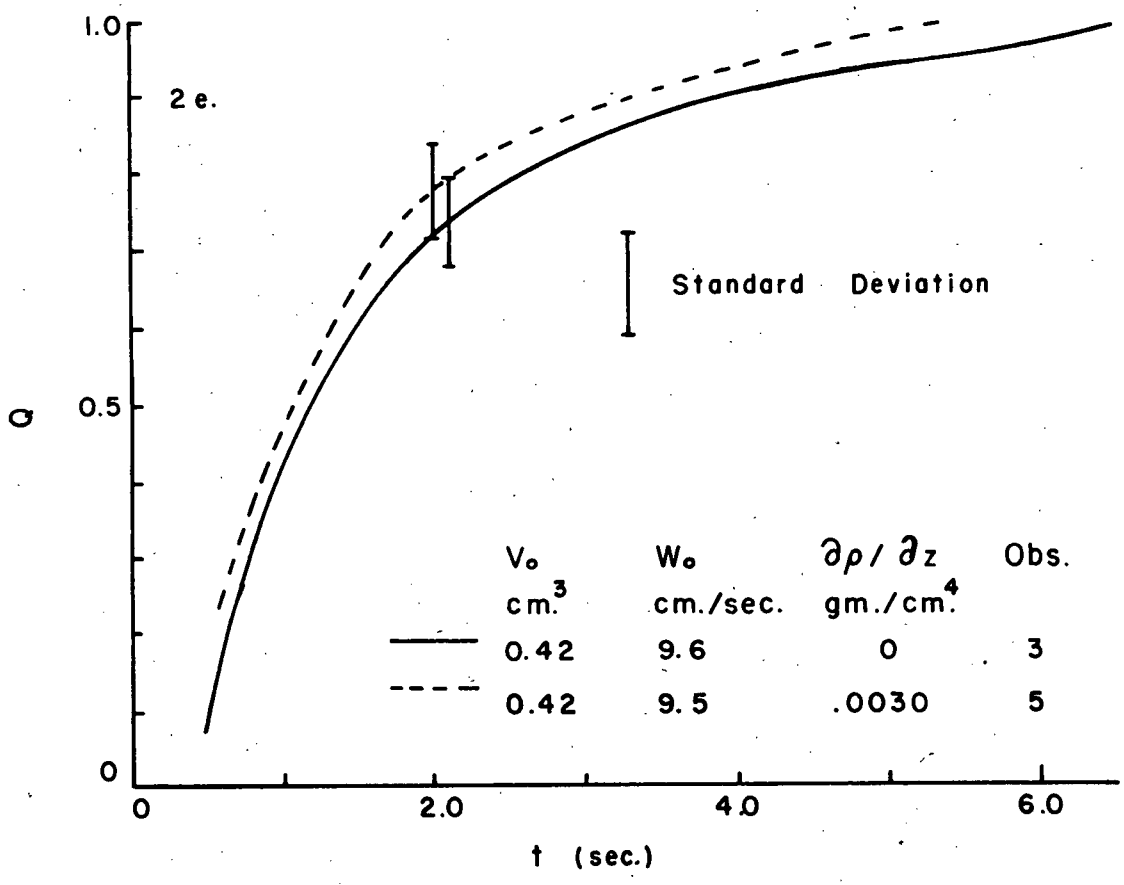

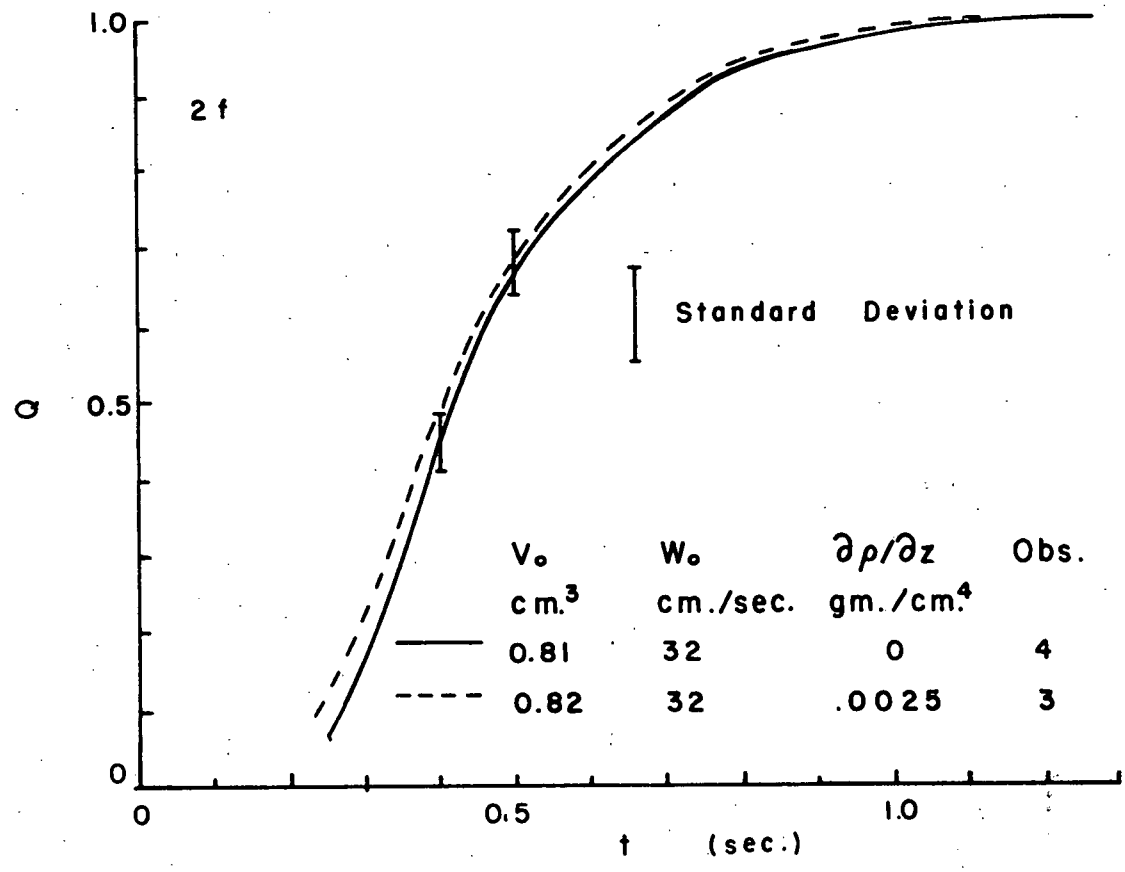

Fig. 2 DETAILED MIXING

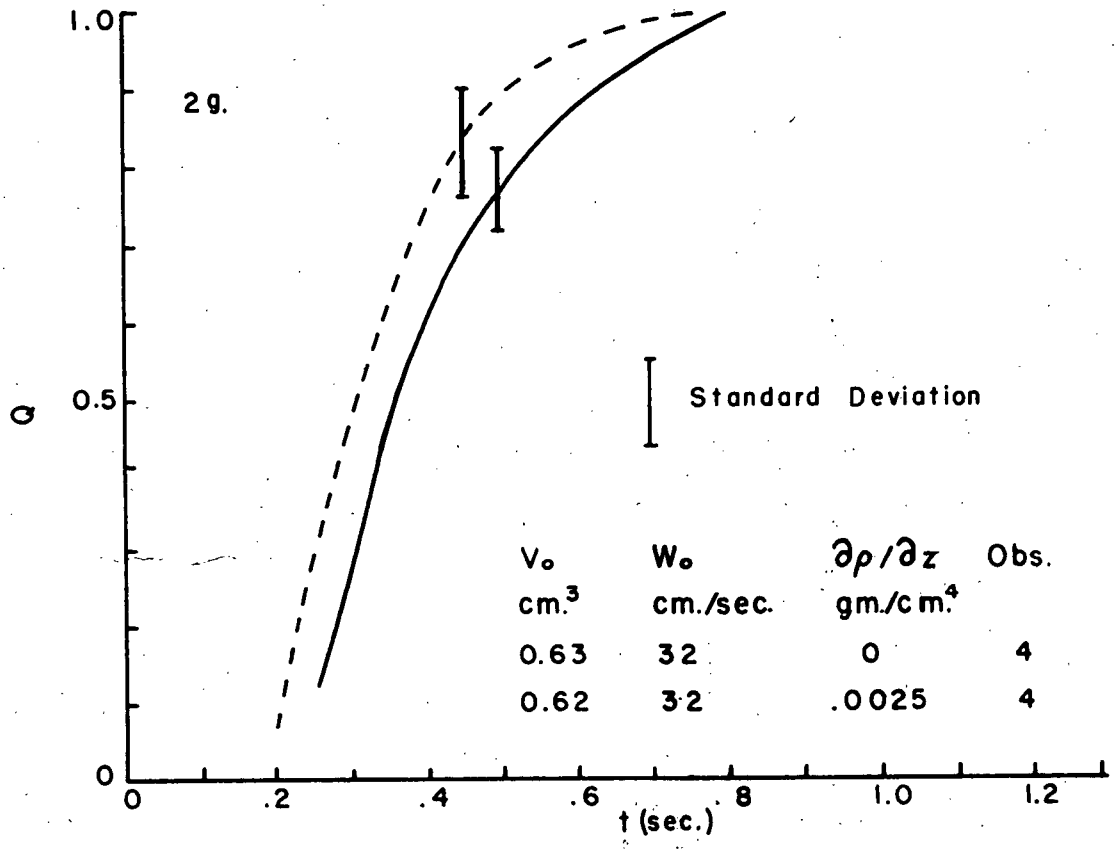

Fig. 2 DETAILED MIXING.

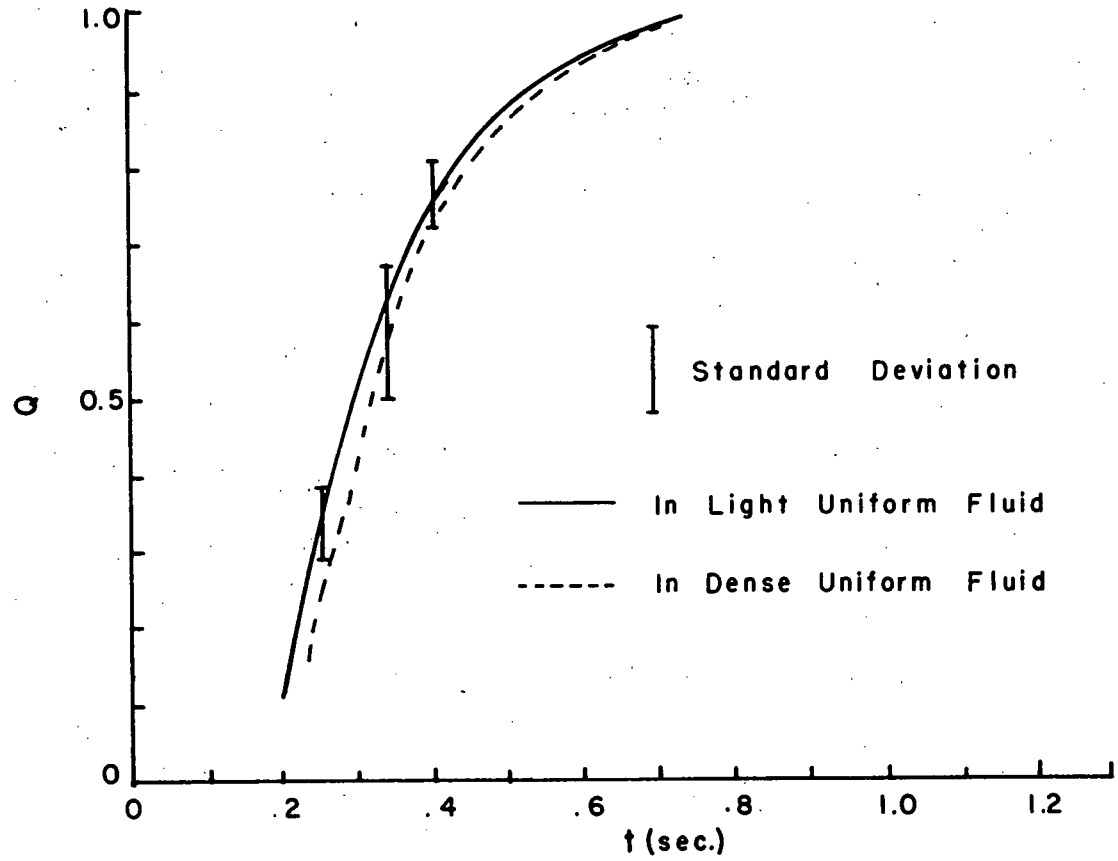

Fig. 3 EFFECT OF SALT UPON MIXING DATA

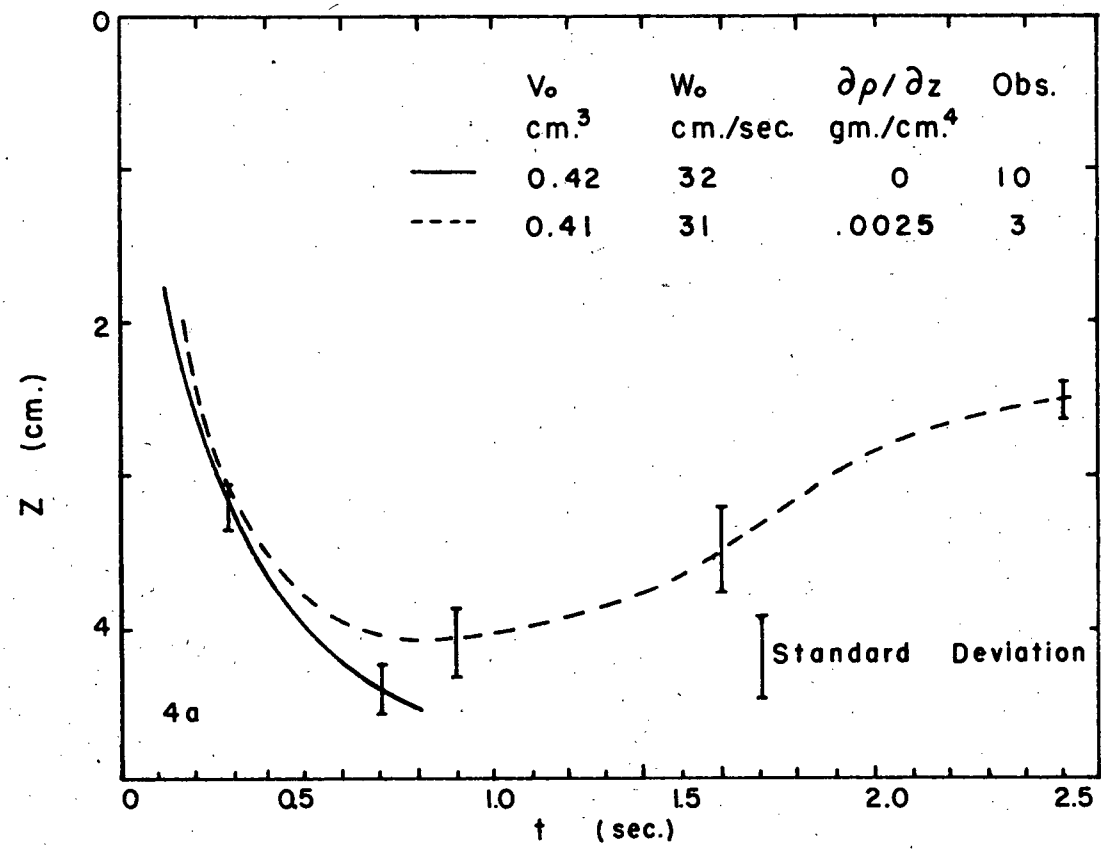

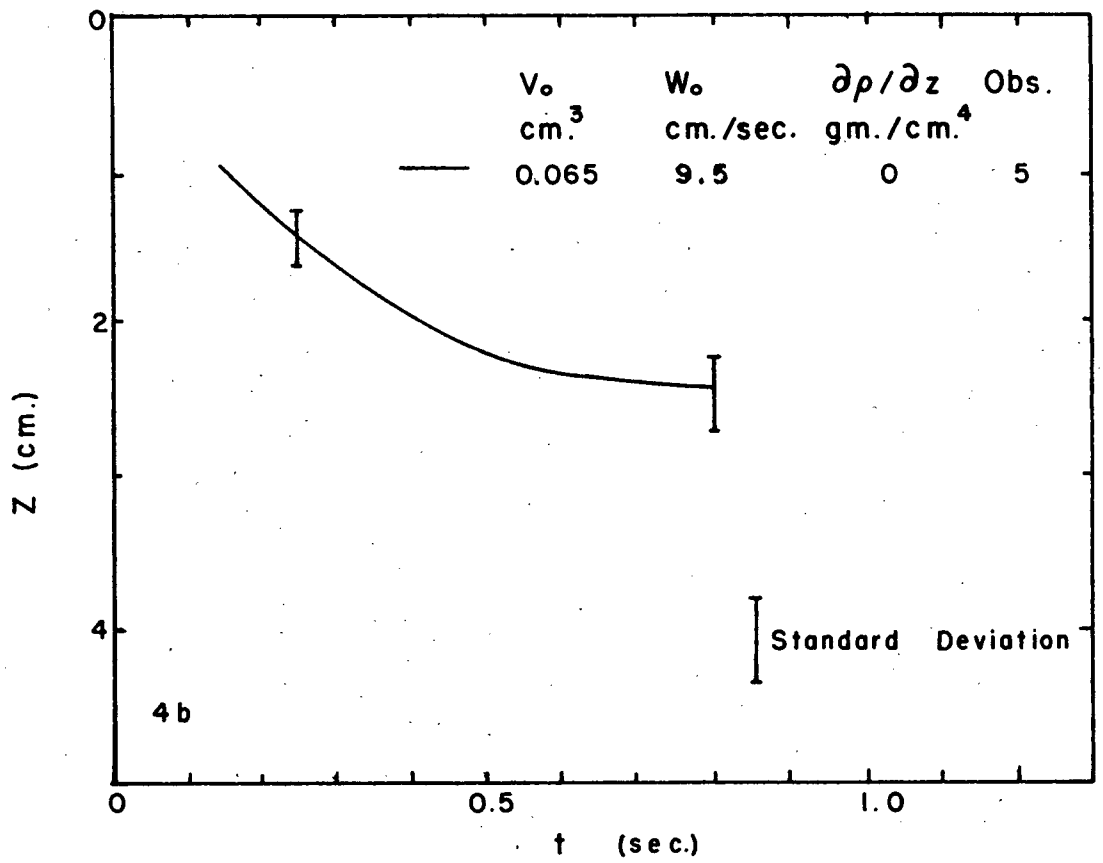

Fig. 4 CENTER DISPLACEMENT

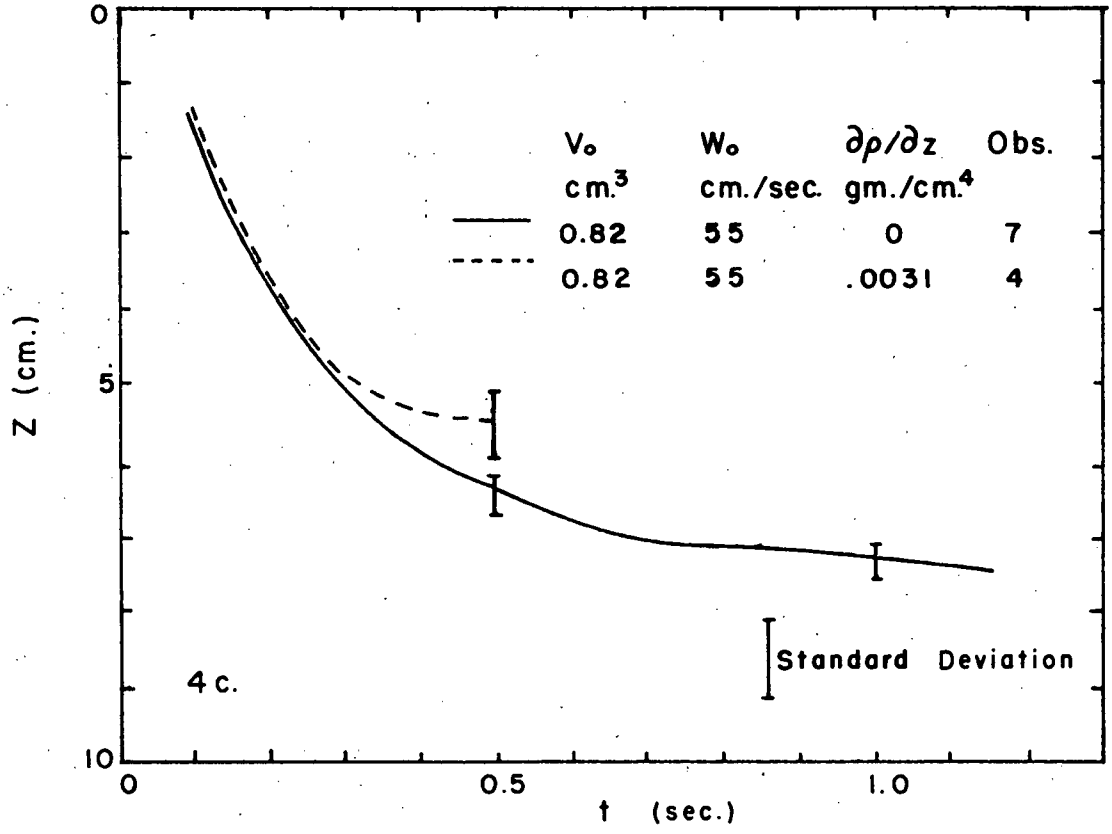

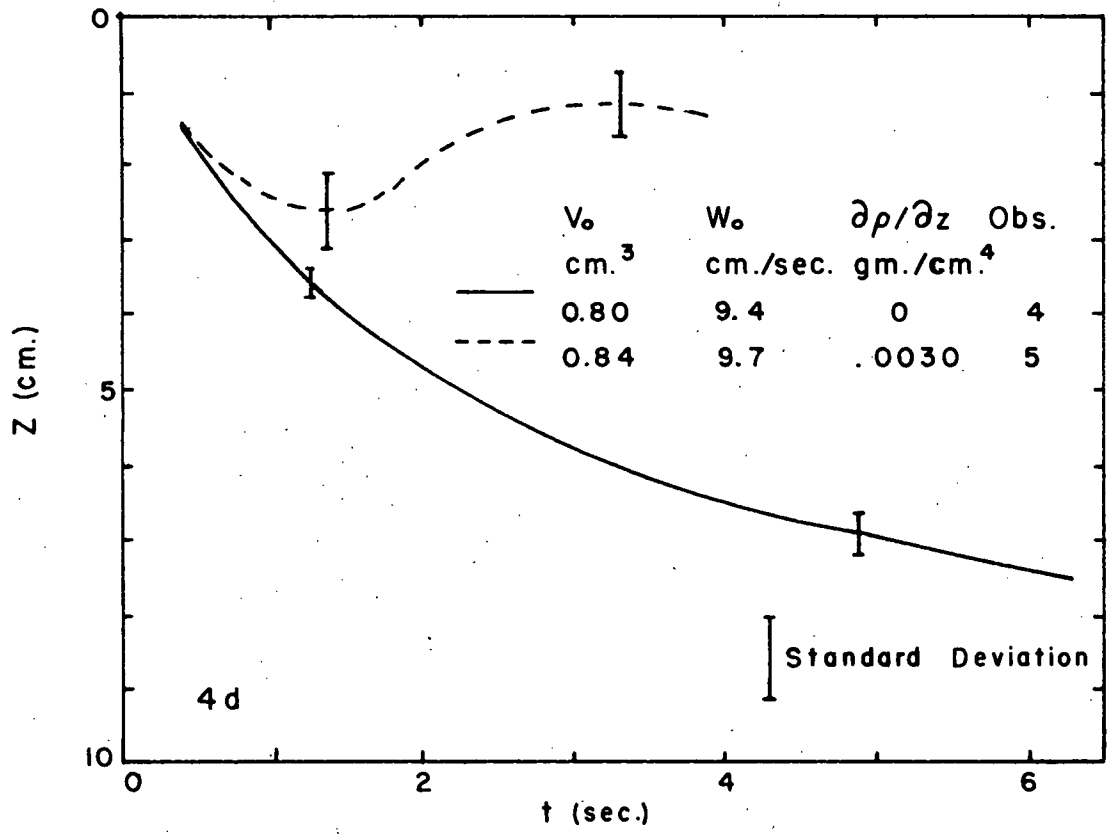

Fig. 4 CENTER DISPLACEMENT

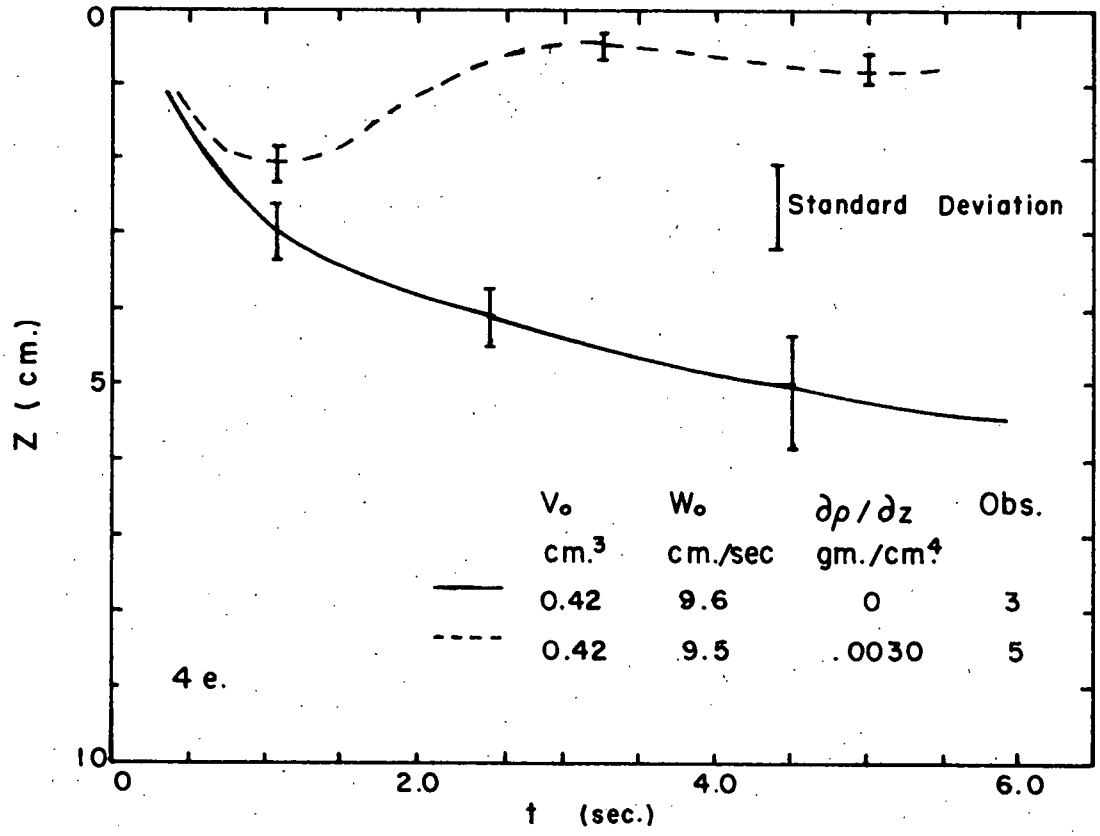

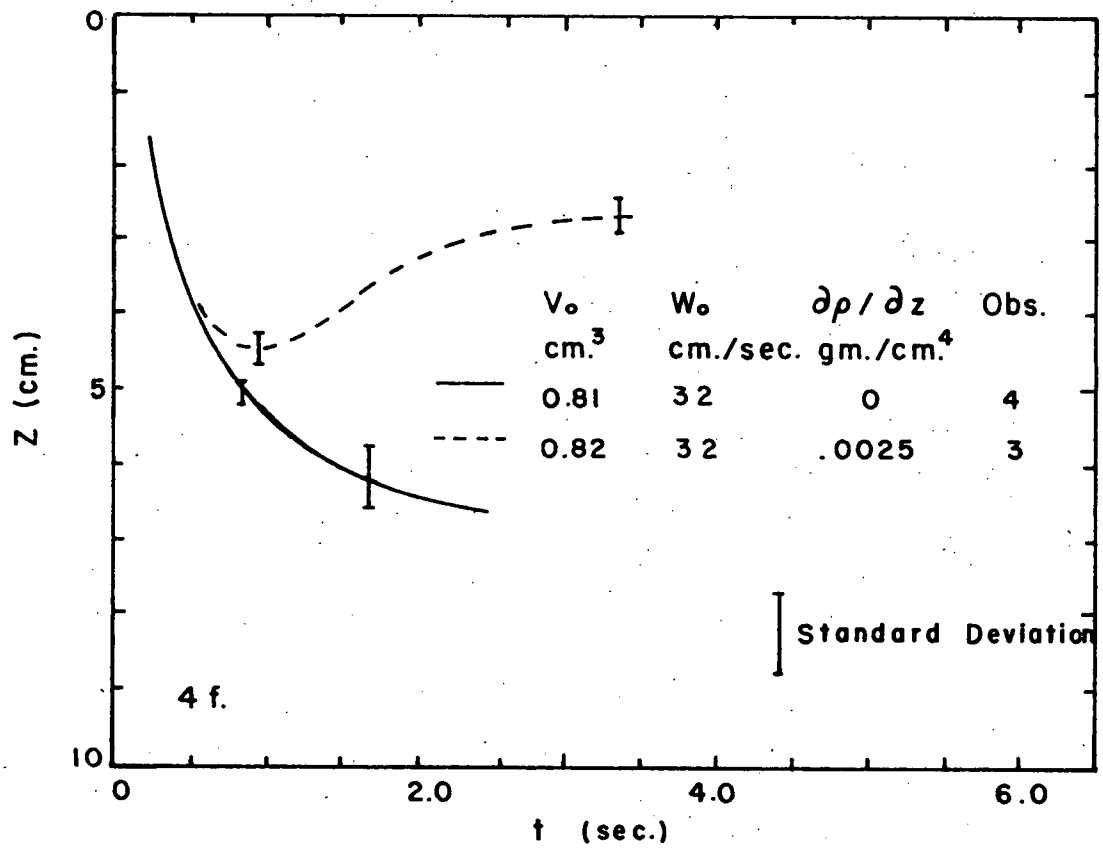

Fig. 4 CENTER DISPLACEMENT

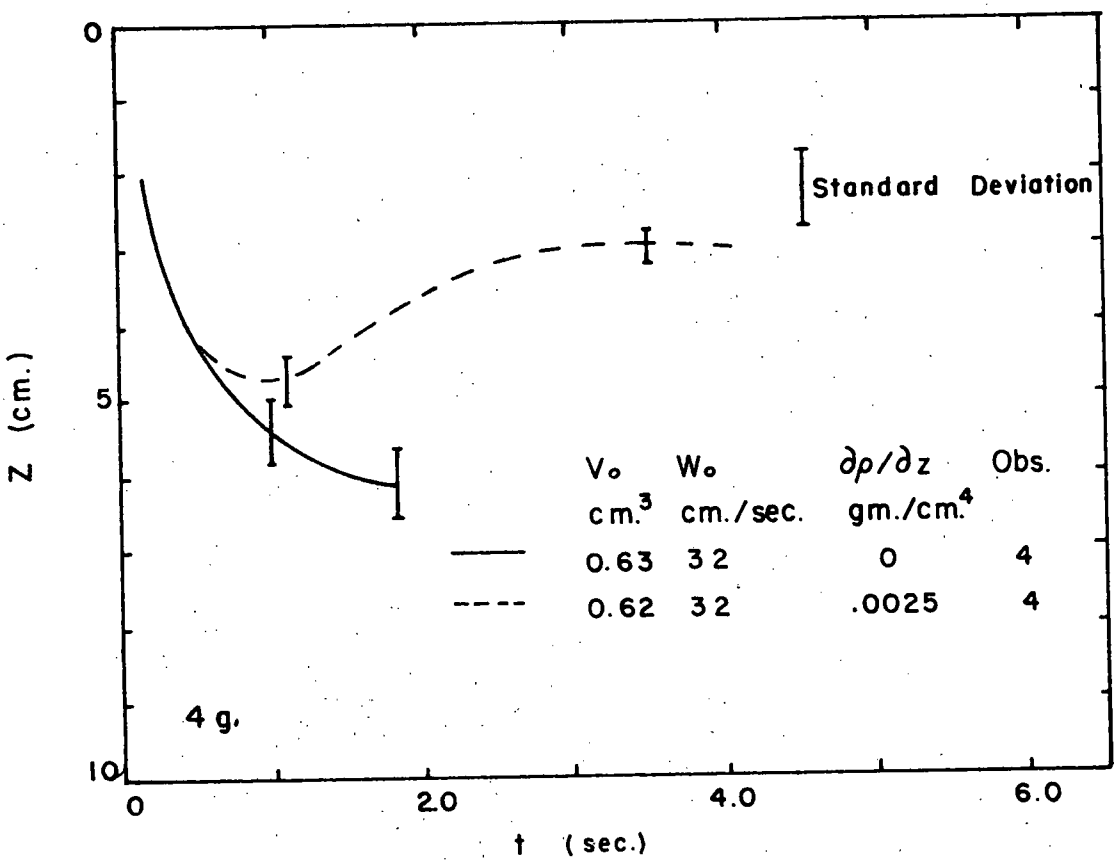

Fig. 4 CENTER DISPLACEMENT

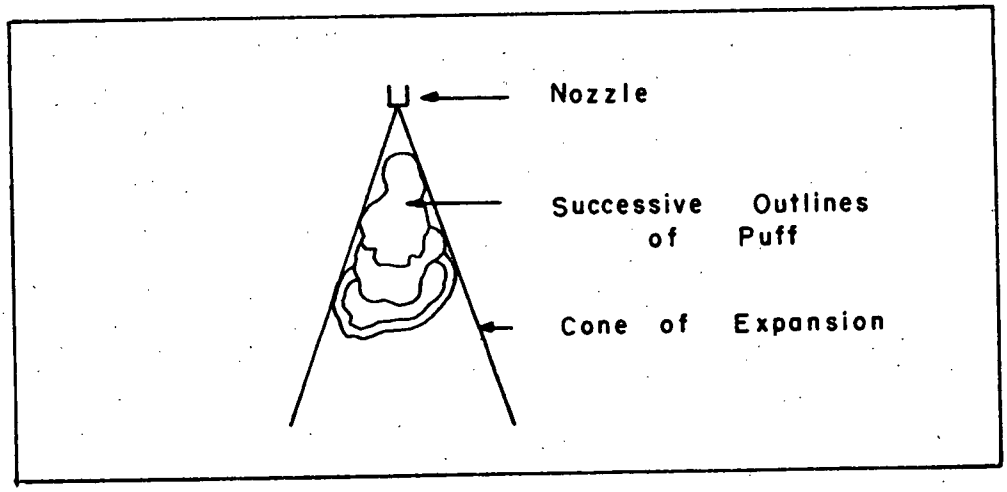

Fig. 5 HORIZONTAL SPREAD IN UNIFORM FLUID

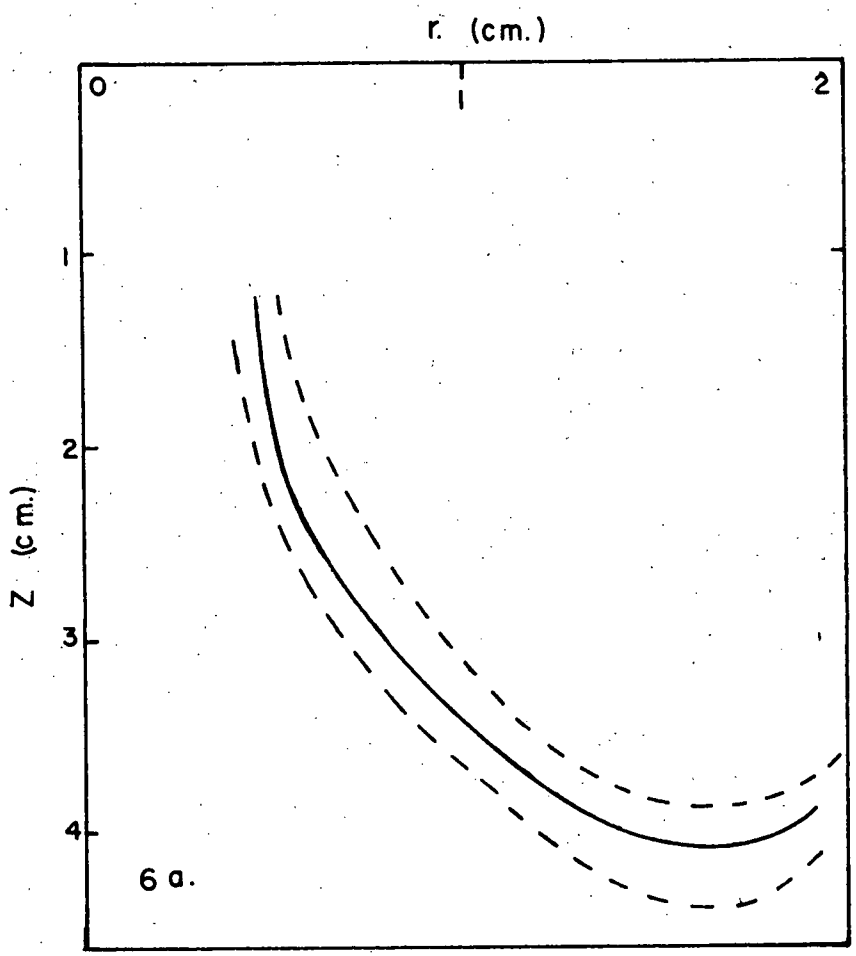

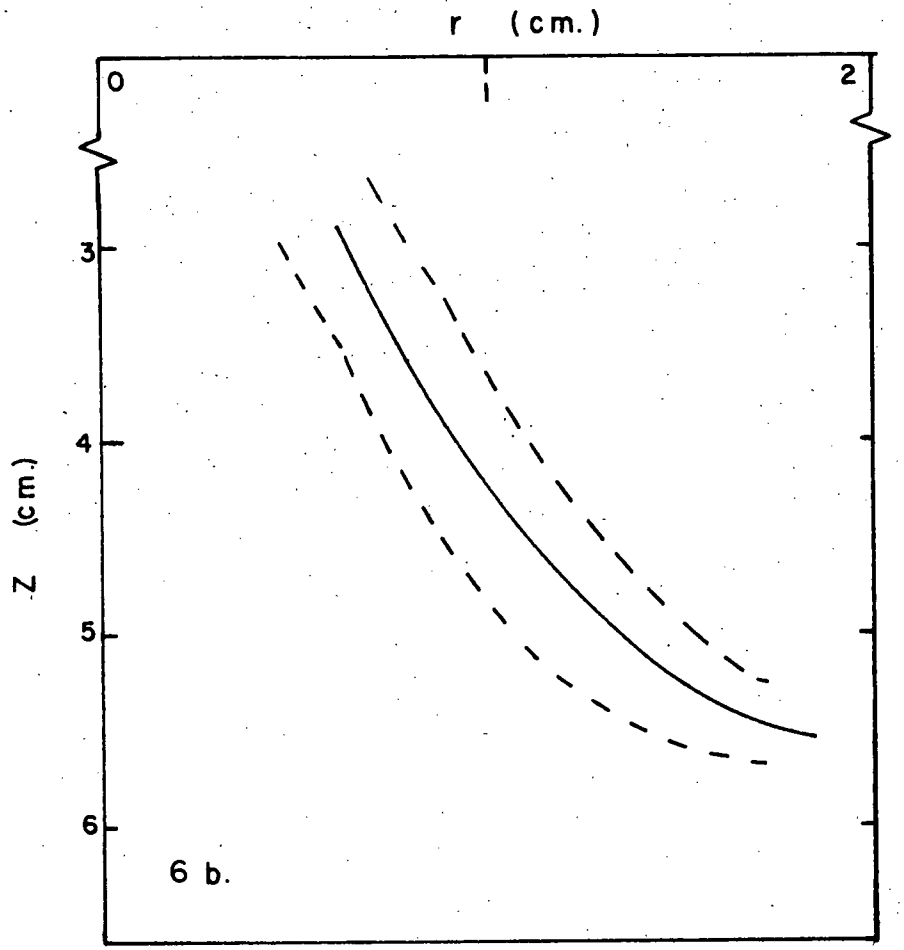

		a	b
V_o	$cm.^3$	0.41	0.82
W_o	cm./sec.	31	55
$\partial\rho/\partial z$	$gm./cm.^4$	.0025	.0031
Obs.		3	4

---- Extremeties of Plotted Points

—— Fitted Line

Fig. 6 HORIZONTAL SPREAD IN STRATIFIED FLUID

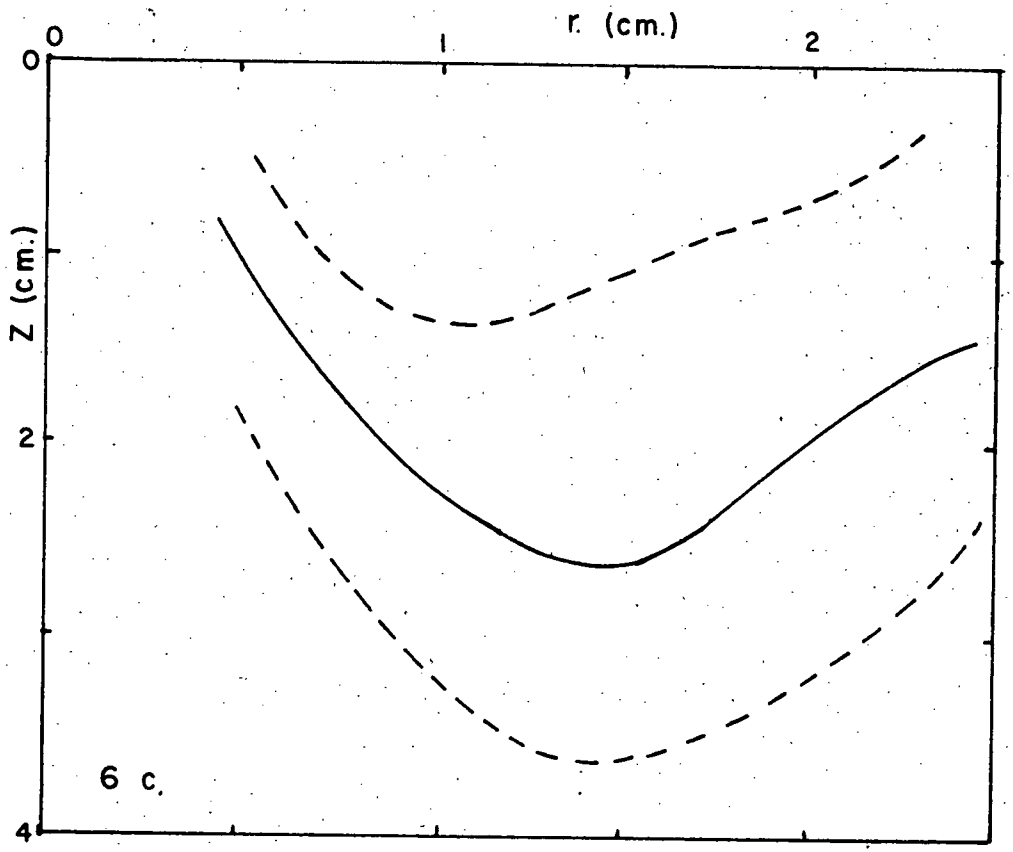

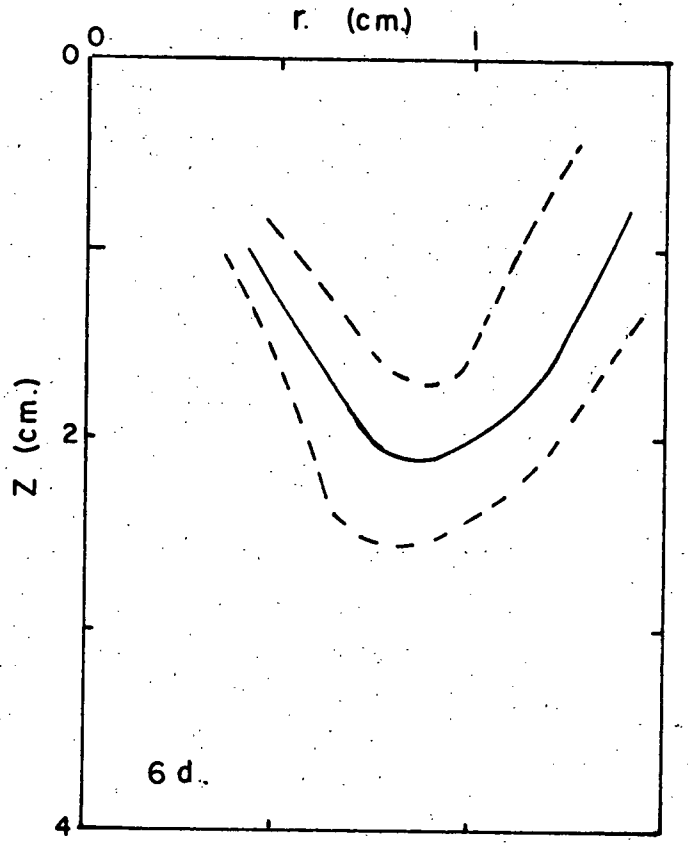

---- Extremeties of Plotted Points

—— Fitted Line

		c	d
V_o	$cm.^3$	0.84	0.42
W_o	cm./sec.	9.7	9.5
$\partial\rho/\partial z$	$gm./cm.^4$	.0030	.0030
Obs.		5	5

Fig. 6 HORIZONTAL SPREAD IN STRATIFIED FLUID

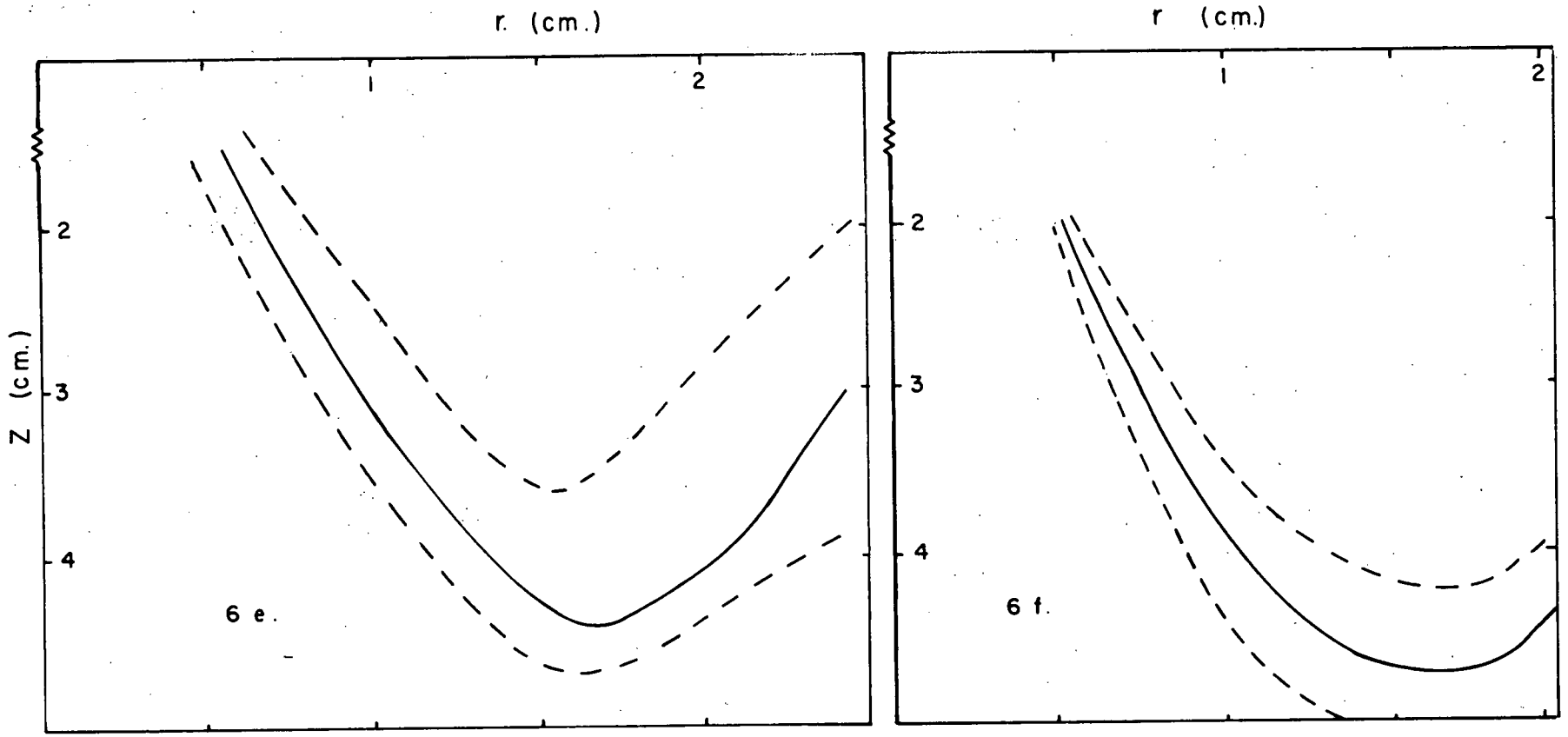

		e	f
V_o	$cm.^3$	0.82	0.62
W_o	cm./sec.	32	32
$\partial\rho/\partial Z$	$gm./cm.^4$	.0025	.0025
Obs.		3	4

-----Extremeties of Plotted Points

——— Fitted Line

Fig. 6 HORIZONTAL SPREAD IN STRATIFIED FLUID

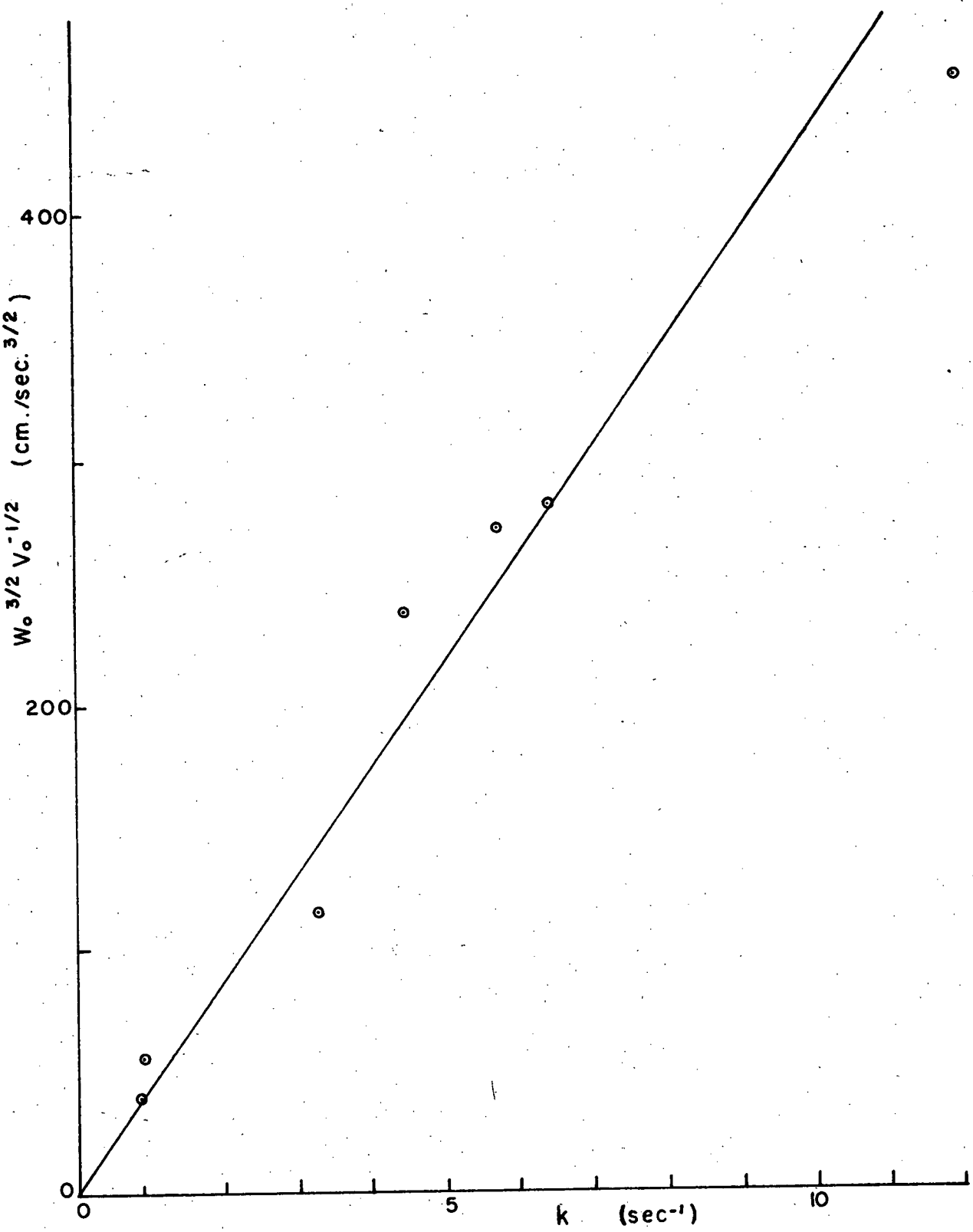

Fig. 7 DEPENDENCE OF MIXING FUNCTION k UPON THE INITIAL CONDITIONS

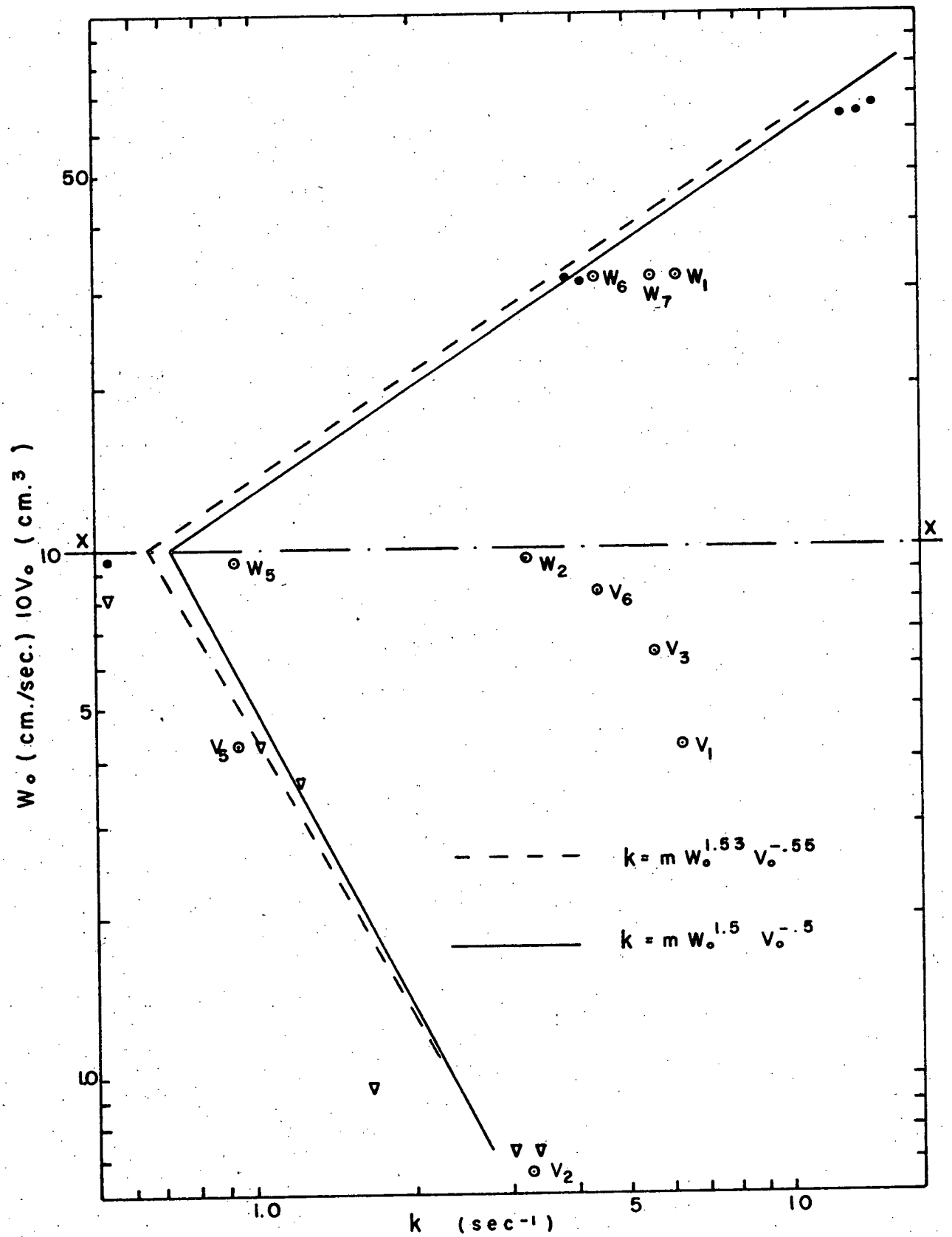

Fig. 8 3-DIMENSIONAL PLOT OF k AGAINST THE INITIAL CONDITIONS

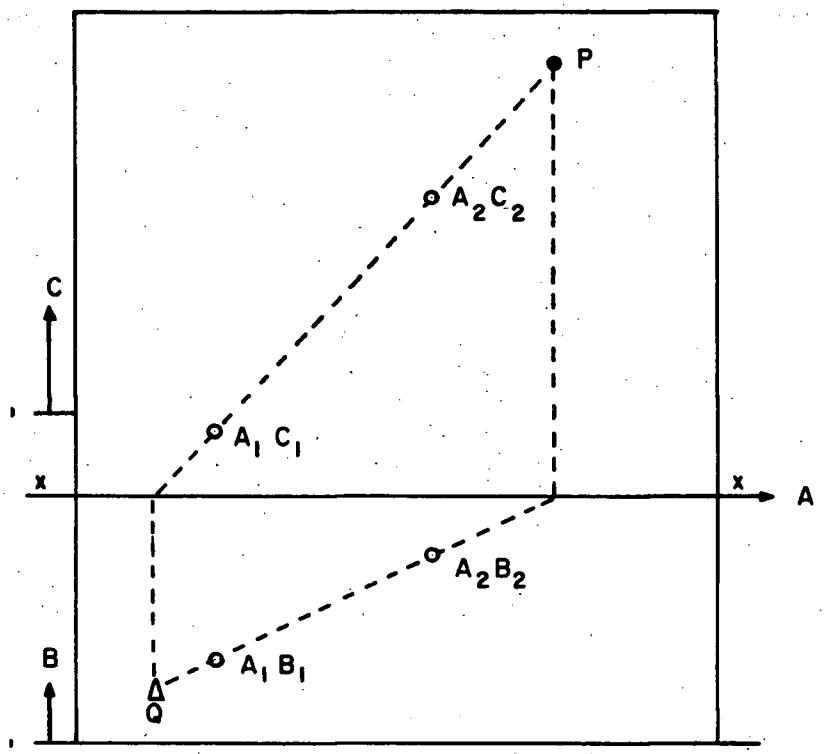

Fig.9 GRAPHICAL DETERMINATION OF POWER LAW FOR 3 VARIABLES

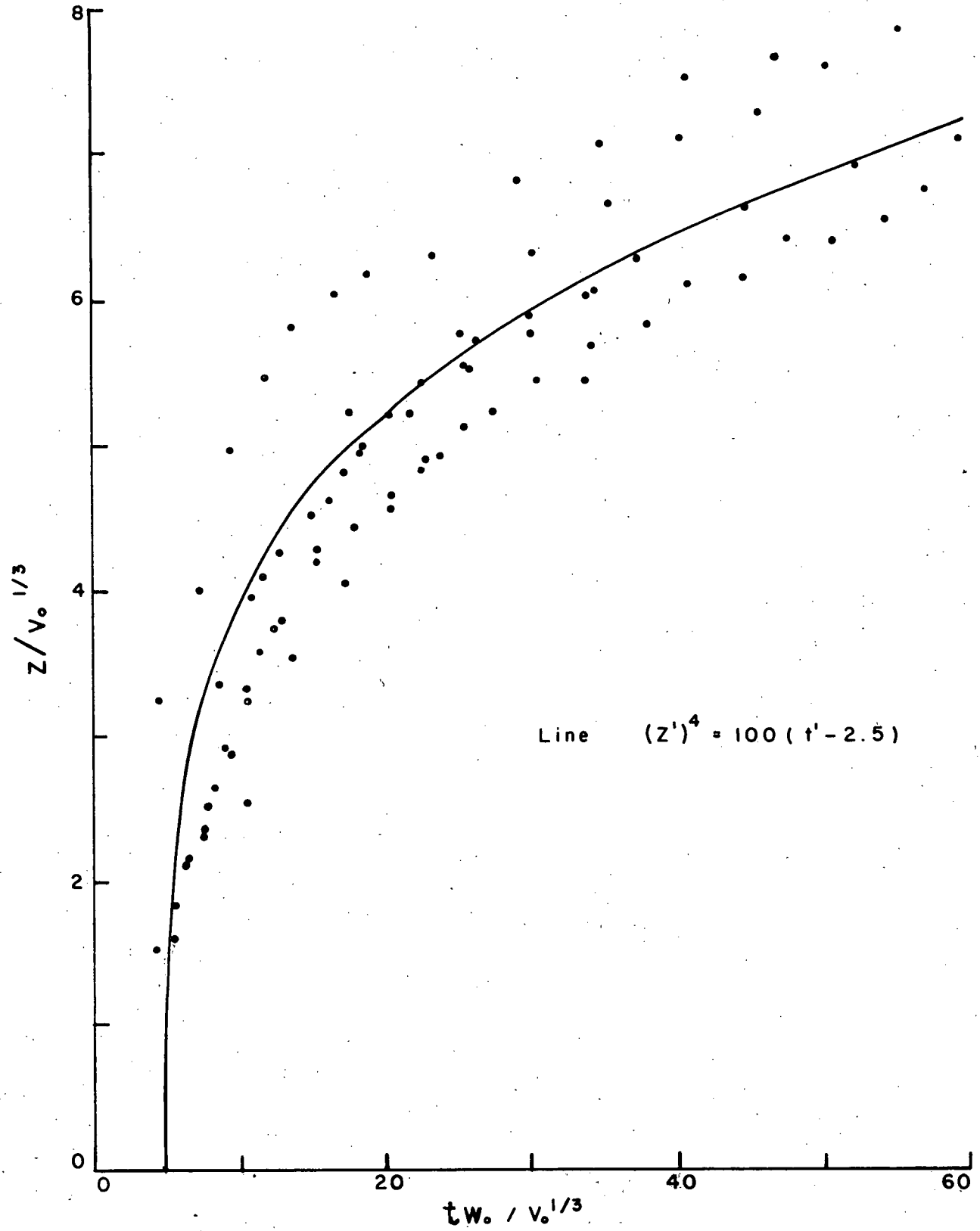

Fig. 10 SIMILARITY IN NEUTRALLY BUOYANT SURROUNDINGS

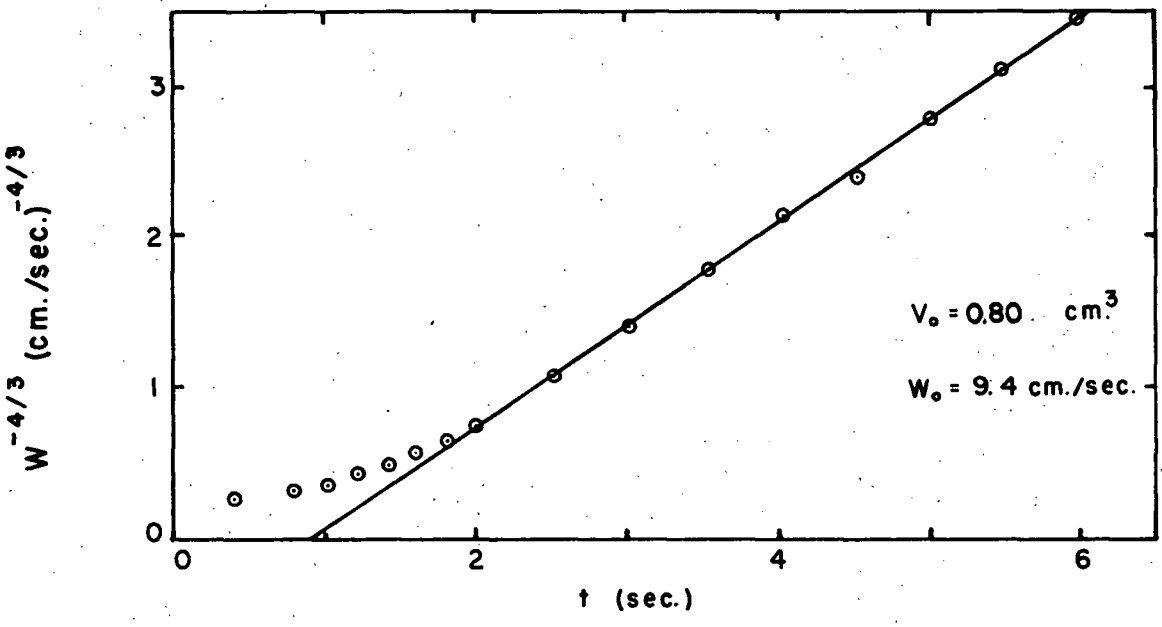

Fig. 11 VELOCITY OF PUFF IN NEUTRALLY BUOYANT SURROUNDINGS

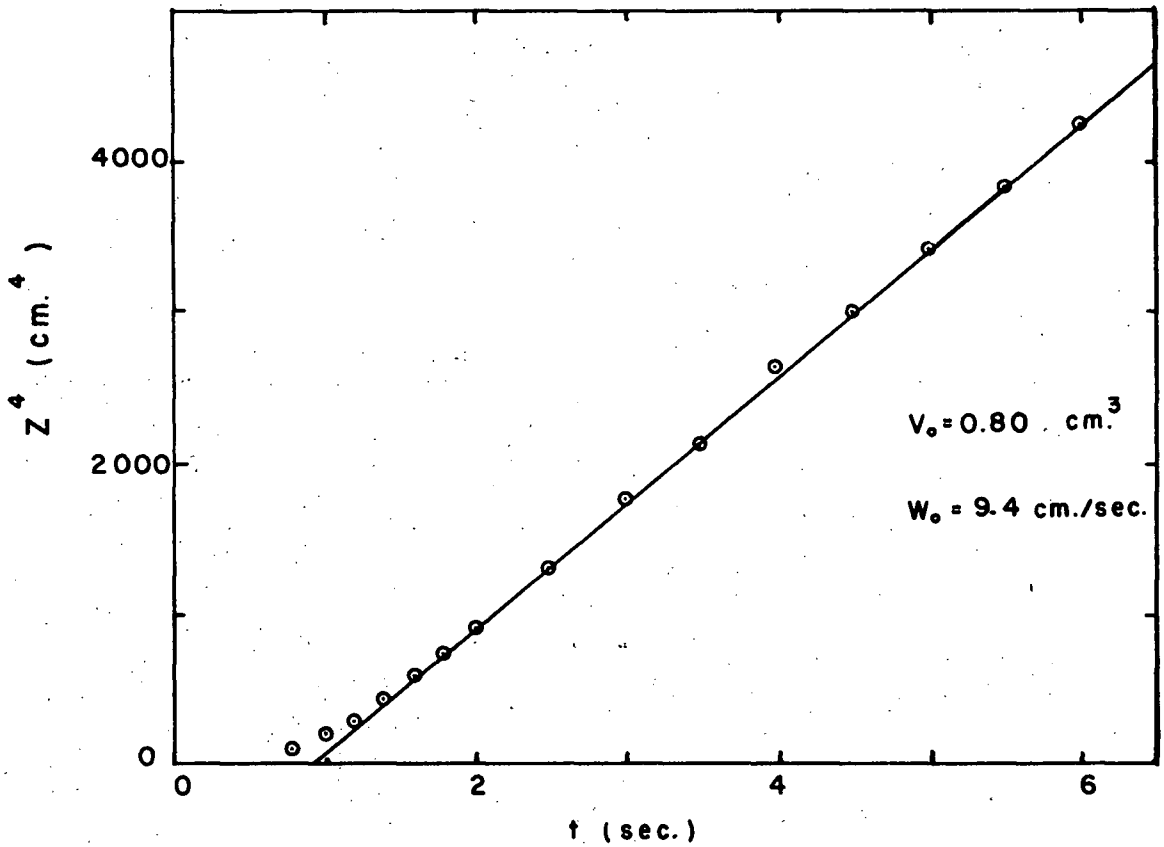

Fig. 12 DISPLACEMENT OF A PUFF IN NEUTRALLY BUOYANT SURROUNDINGS

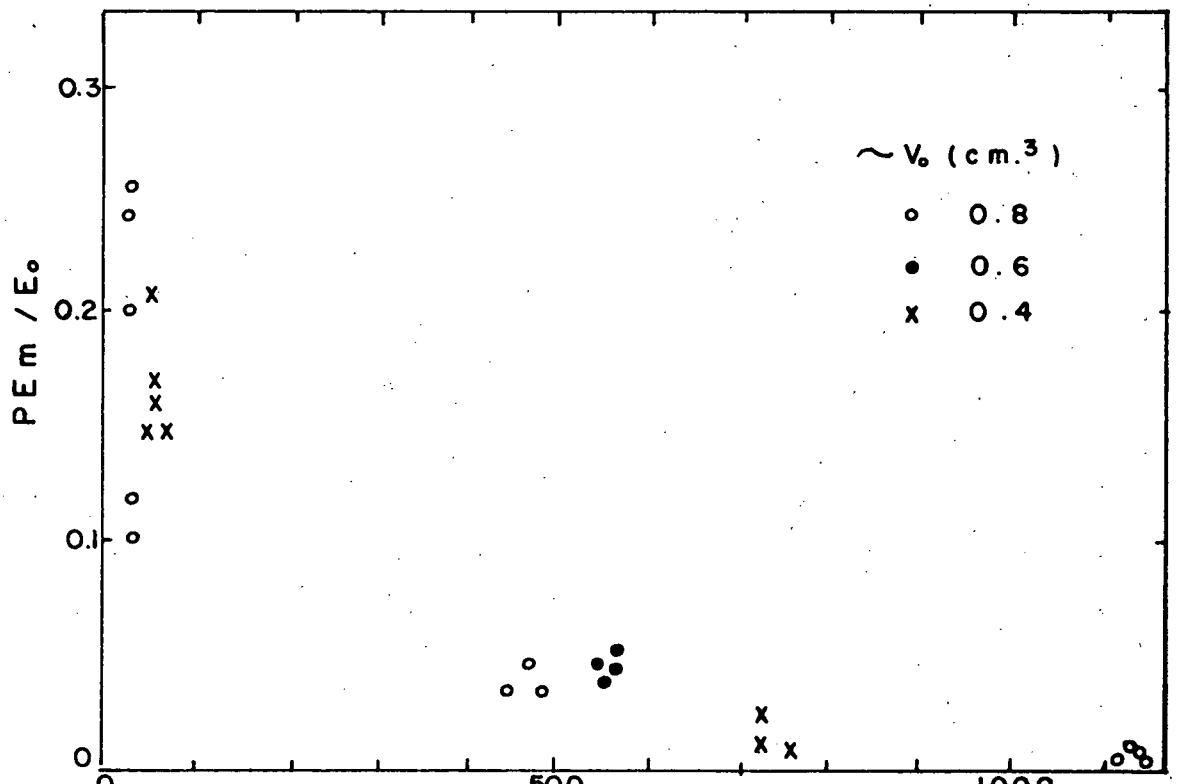

$$\frac{1}{R_1} = \frac{\rho_0 W_0^2}{g \, \partial\rho / \partial z \, V_0^{2/3}}$$

Fig. 13 POTENTIAL ENERGY AT MAXIMUM PENETRATION / INITIAL ENERGY

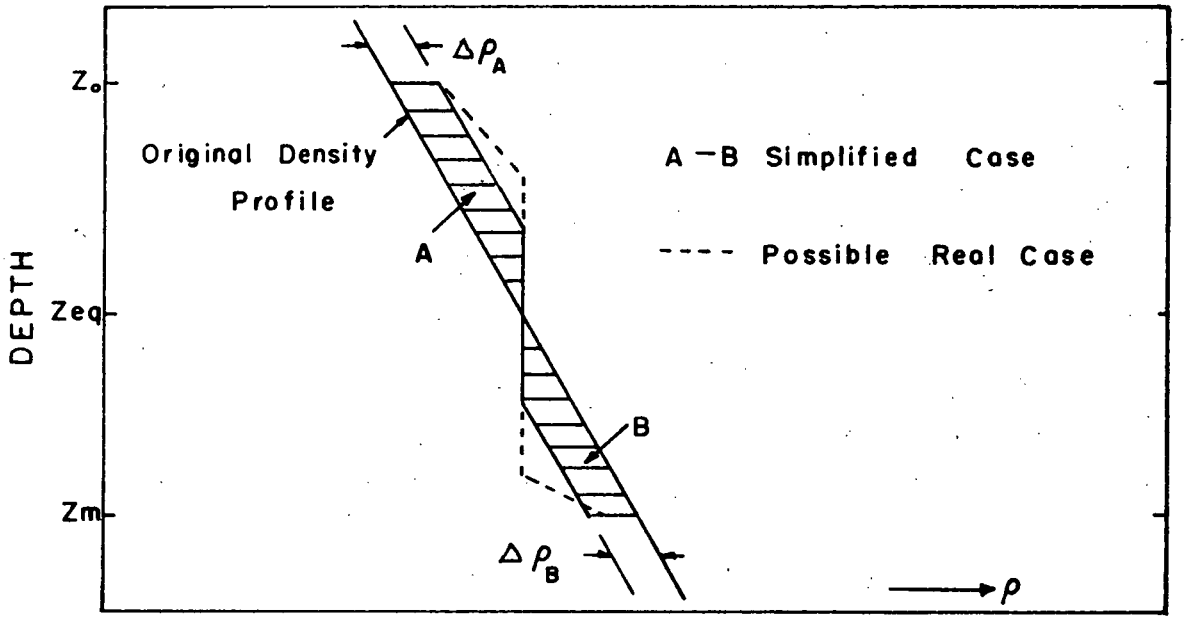

Fig. 14 ALTERATION IN DENSITY STRUCTURE

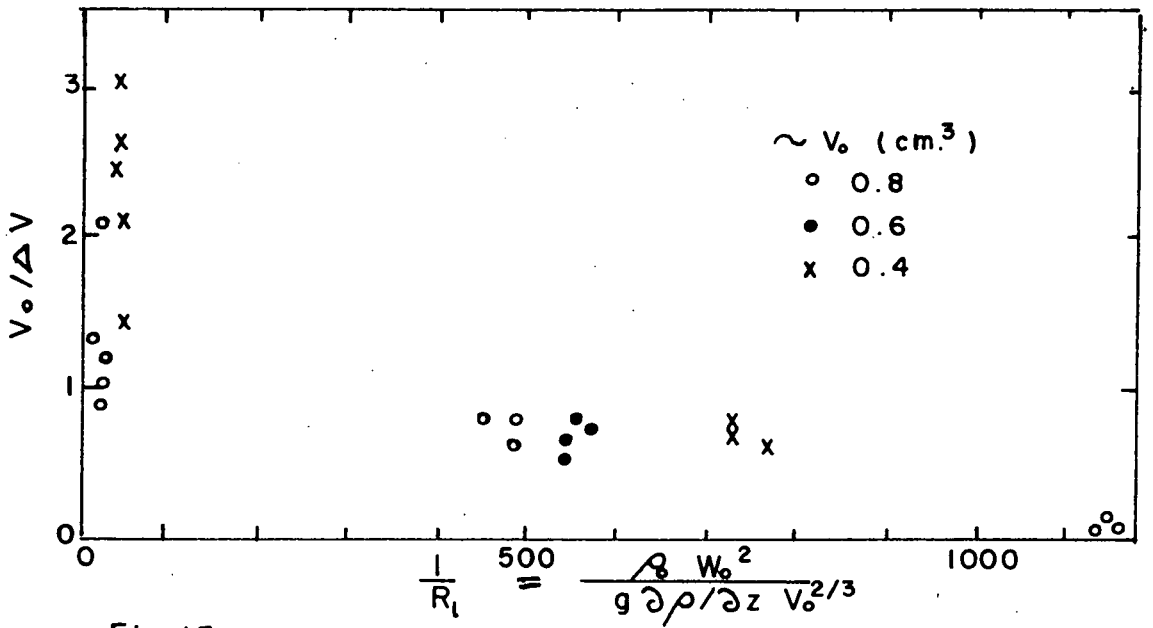

Fig. 15

RATIO $\frac{\text{INITIAL VOLUME}}{\text{VOLUME ENTRAINED}}$

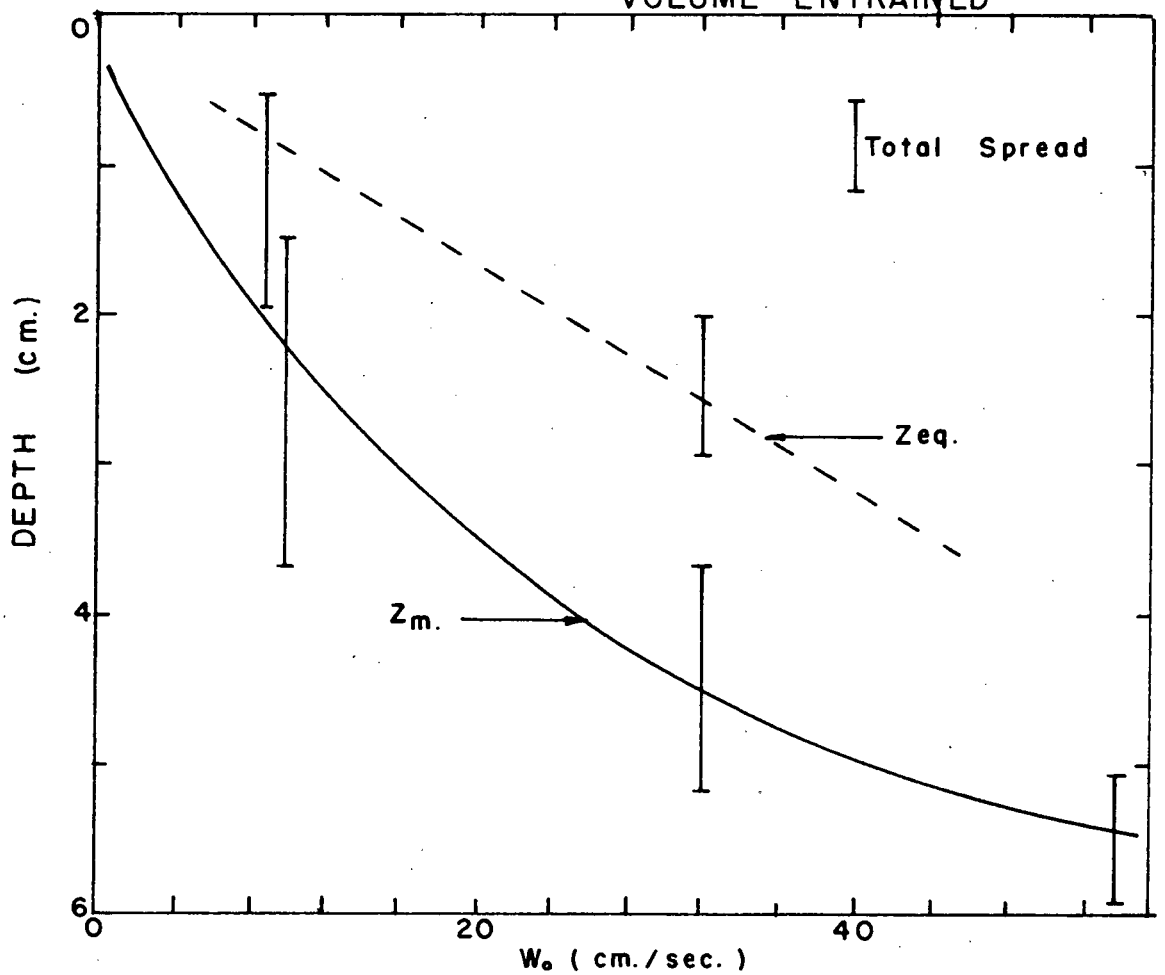

Fig. 16

MAXIMUM PENETRATION (Z_m)
AND EQUILIBRIUM DEPTH ($Z_{eq.}$)

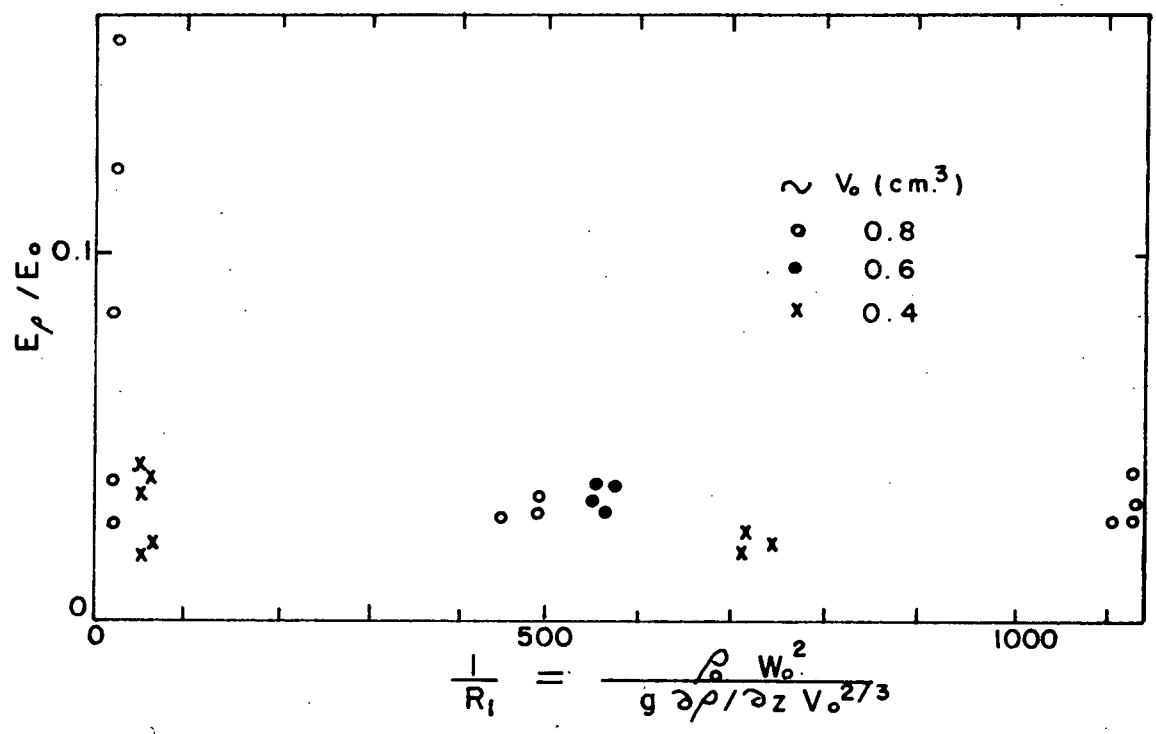

Fig. 17 ENERGY LOST TO DENSITY STRATIFICATION / INITIAL ENERGY

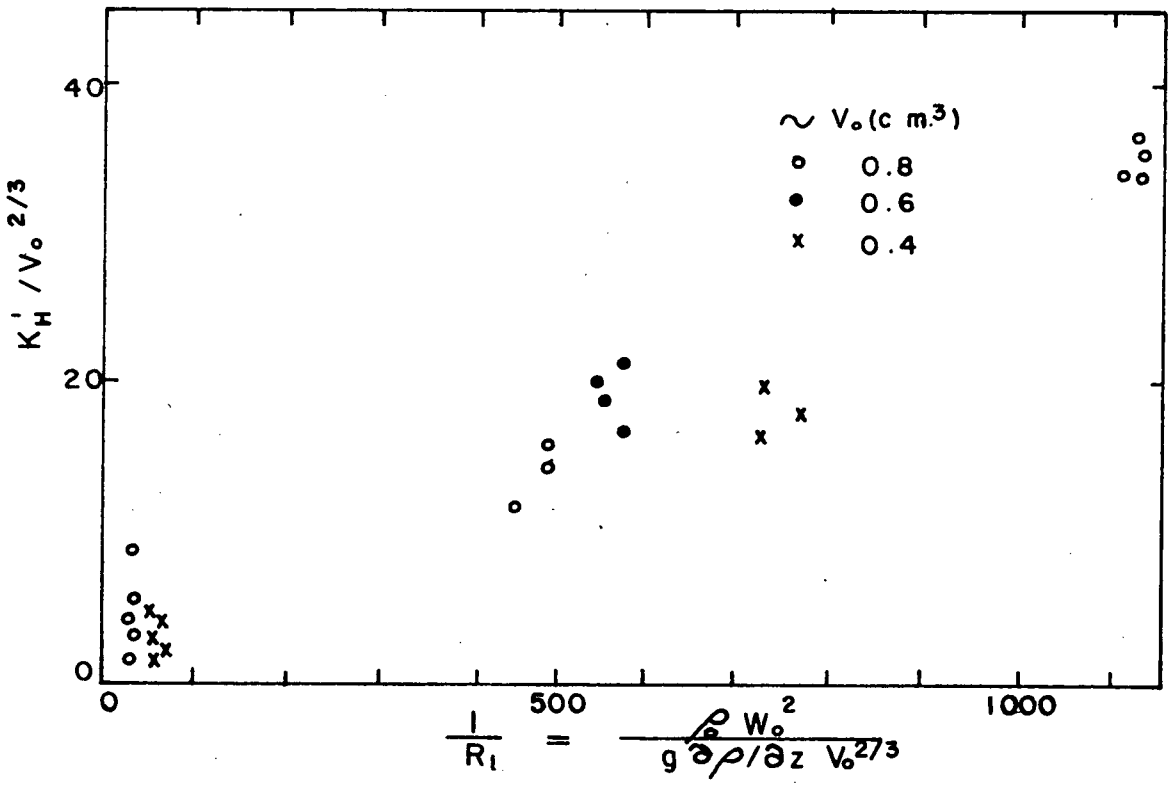

Fig. 18 NET DENSITY TRANSFER COEFFICIENTS

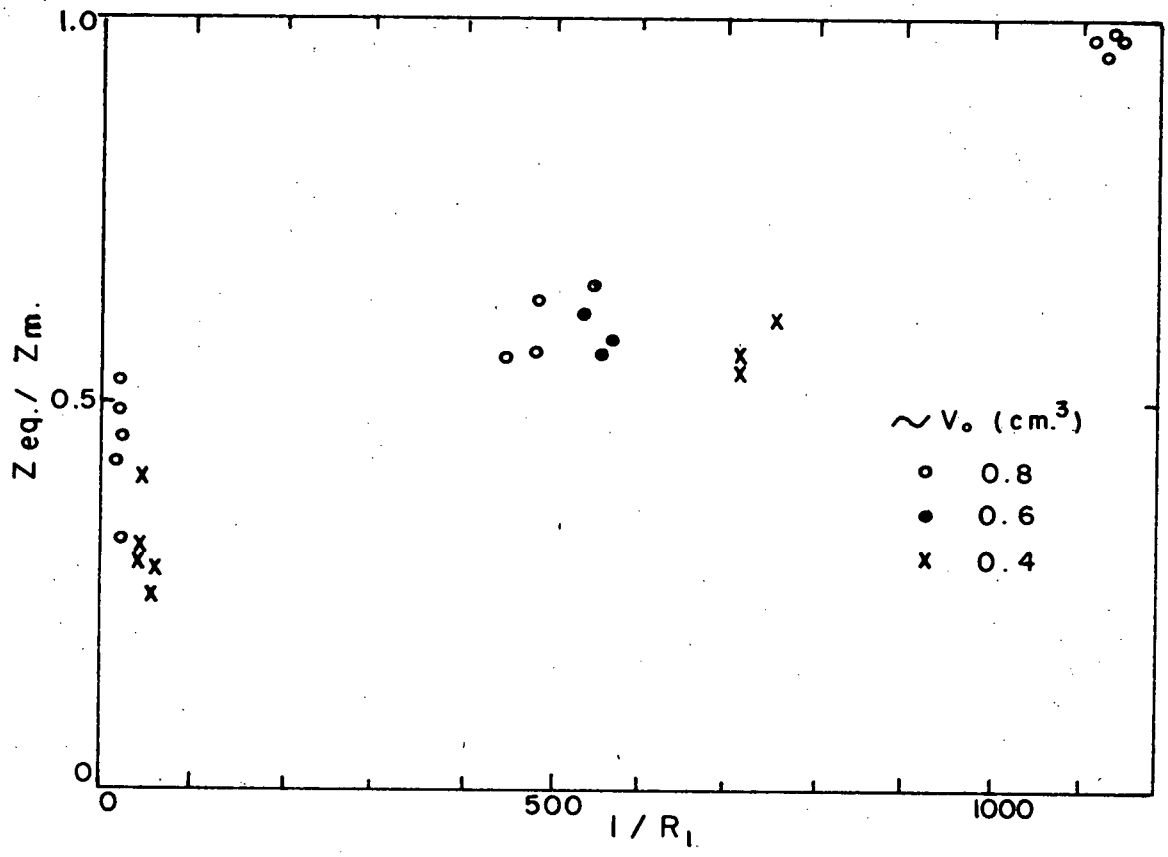

Fig. 19 EQUILIBRIUM DISTANCE / MAXIMUM PENETRATION

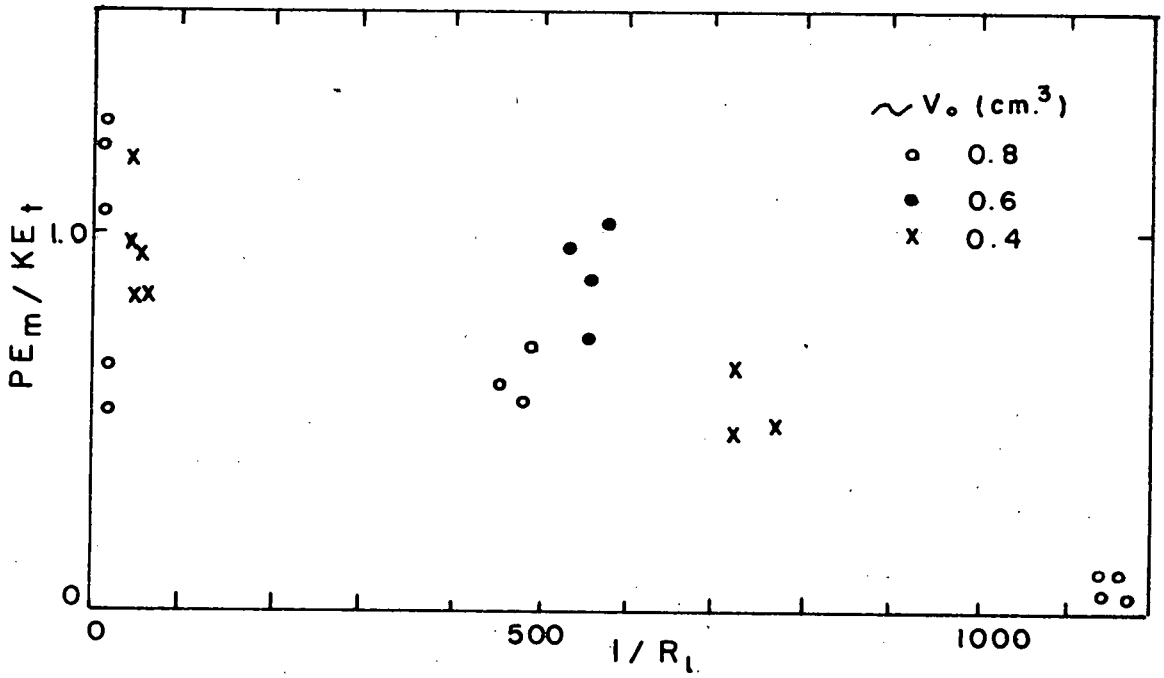

Fig. 20 POTENTIAL ENERGY AT MAXIMUM PENETRATION / KINETIC ENERGY AT SAME TIME IN NEUTRAL SURROUNDINGS

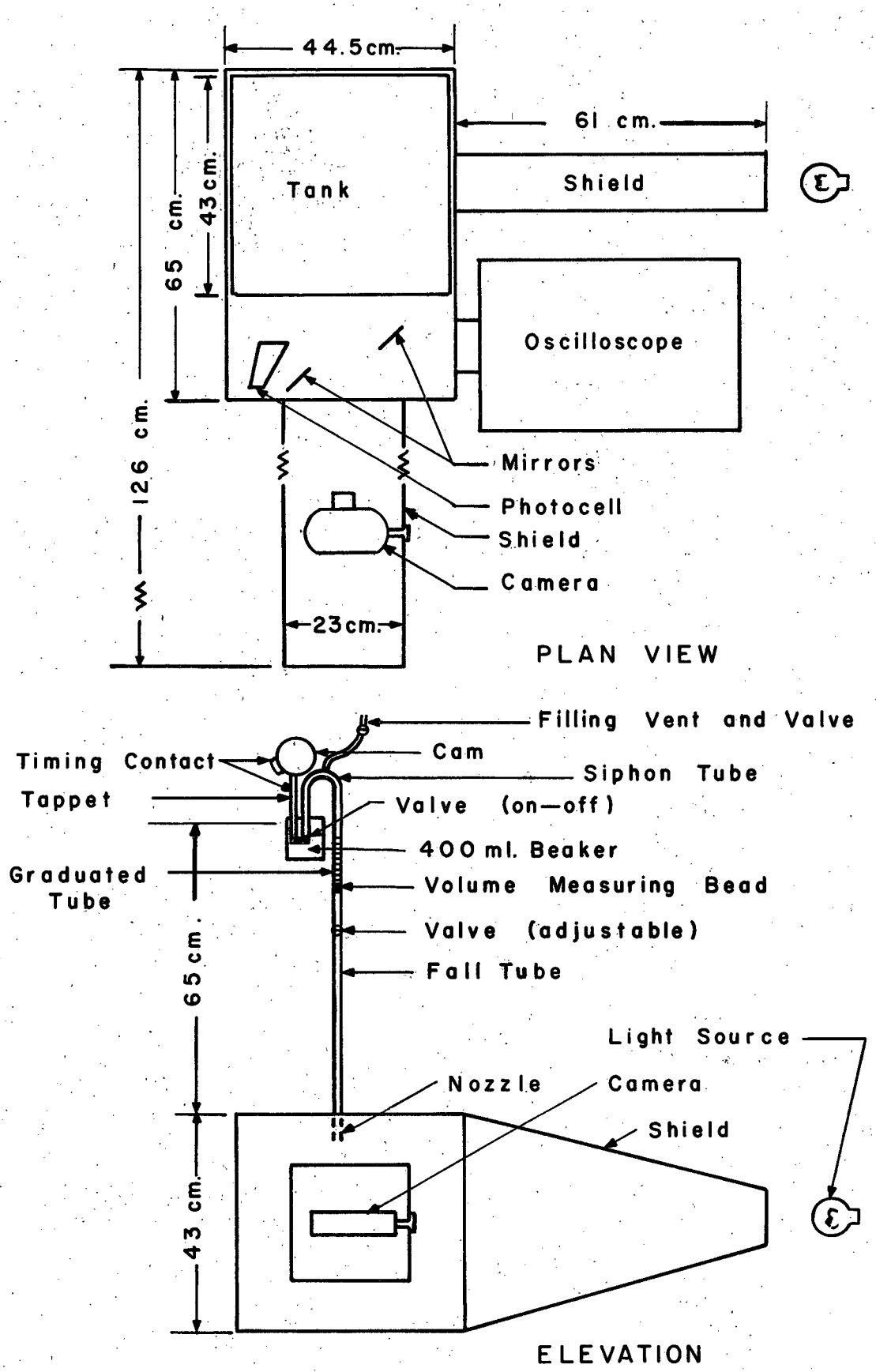

Fig. I APPARATUS

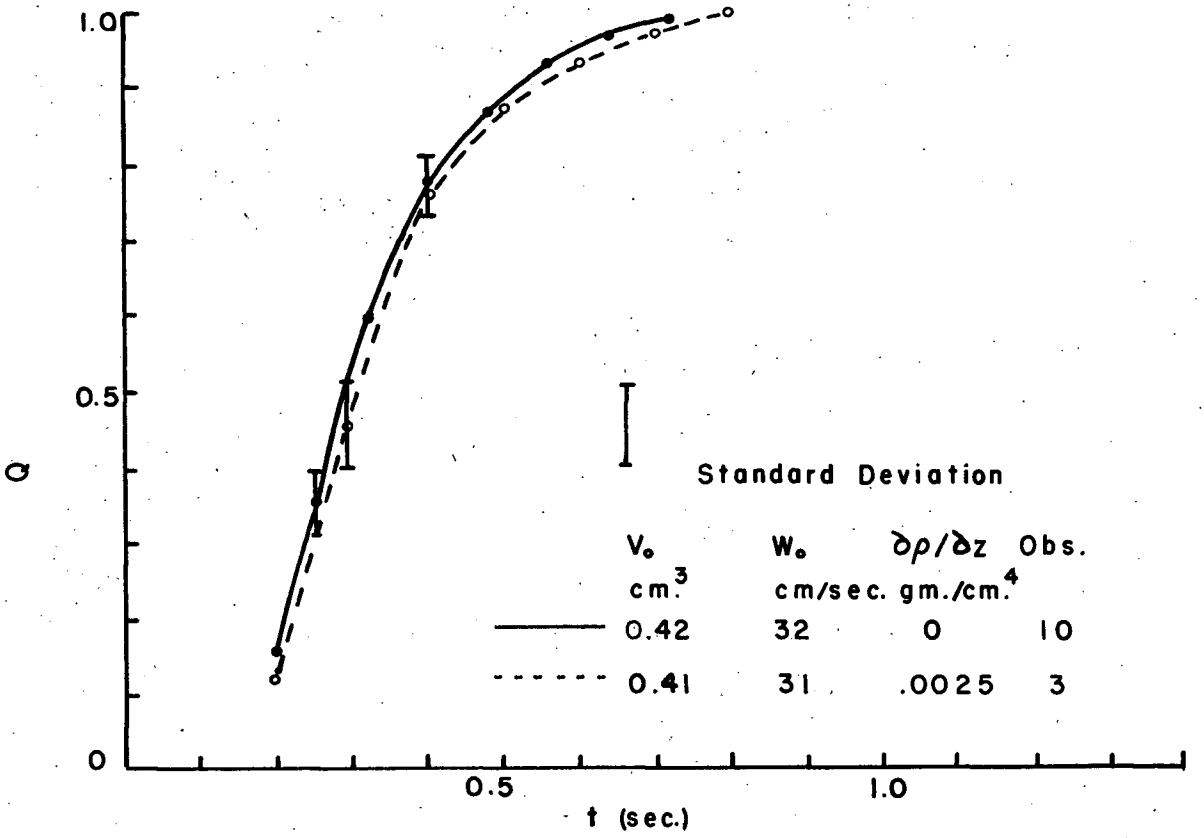

Fig. 2a

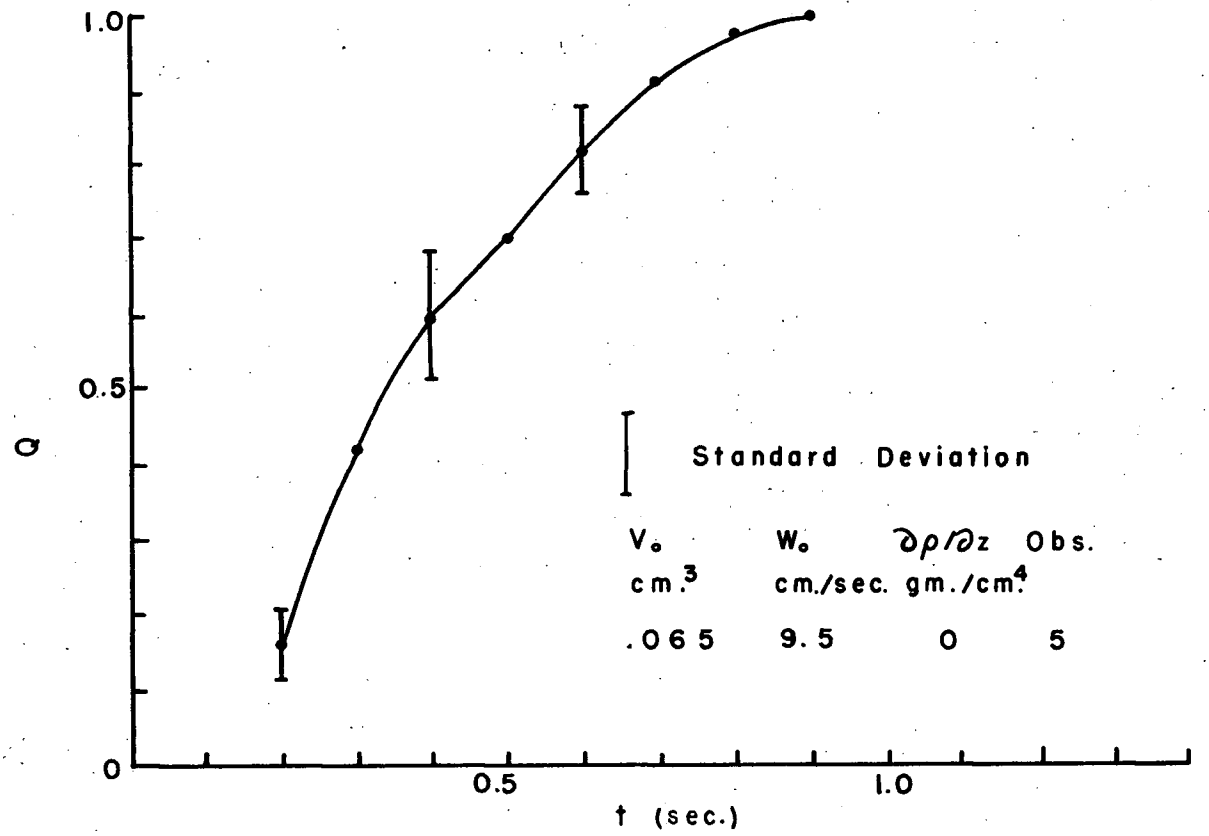

Fig. 2b DETAILED MIXING

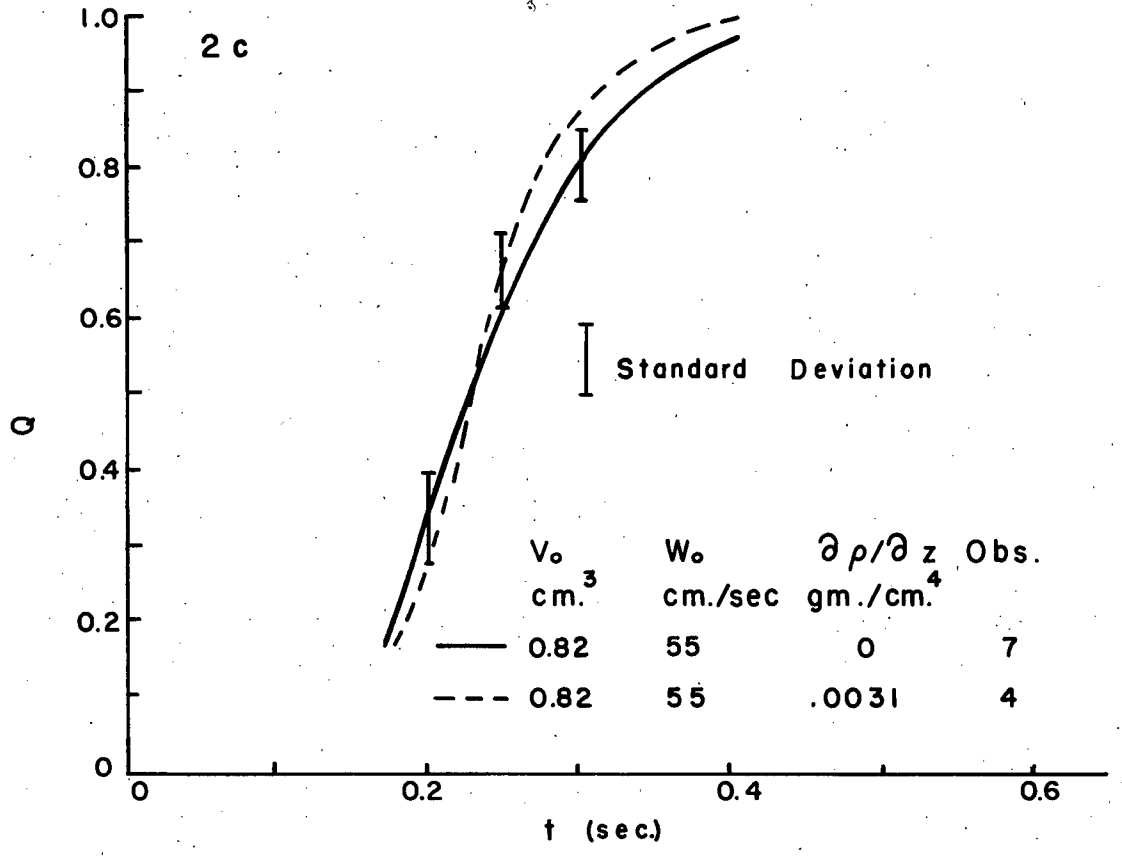

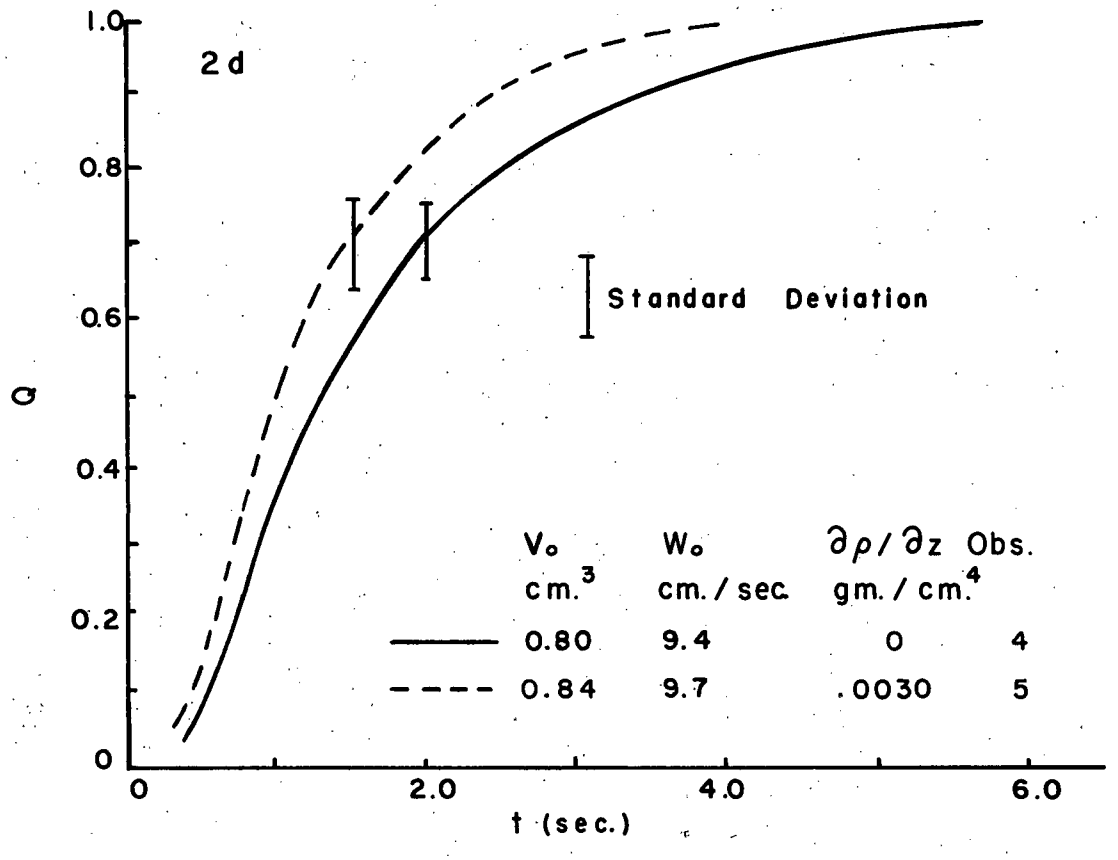

Fig. 2 DETAILED MIXING

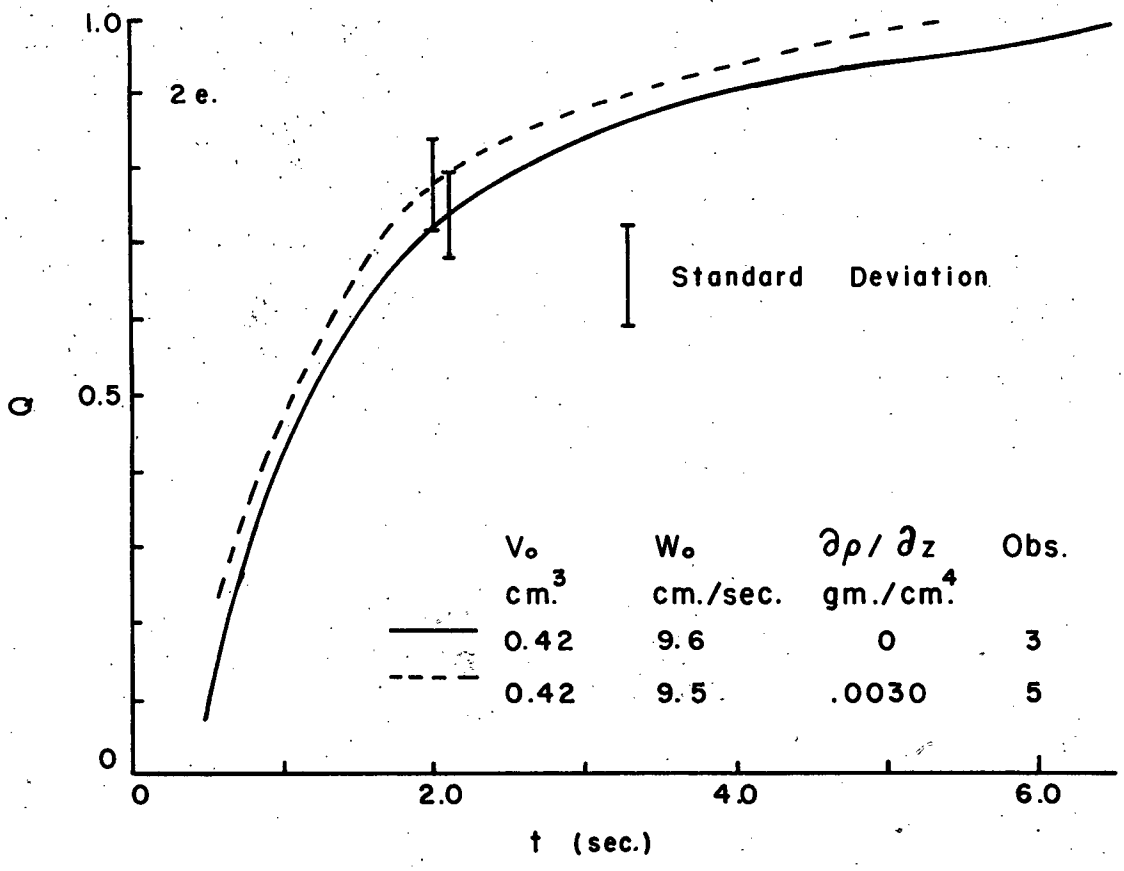

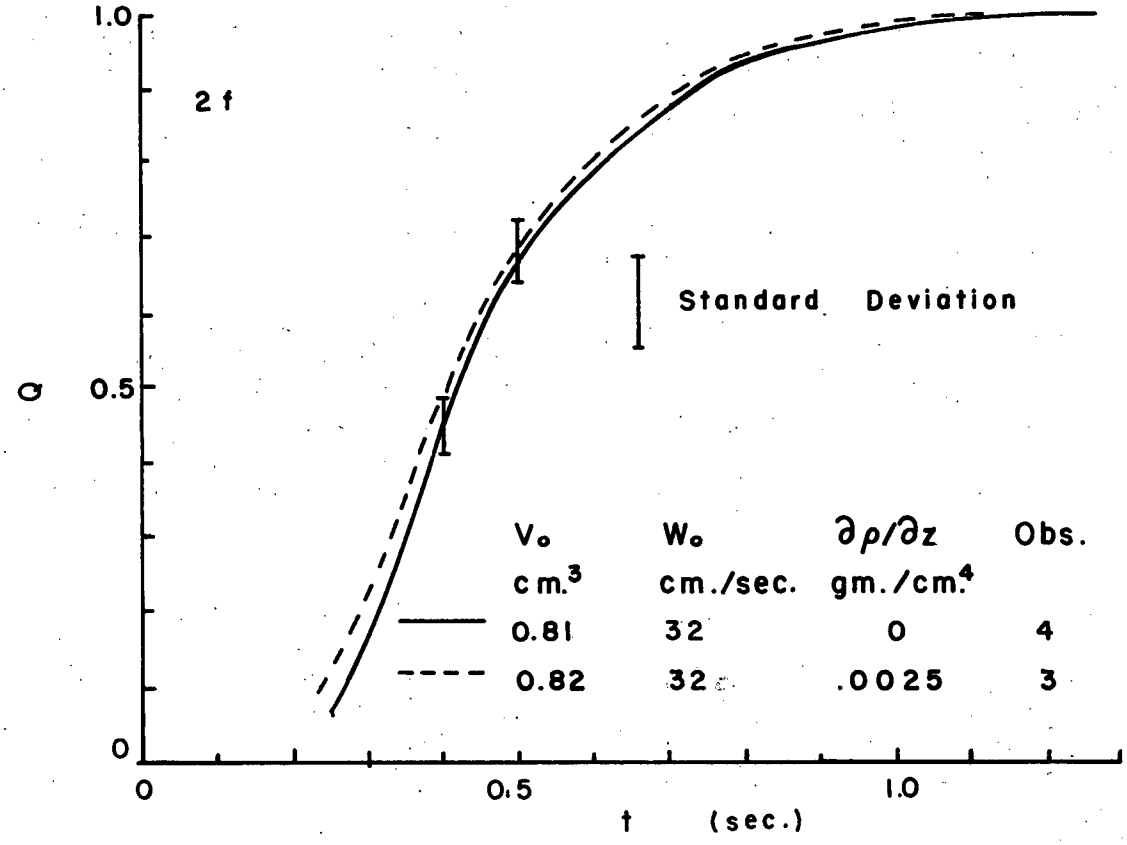

Fig. 2 DETAILED MIXING

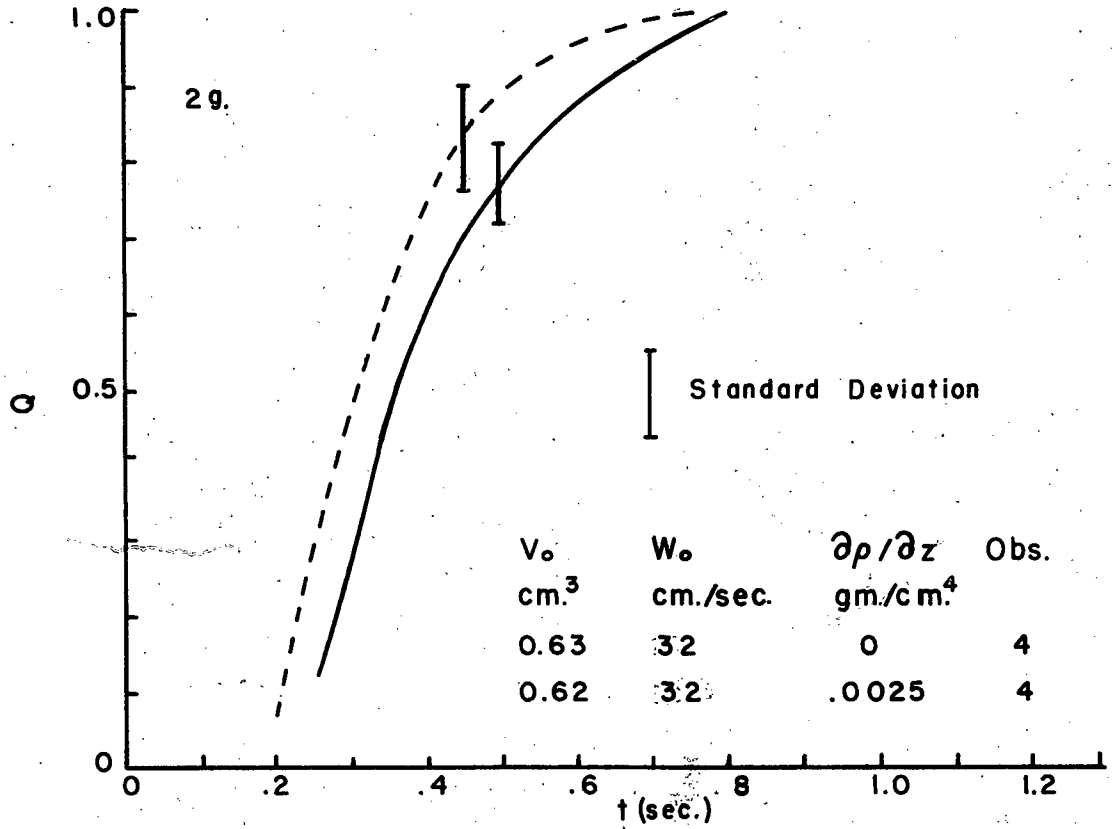

Fig. 2 DETAILED MIXING.

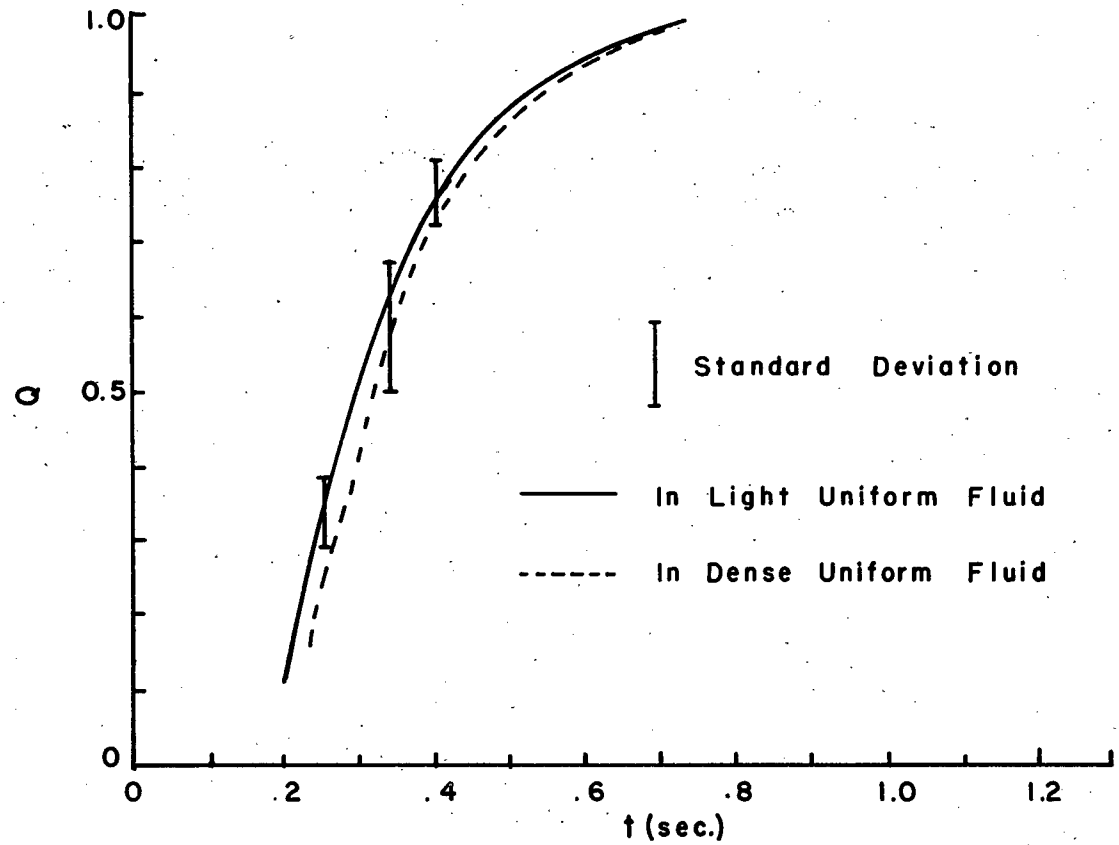

Fig. 3 EFFECT OF SALT UPON MIXING DATA

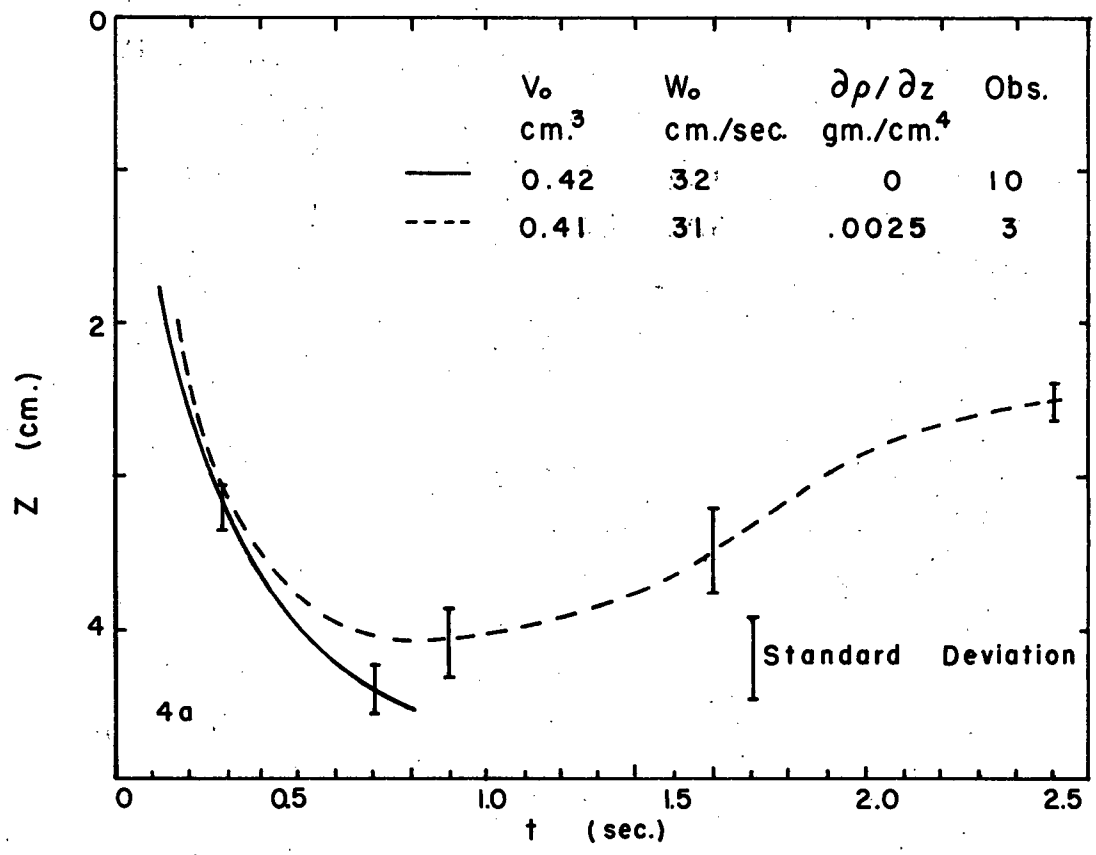

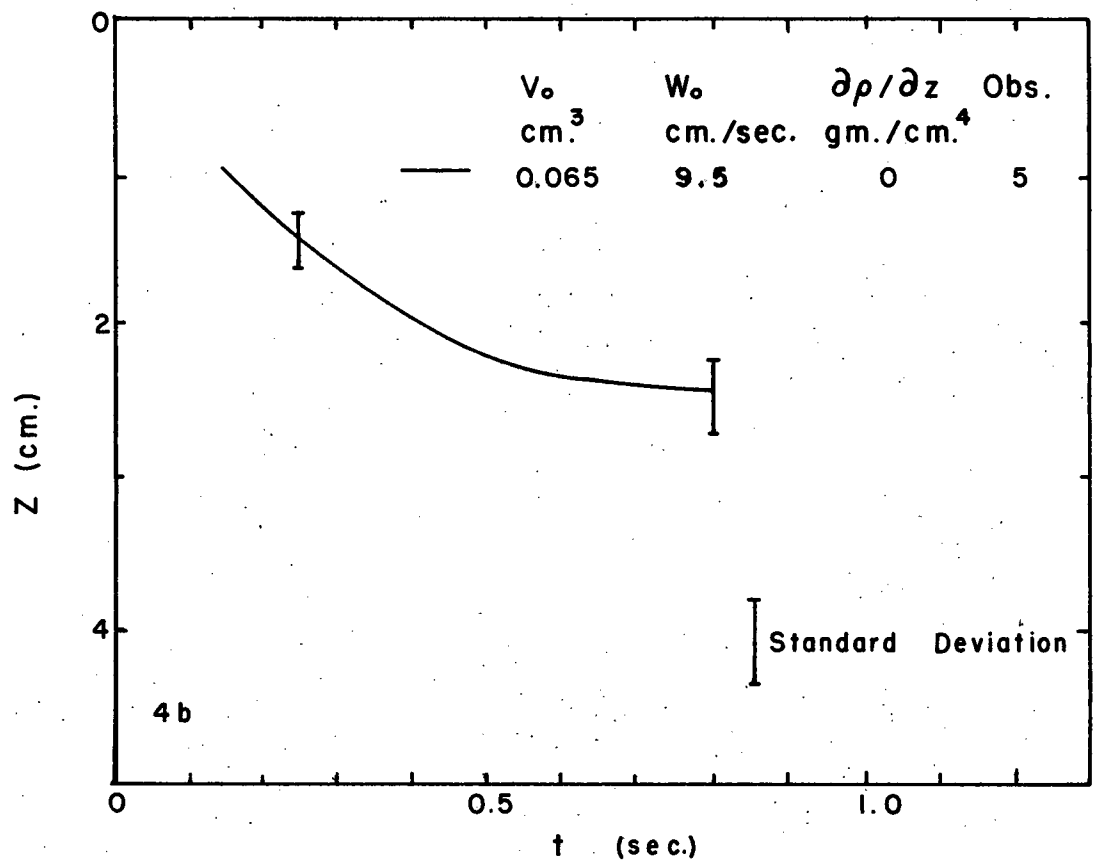

Fig. 4 CENTER DISPLACEMENT

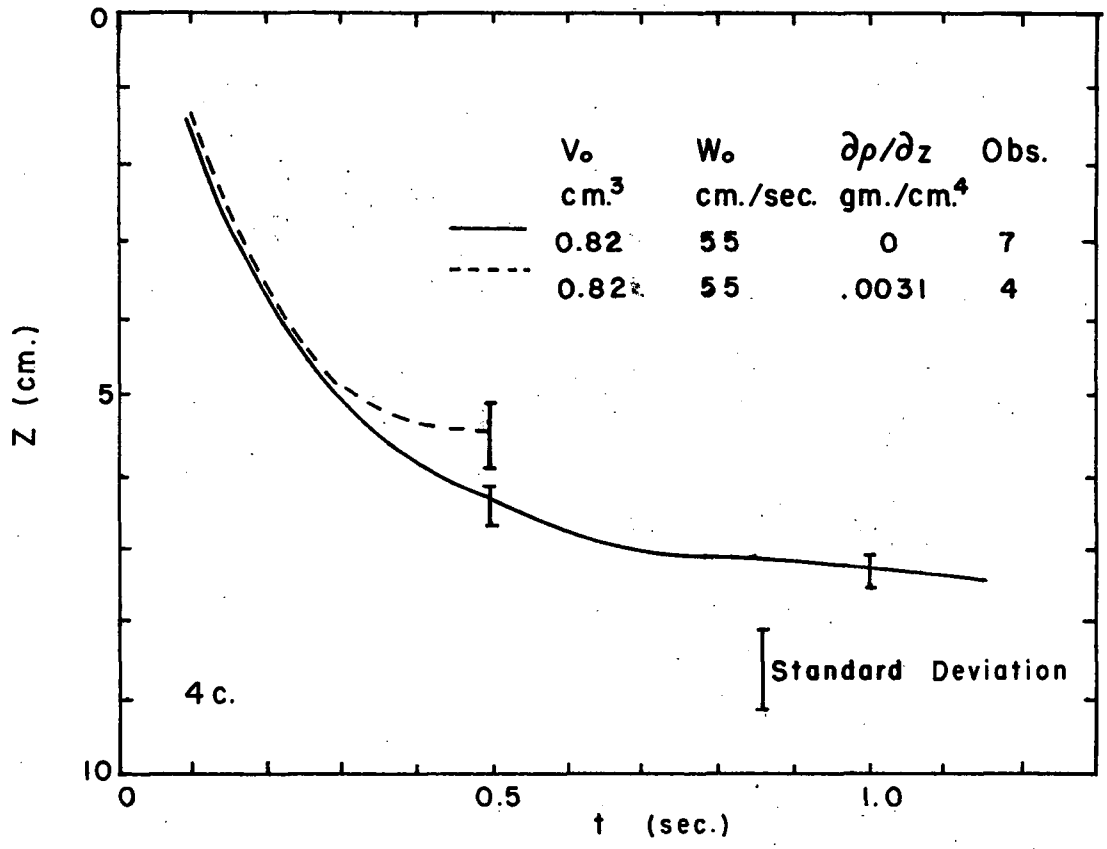

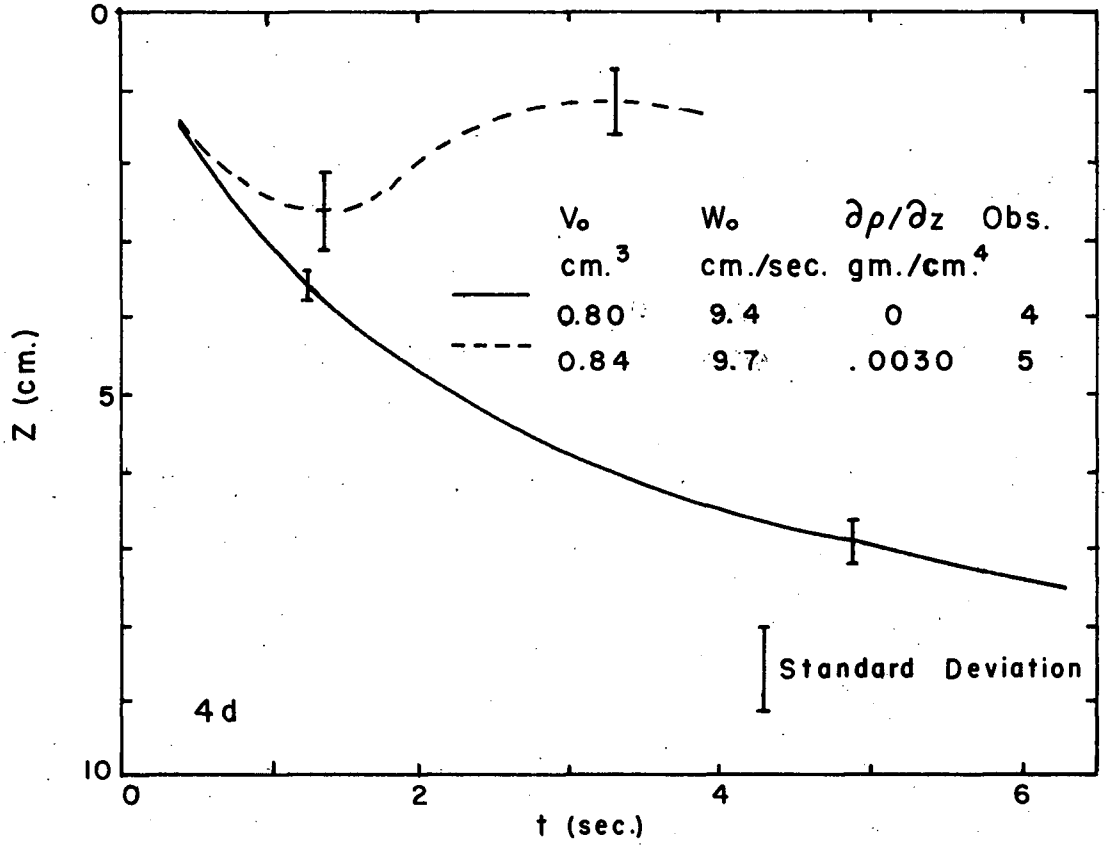

Fig. 4 CENTER DISPLACEMENT

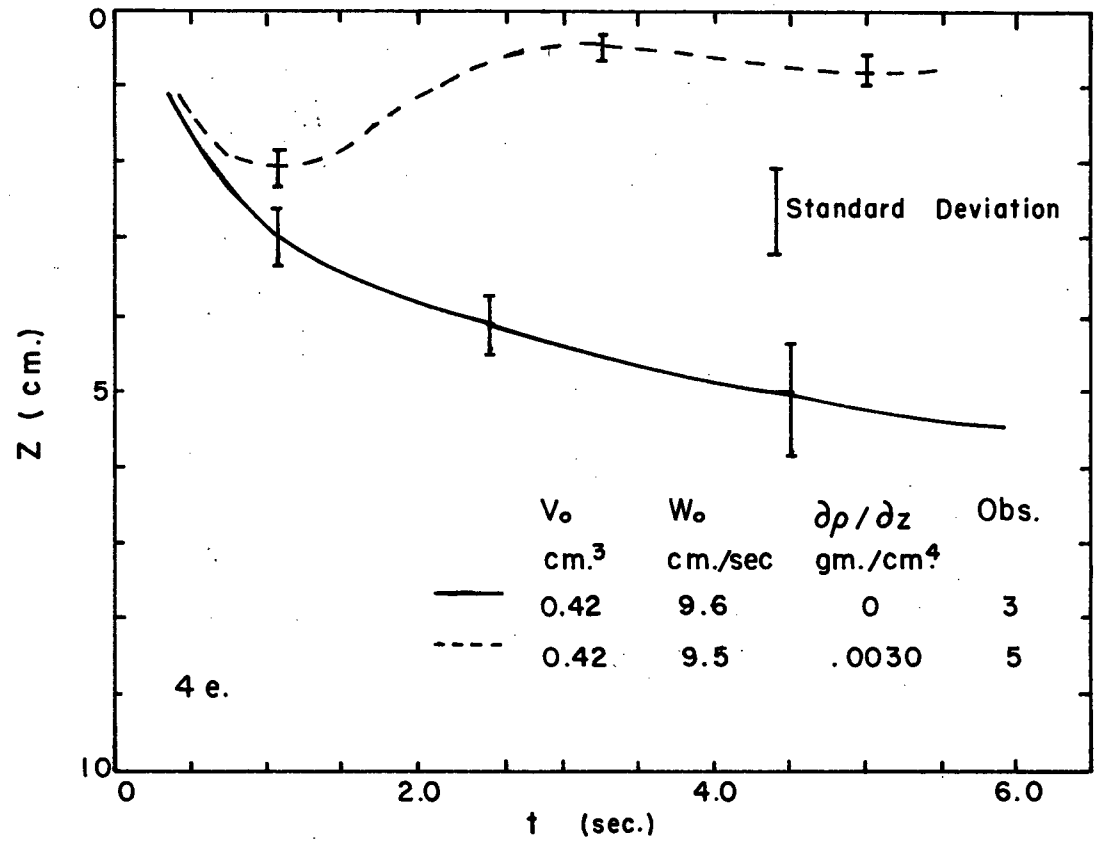

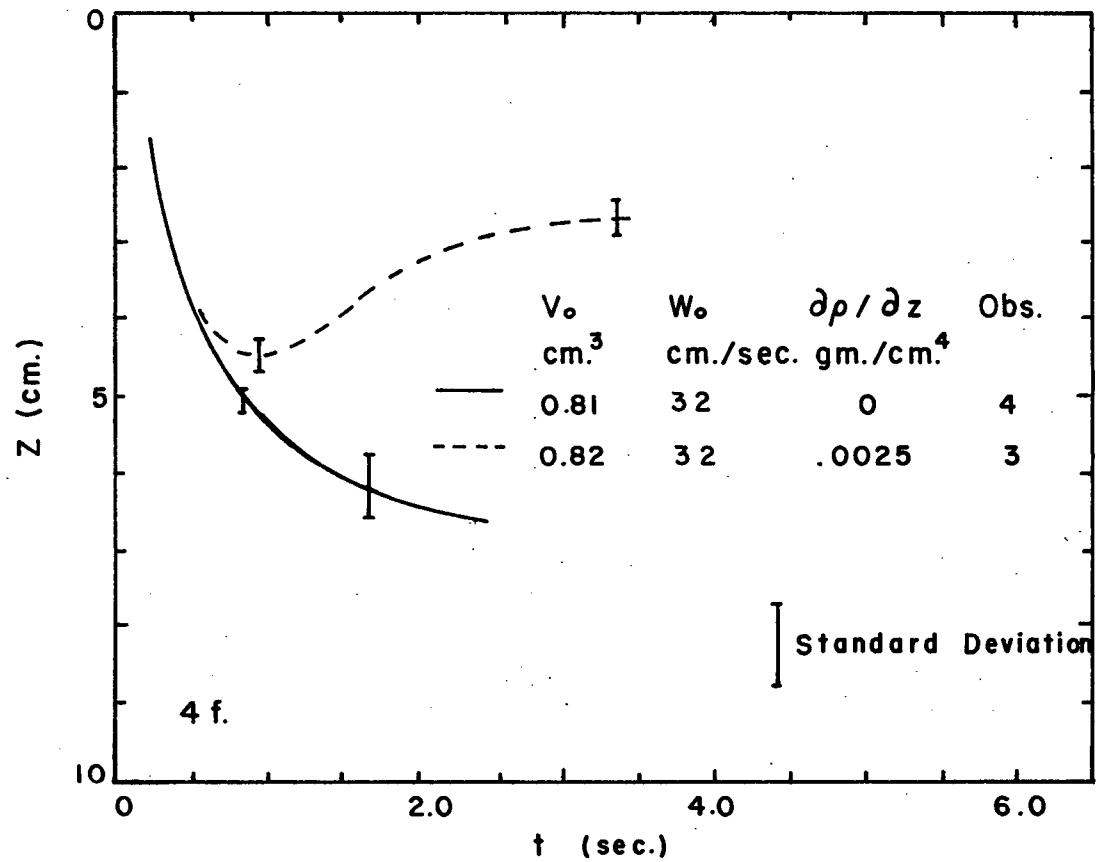

Fig. 4 CENTER DISPLACEMENT

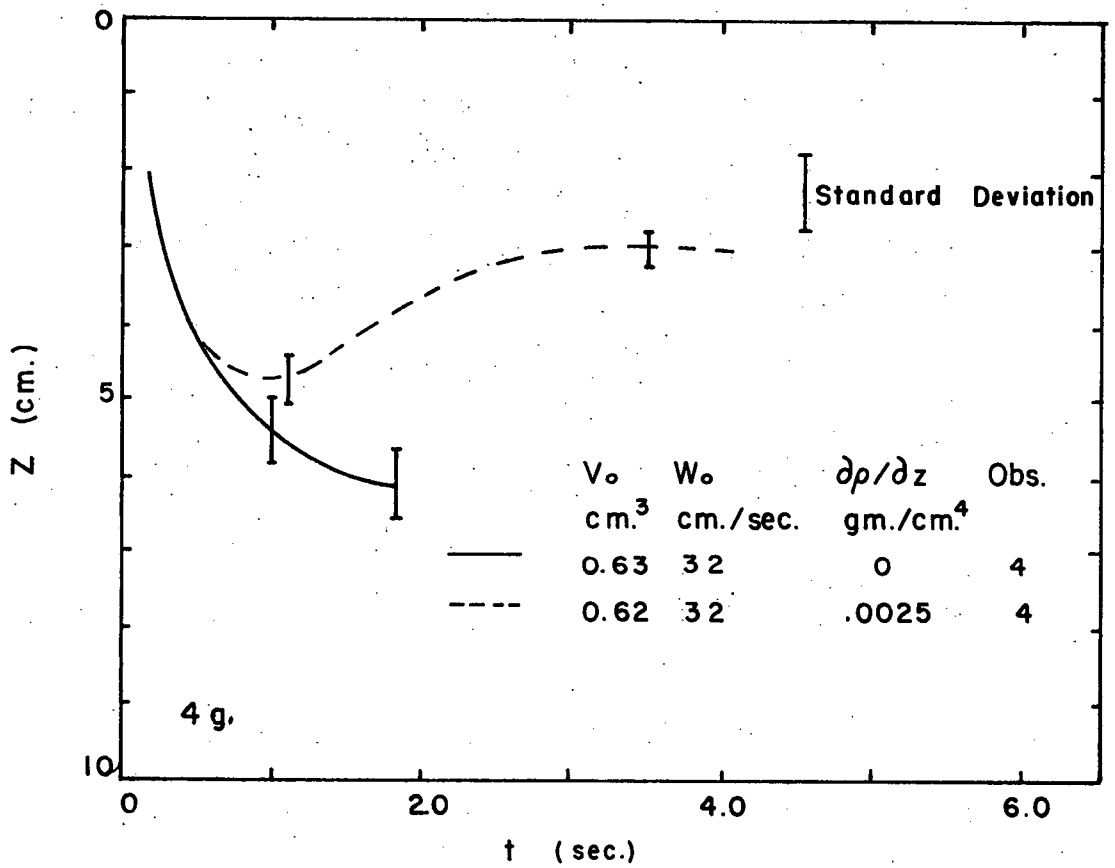

Fig. 4 CENTER DISPLACEMENT

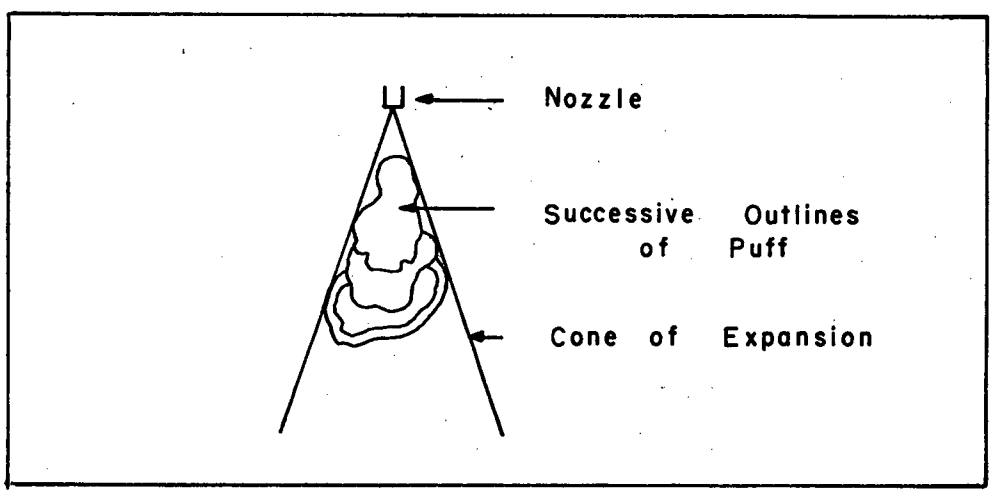

Fig. 5 HORIZONTAL SPREAD IN UNIFORM FLUID

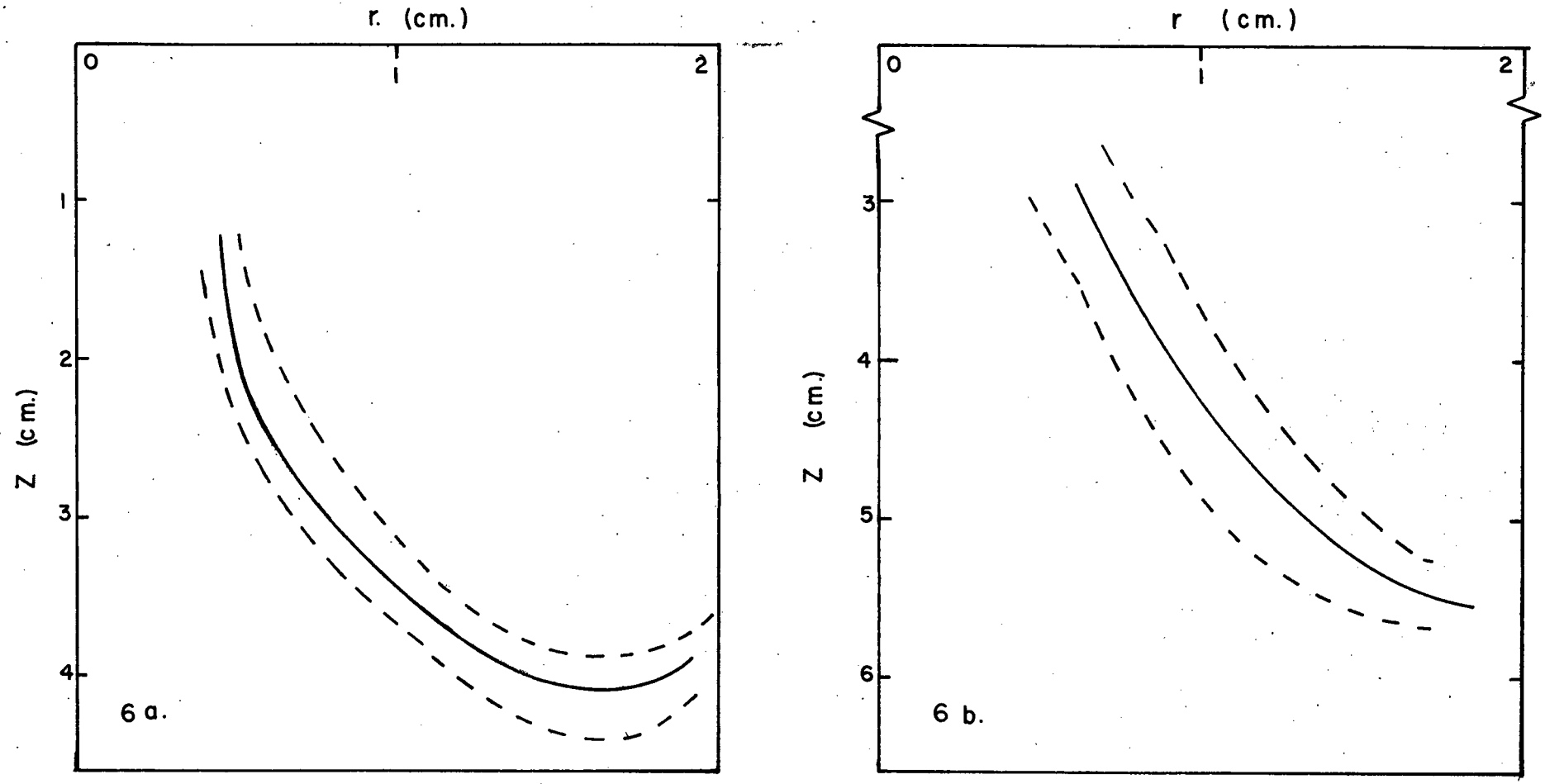

		a	b
V_o	$cm.^3$	0.41	0.82
W_o	cm./sec.	31	55
$\partial\rho/\partial z$	$gm./cm.^4$	.0025	.0031
Obs.		3	4

---- Extremeties of Plotted Points

——— Fitted Line

Fig. 6 HORIZONTAL SPREAD IN STRATIFIED FLUID

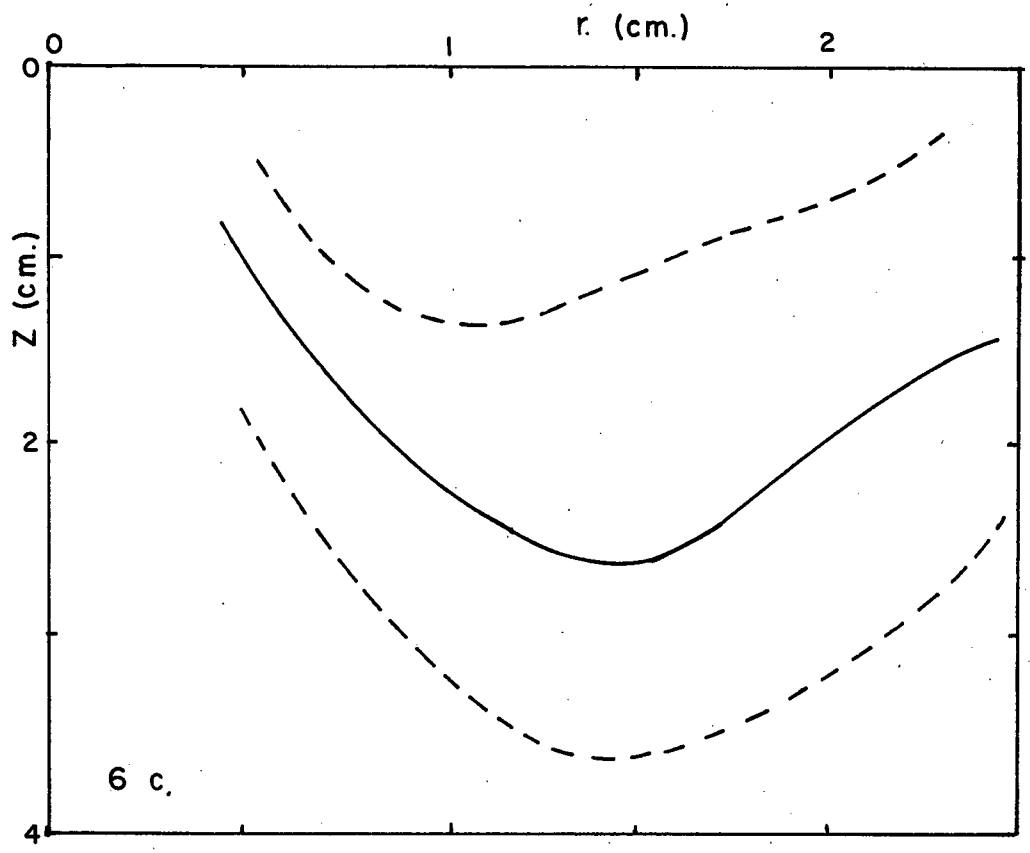

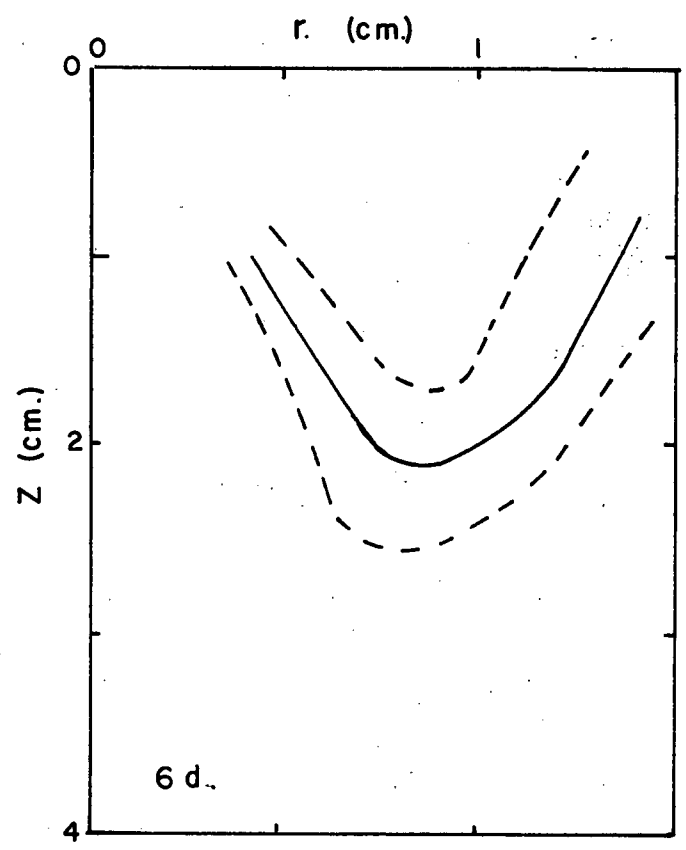

------ Extremeties of Plotted Points

——— Fitted Line

		c	d
V_o	$cm.^3$	0.84	0.42
W_o	cm./sec.	9.7	9.5
$\partial\rho/\partial z$	$gm./cm.^4$	.0030	.0030
Obs.		5	5

Fig. 6 HORIZONTAL SPREAD IN STRATIFIED FLUID

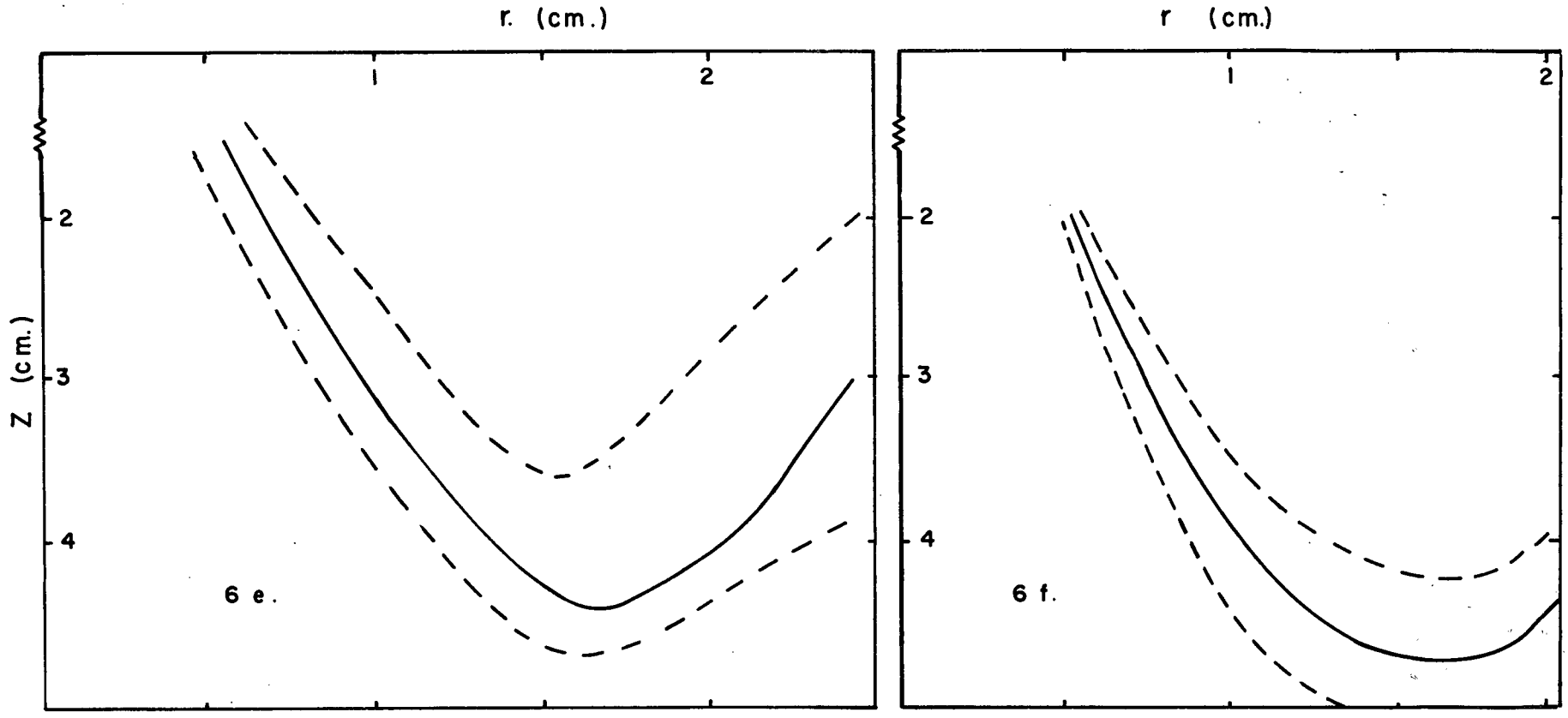

		e	f
V_o	$cm.^3$	0.82	0.62
W_o	cm./sec.	32	32
$\partial\rho/\partial Z$	$gm./cm.^4$	.0025	.0025
Obs.		3	4

----- Extremeties of Plotted Points

—— Fitted Line

Fig. 6 HORIZONTAL SPREAD IN STRATIFIED FLUID

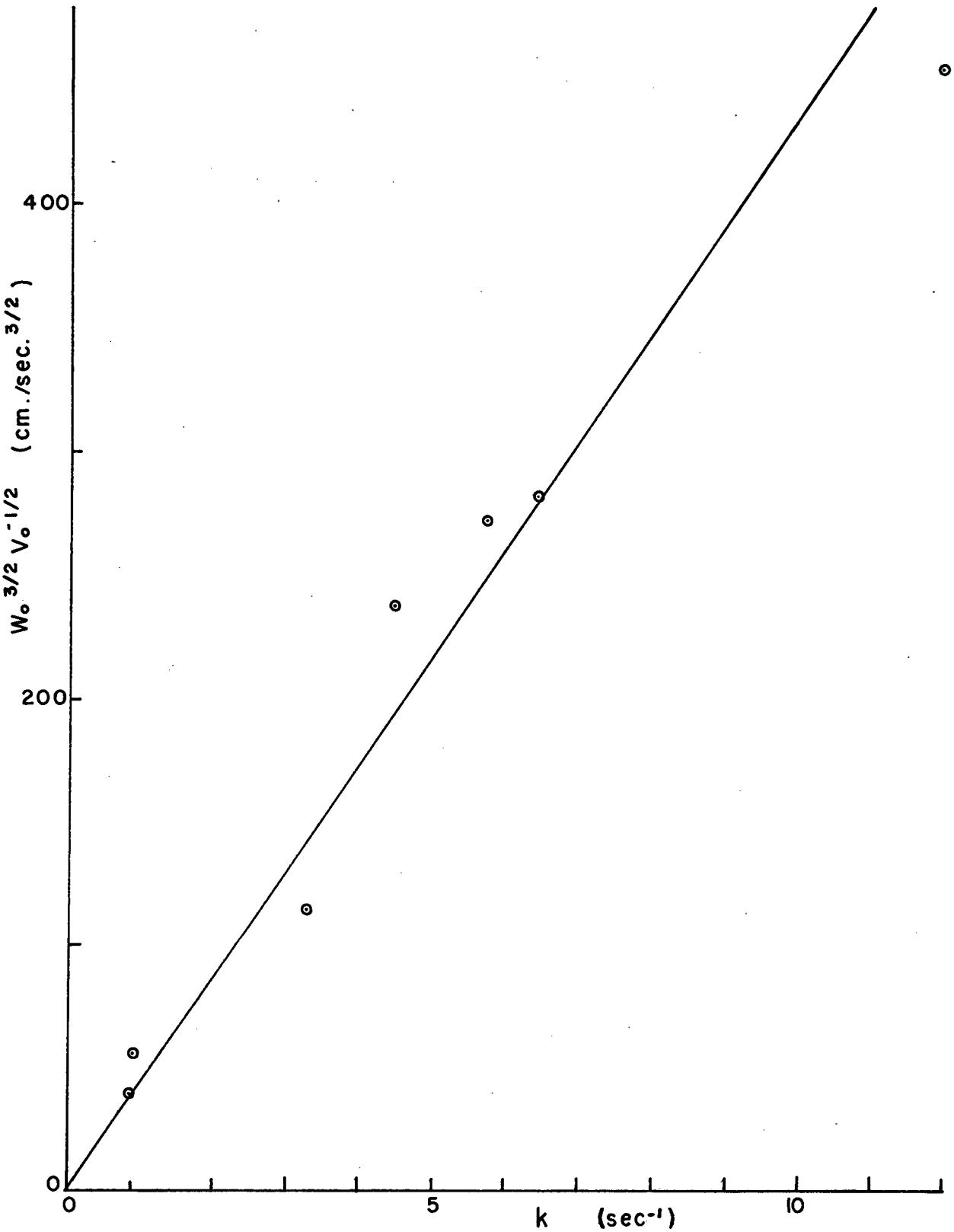

Fig. 7 DEPENDENCE OF MIXING FUNCTION k UPON THE INITIAL CONDITIONS

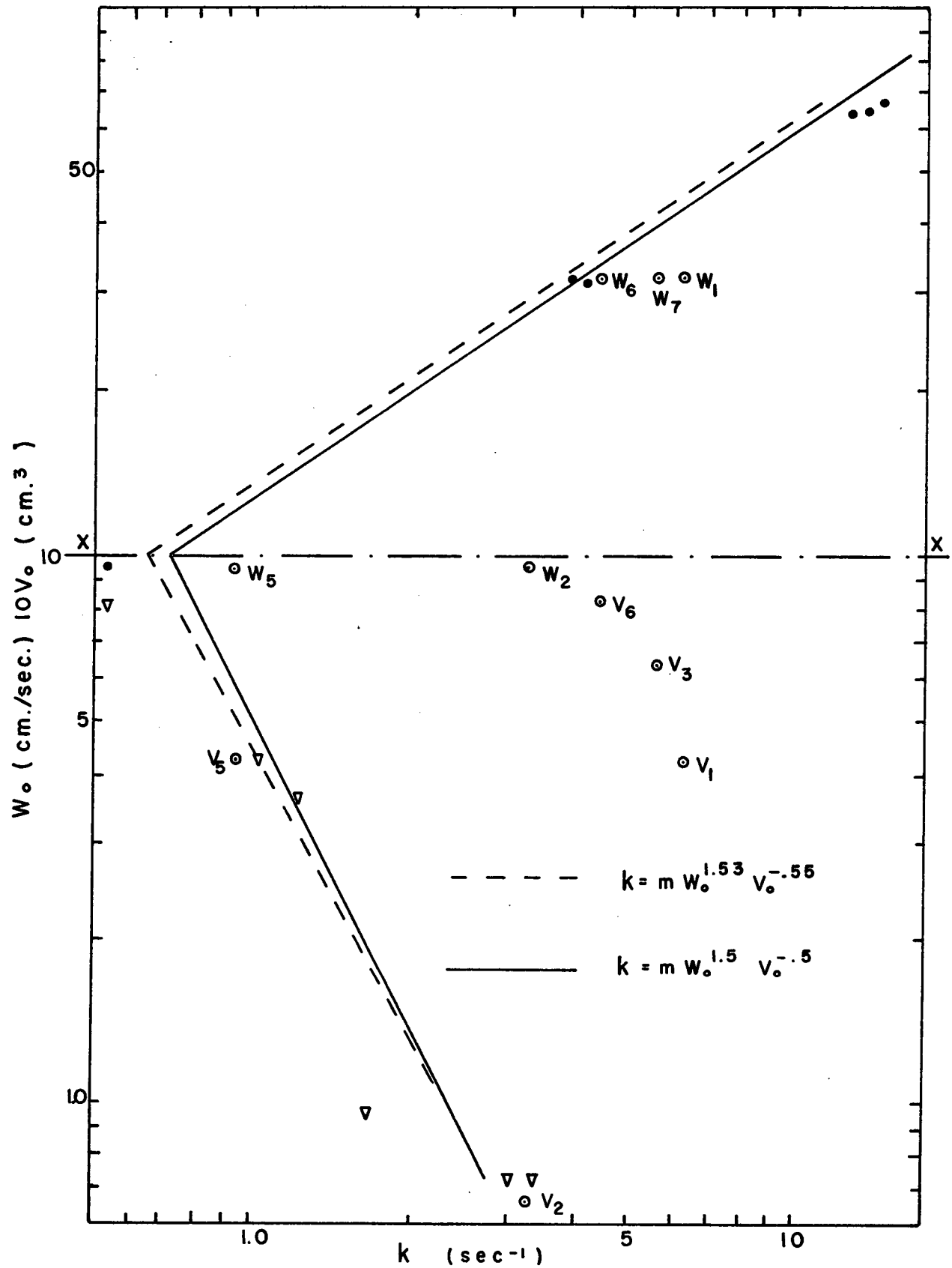

Fig. 8 3-DIMENSIONAL PLOT OF k AGAINST THE INITIAL CONDITIONS

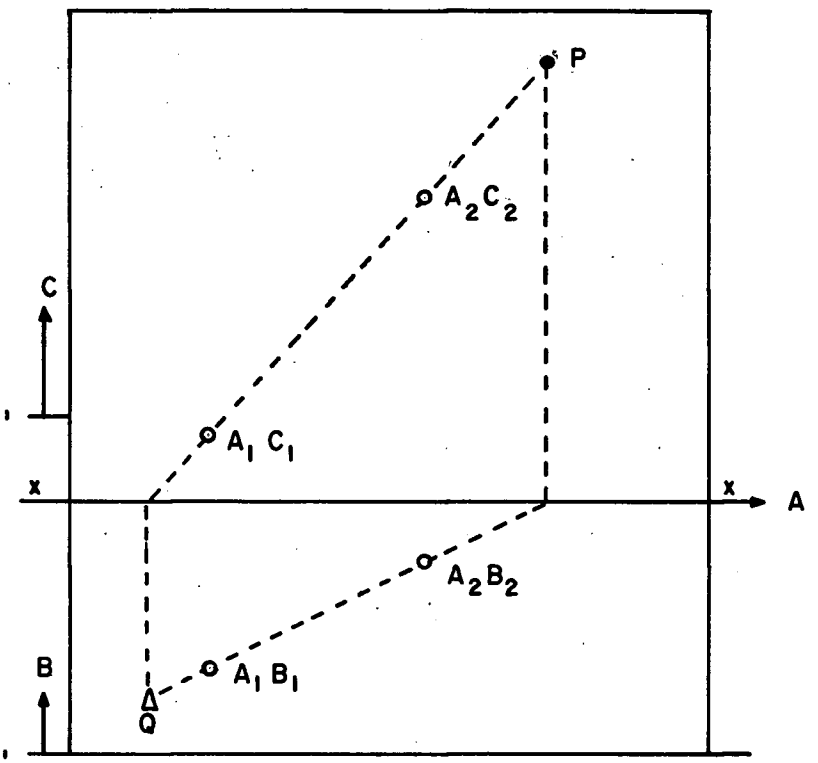

Fig.9 GRAPHICAL DETERMINATION OF POWER LAW FOR 3 VARIABLES

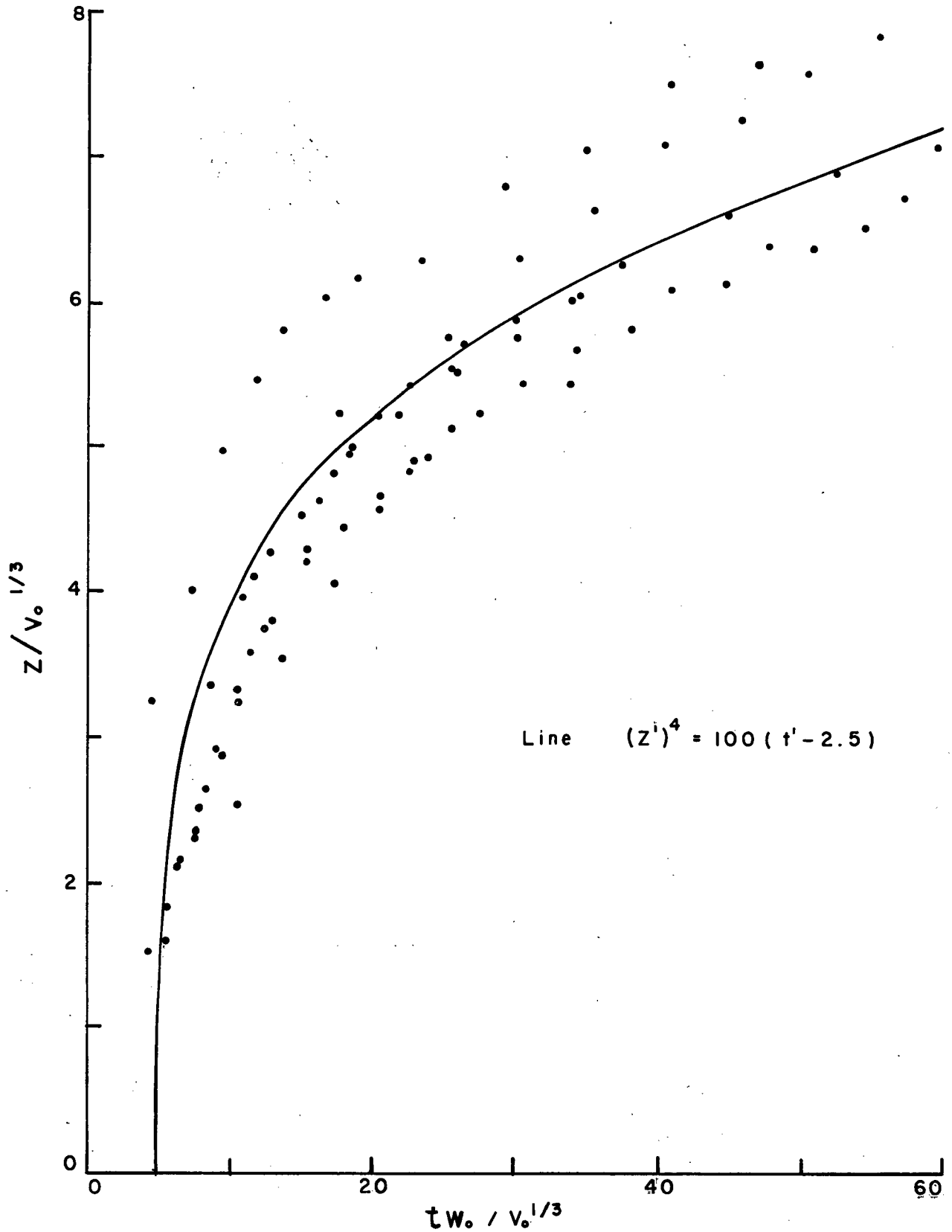

Fig. 10 SIMILARITY IN NEUTRALLY BUOYANT SURROUNDINGS

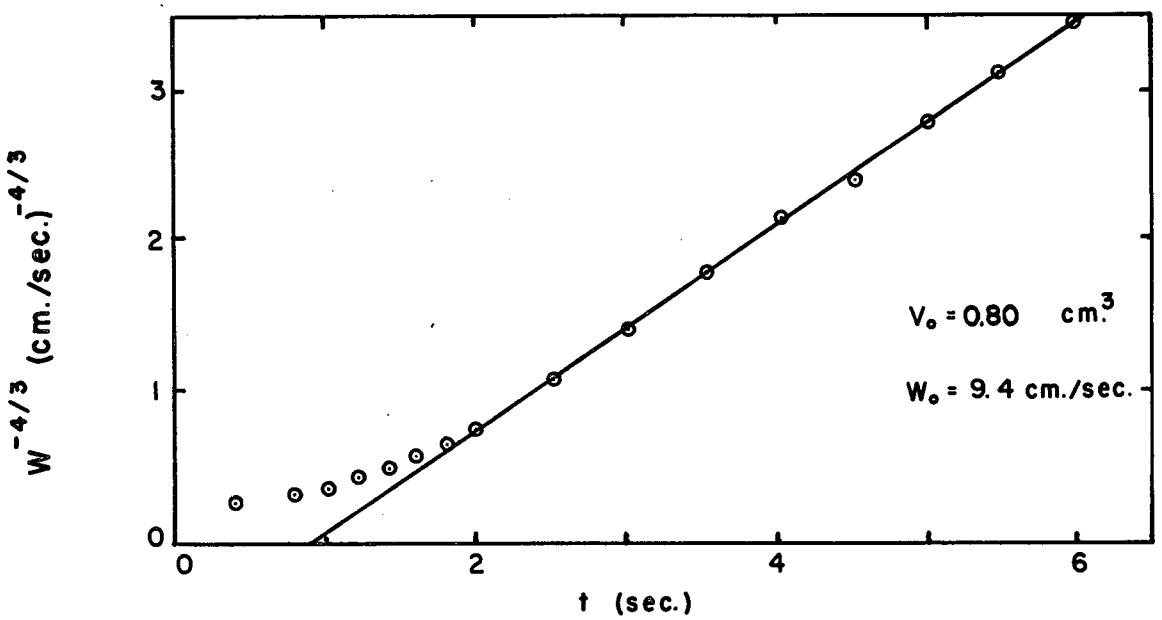

Fig. 11 VELOCITY OF PUFF IN NEUTRALLY BUOYANT SURROUNDINGS

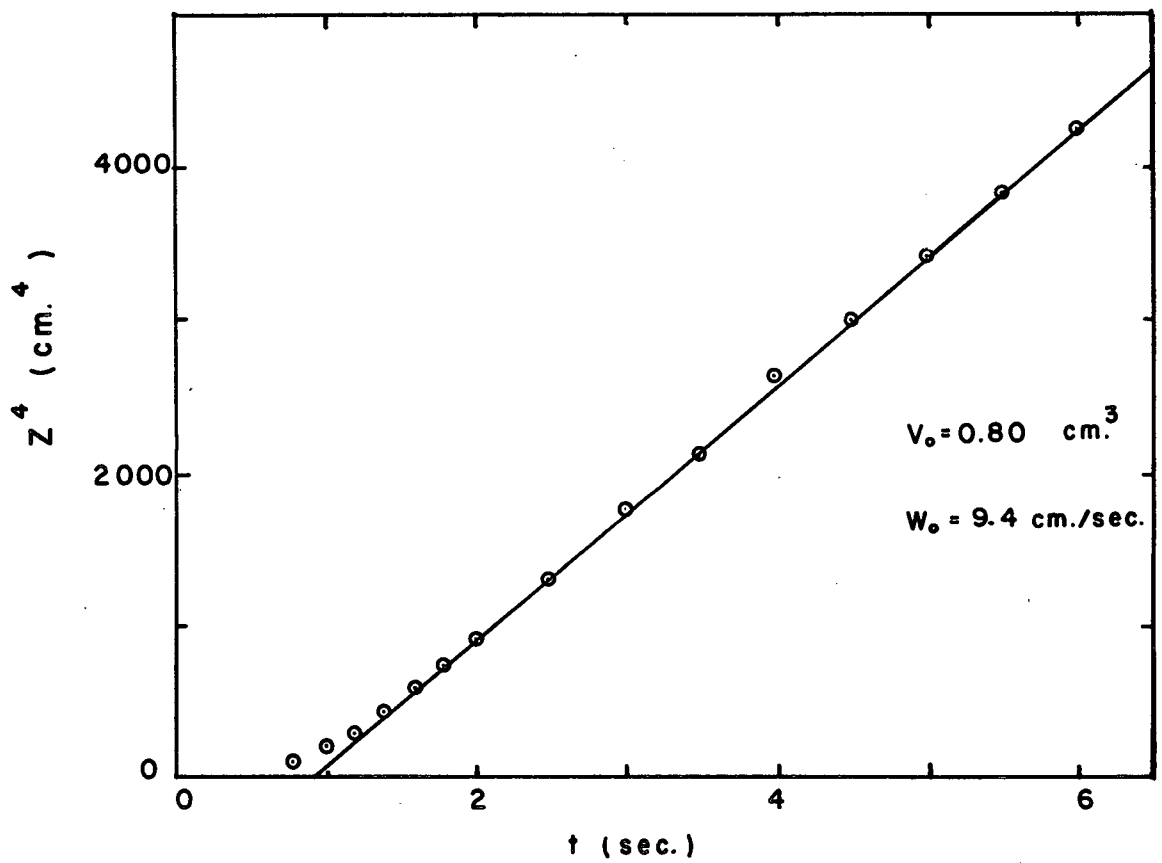

Fig. 12 DISPLACEMENT OF A PUFF IN NEUTRALLY BUOYANT SURROUNDINGS

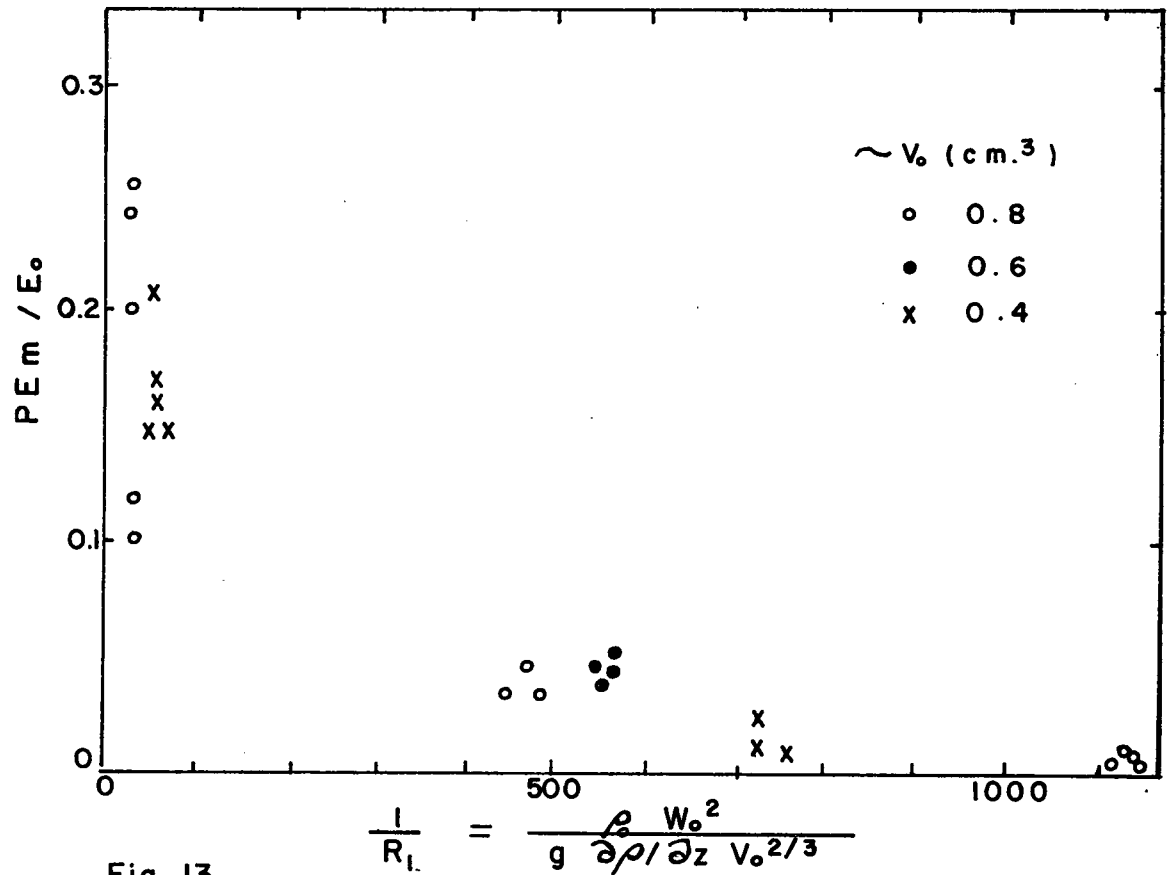

$$\frac{1}{R_L} = \frac{\rho_0 W_0^2}{g \, \partial\rho/\partial z \, V_0^{2/3}}$$

Fig. 13 POTENTIAL ENERGY AT MAXIMUM PENETRATION / INITIAL ENERGY

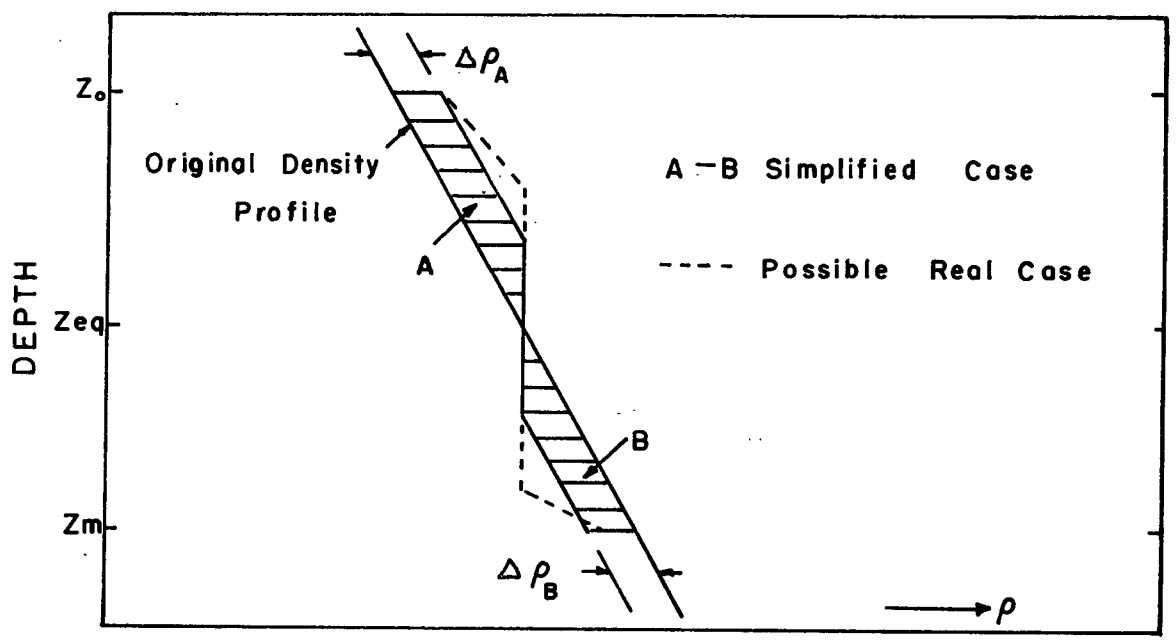

Fig. 14 ALTERATION IN DENSITY STRUCTURE

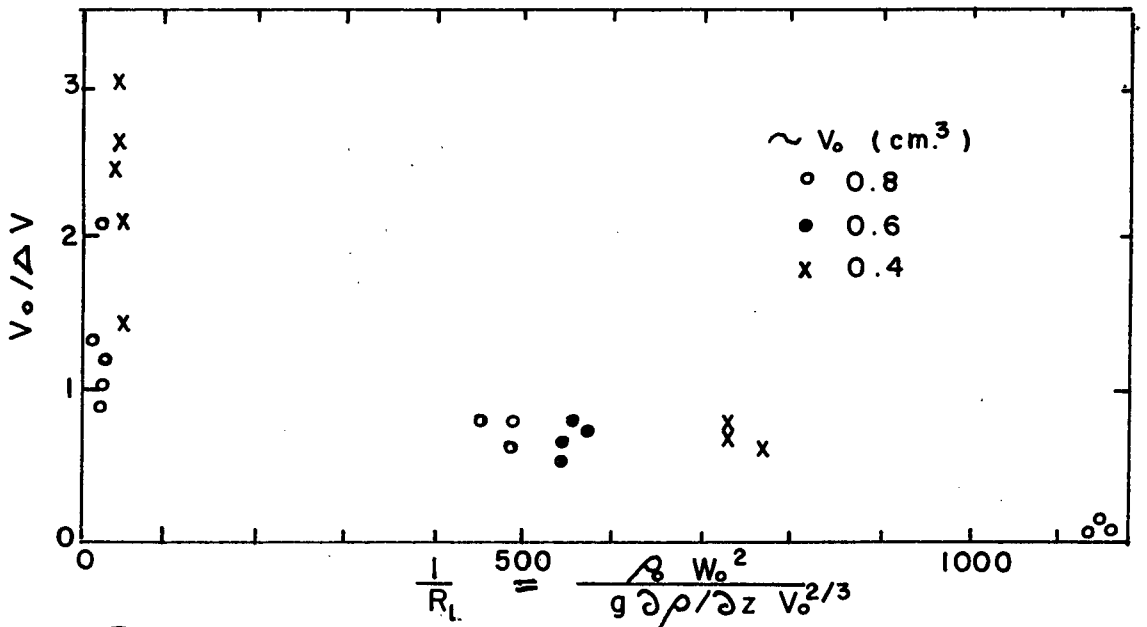

Fig. 15

RATIO $\frac{\text{INITIAL VOLUME}}{\text{VOLUME ENTRAINED}}$

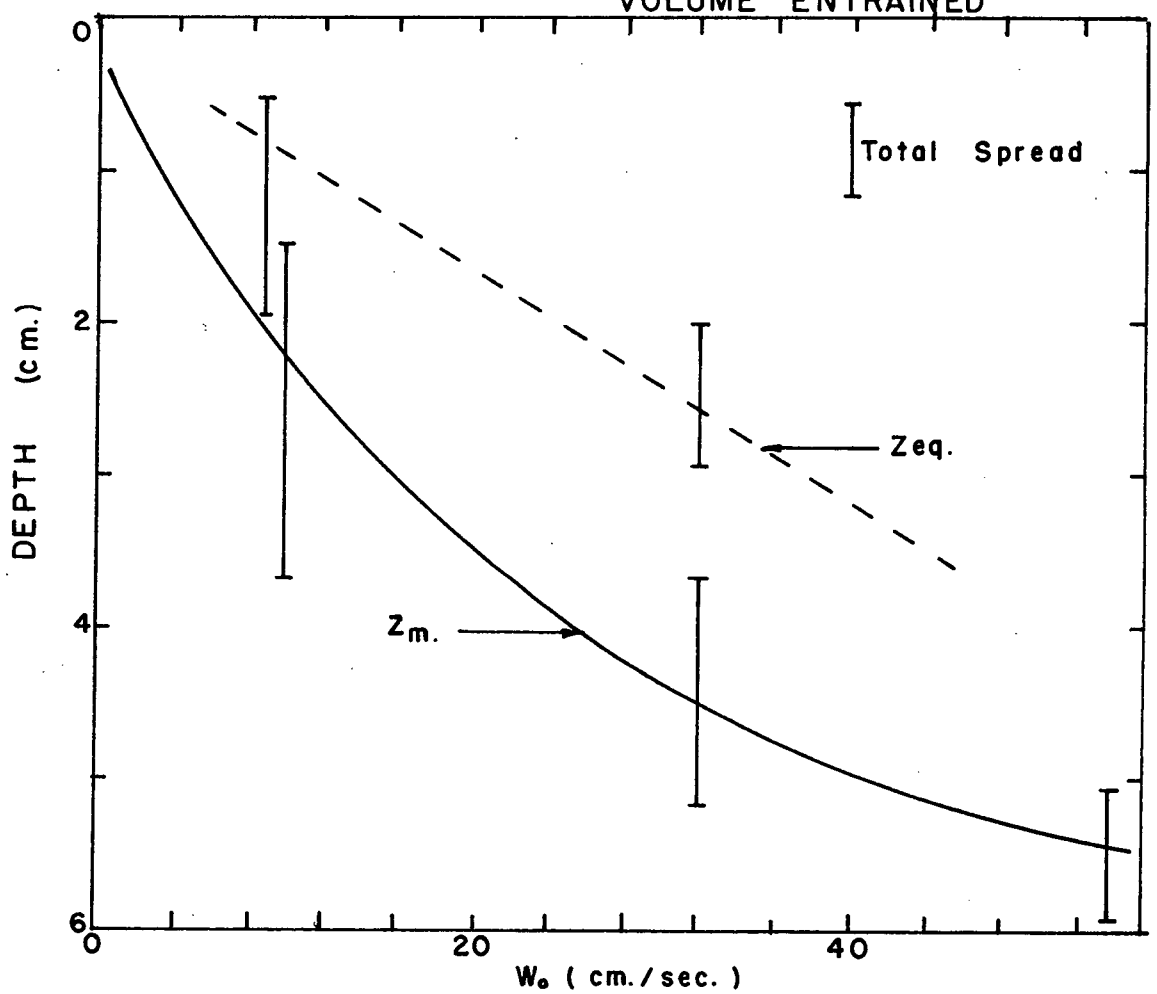

Fig. 16

MAXIMUM PENETRATION (Z_m)
AND EQUILIBRIUM DEPTH ($Z_{eq.}$)

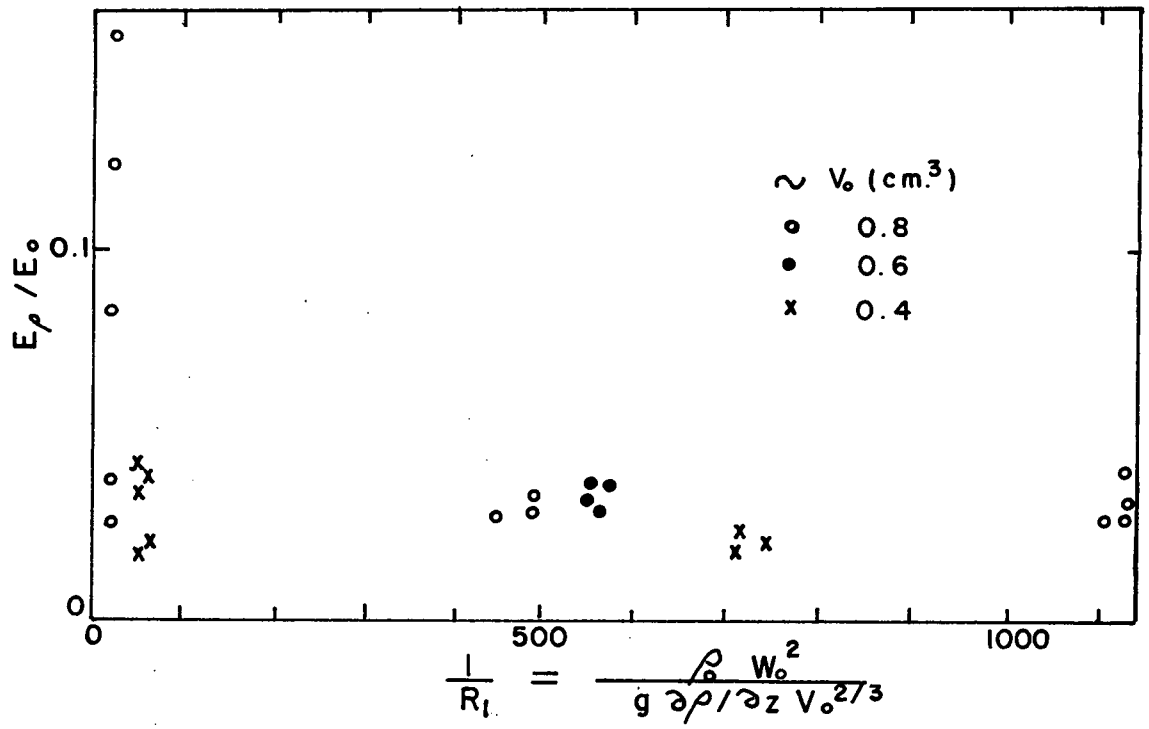

Fig. 17 ENERGY LOST TO DENSITY STRATIFICATION / INITIAL ENERGY

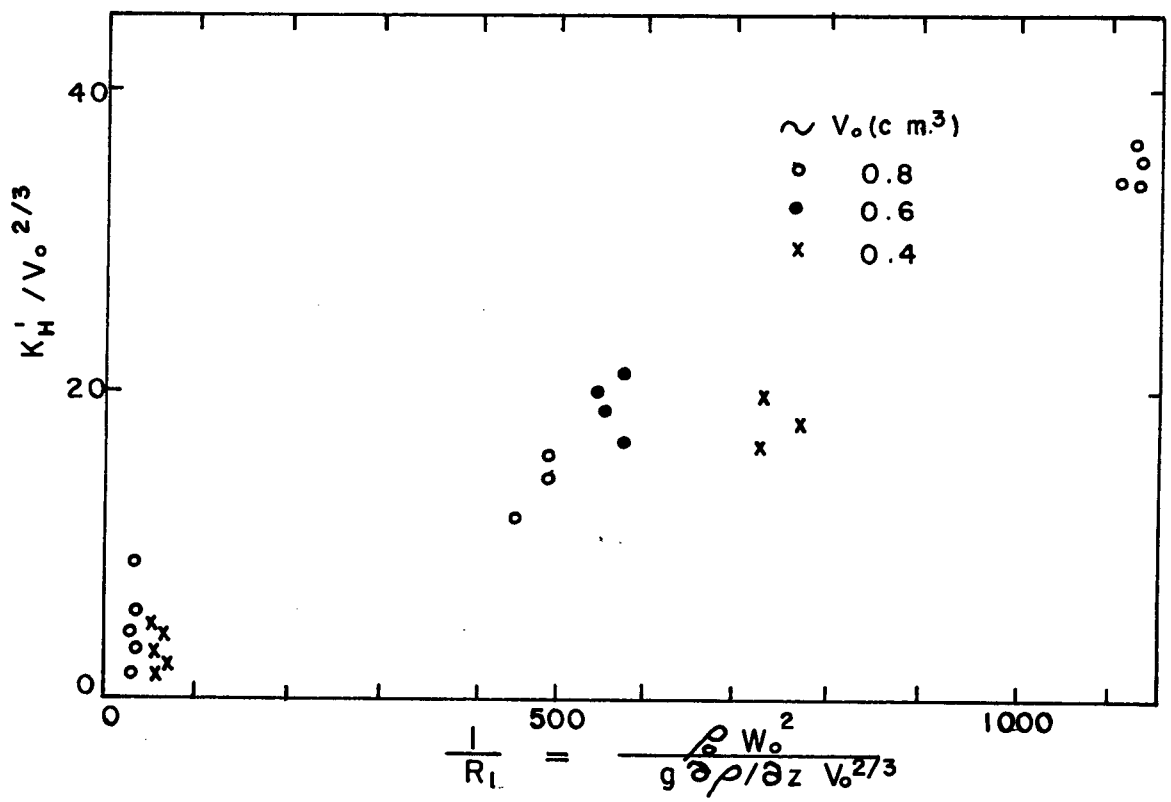

Fig. 18 NET DENSITY TRANSFER COEFFICIENTS

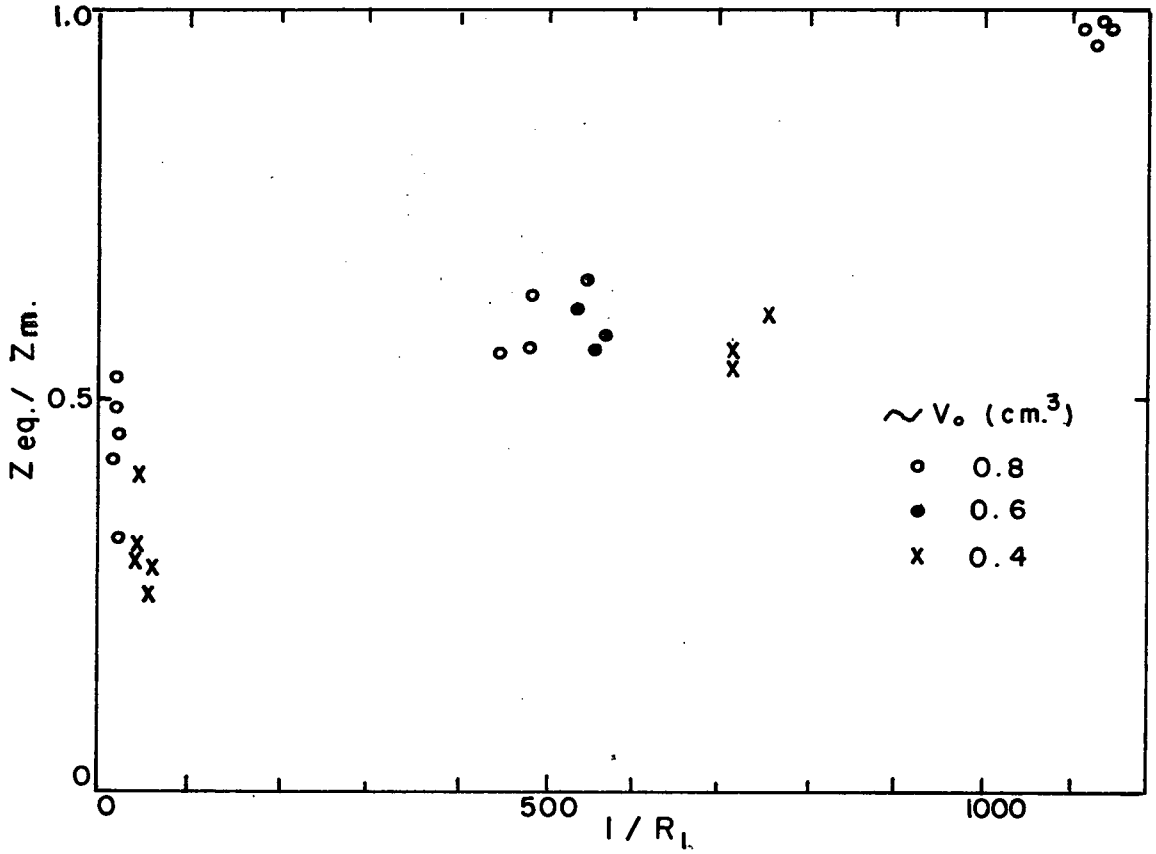

Fig. 19 EQUILIBRIUM DISTANCE / MAXIMUM PENETRATION

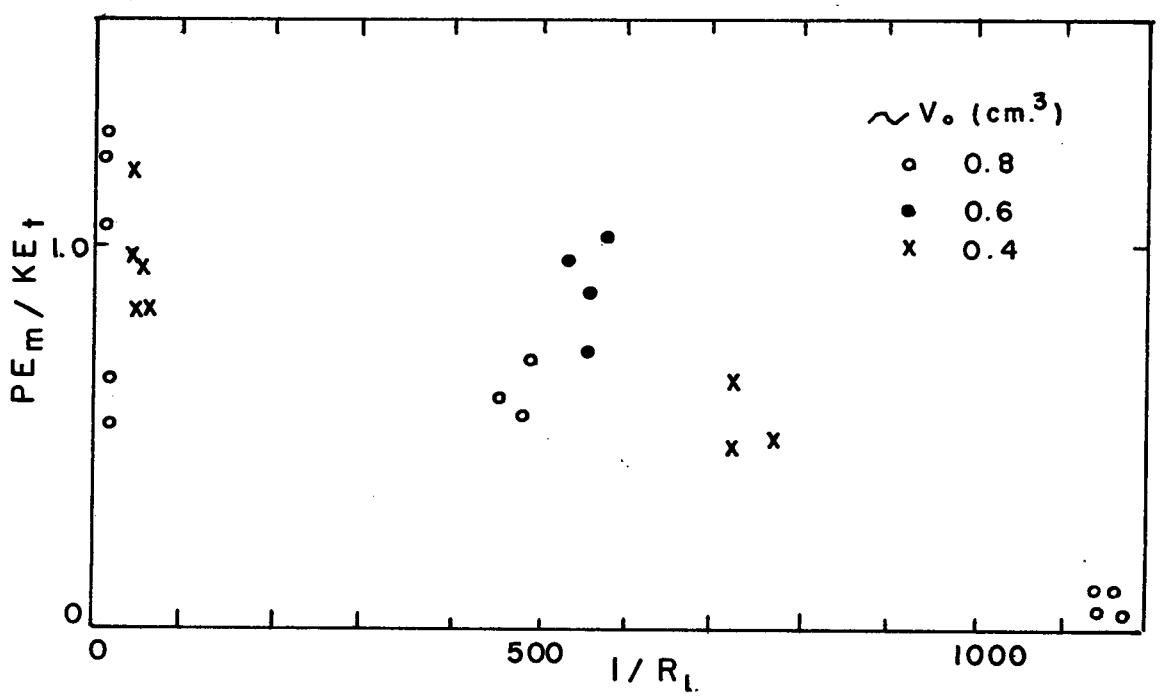

Fig. 20 POTENTIAL ENERGY AT MAXIMUM PENETRATION / KINETIC ENERGY AT SAME TIME IN NEUTRAL SURROUNDINGS